**ECM regulates morphogenesis and function of ciliated sensory organs**

By

DEANNA MICHELE DE VORE

A dissertation submitted to the

School of Graduate Studies

Rutgers, The State University of New Jersey

In partial fulfillment of the requirements

For the degree of

Doctor of Philosophy

Graduate Program in Cell and Developmental Biology

Written under the direction of

Maureen Barr

And approved by

_____

_____

_____

_____

New Brunswick, New Jersey

October 2018

**ABSTRACT OF THE DISSERTATION**

**Extracellular matrix regulates morphogenesis and function of ciliated sensory organs**

**by DEANNA MICHELE DE VORE**

**Dissertation Director**

**Maureen Barr**

Extracellular matrix (ECM) is made up of a network of interacting proteins that surround and support cells for mechanosensation, attachment, and signaling. Alterations in ECM quality and quantity contribute to many human diseases and disorders (Bruckner-Tuderman & Bruckner, 1998; Kain, 2010). ECM proteins have been implicated in cilia formation, cilia retraction/elongation, and cell-to-cell junction signaling, which are impaired in human ciliopathies (Marta Andrés, Enrique Turiégano, Martin C Göpfert, Inmaculada Canal, & Laura Torroja, 2014a; Rondanino et al., 2011; Seeger-Nukpezah & Golemis, 2012). Abnormal ECM is observed in ciliopathies such as Bardet-Biedl Syndrome, nephronophthisis, and polycystic kidney disease (PKD).

PKD1 and PKD2 encode transient receptor potential polycystin channel receptor proteins found in primary cilia of mammalian cells and sensory cilia of *Caenorhabditis elegans (C. elegans)* neurons. In humans, PKD1 and PKD2 mutations result in autosomal dominant polycystic kidney disease (ADPKD). Given the ancient and evolutionarily conserved role for polycystins in cilia, we used *C.*

*elegans* to identify new genes required for ciliary receptor localization and found that ECM components play multifaceted roles in ciliated sensory neurons. ECM formation, secretion, and integrity have been shown to be a primary factor in PKD (Mangos et al., 2010). *mec-1, mec-5,* and *mec-9* encode ECM components that play a role in mechanosensation and degenerin/epithelial sodium channel localization in non-ciliated touch receptor neurons (Du, Gu, William, & Chalfie, 1996; Emtage, Gu, Hartwieg, & Chalfie, 2004) .

Here, I show the ECM-encoding genes *mec-1*, *mec-5*, and *mec-9* play complex roles in *C. elegans* ciliated sensory organs. *mec-1* and *mec-9* encode proteins that contain multiple epidermal growth factor and Kunitz protease inhibitor domains; *mec-5* encodes a collagen (Du et al., 1996; Emtage et al., 2004). These ECM components regulate polycystin localization and polycystin-mediated male mating behaviors; control ciliary, dendritic, and glia integrity; and modulate the release of ciliary extracellular vesicles. Intriguingly, *mec-9* has cell-specific functions that are controlled by a short isoform that is differentially expressed in the ciliated nervous system. My findings reveal expanded roles of these ECM components by exposing their activity in ciliated neurons of the worm. I show that ECM proteins regulate aspects of extracellular vesicle biology, control ciliated neuron morphology and activity, and are necessary for ciliary localization of sensory receptors like PKD-2 and LOV-1. These findings expand the options for treatment of ADPKD and advance the front-line research of extracellular vesicle biology.

**Acknowledgements and Dedication**

**Maureen Barr**-I appreciate you. Thank you for sharing your expertise, knowledge, and all the excellence that is Barr lab. Thank you for your patience, support, and confidence boosts while I traveled this winding road. You helped me become a scientist.

**Committee Members: Monica Driscoll, Sunita Kramer, and Marion Gordon.** Thank you for your expertise, patience, and encouragement.

**David Hall and Ken Nguyen**-Much appreciation for EM data and decryption.

**NIH** for financial support at all stages of this research.

**Barr Lab Members: present and past**-**Juan, Bob, Shilpa, Yasmin, Gloria, Kumar, Kate and the Undergrads Extraordinaire**- YOU GUYS ARE AWESOME! Thank you for your uncountable hours of direction, advice, support, companionship, and entertainment.

**My Rutgers Support System:** *C. elegans* group, IMSD, INSPIRE, Waksman Band, LSB office staff, CDB staff, GSBS…

**Olivet Good Shepherd Church of Christ**, Paterson, NJ- Thank you for all the needed prayers and support. You helped my keep my eyes on my Help.

**Mom and Dad, Karen and David, my siblings here and gone, family and friends**-You kept me balanced.

**Bryanna and Jared**-I missed a lot of your things by doing this thing. Instead of complaining, you expressed your pride for my work-Thank you.

**Rodney De Vore**- There are not enough words. You stuck with me through it all. I thank you.

**Table of Contents**

Abstract .....ii

Acknowledgement and Dedication .....iv

Table of Contents ..... v

1 **Chapter 1 Introduction** ..... 1

1.1 Focus of research: Focus of research: *mec-1*, *mec-5* and *mec-9* ECM genes regulate anatomy and physiology of male specific and amphid organs in *C. elegans* ..... 1

1.2 Extracellular matrix is necessary for cellular support and interaction .... 2

1.2.1 Collagen fibers provide strength ..... 3

1.2.2 Adhesive ECM proteins interact and bind ..... 3

1.2.3 Extracellular Vesicles are ECM components ..... 4

1.2.4 ECM in *C. elegans* ..... *5*

.....

1.3 *Caenorhabditis elegans* is a powerful model organism ..... 6

1.3.1 Hermaphrodites and males ..... 7

1.3.2 *C. elegans* neurons of interest ..... 7

1.4 Cilia and ciliopathies ..... 10

1.4.1 Cilia are sensory organelles that interact with ECM ..... 10

1.4.2 Ciliopathies are disorders characterized by abnormal and dysfunctional cilia ..... 11

1.4.3 ADPKD: ciliopathy caused by PKD protein mutations ..... 12

1.4.4 Polycystins are conserved from humans to worms ..... 13

1.5 Mec ECM Proteins: Background ..... 15

1.5.1 MEC-1, MEC-5, and MEC-9 act as a cohort ..... 15

1.5.2 *mec-9* is necessary for mechanosensation and transcription factor regulation ..... 17

1.5.3 MEC-9 has EGF, Kunitz, and glutamic acid rich domains..... 18

1.5.4 *mec-9(ok2853)* deletion interrupts EGF like domains ..... 19

1.5.5 *mec-9* long and short isoforms have differing expression patterns ..... 20

.....

1.5.6 MEC-9 short protein localization is not clearly discernable ..... 20

**2 Chapter 2: ECM regulates morphogenesis and function of ciliated sensory organs** ..... 41

2.1 Introduction ..... 41

2.2 Results ..... 46

2.2.1 *mec-1*, *mec-5* and *mec-9* regulate PKD-2::GFP localization..... 46

2.2.2 *mec-1*, *mec-5* and *mec-9* regulate male mating behaviors ..... 50

2.2.3 *mec-9* long and short isoforms have distinct expression patterns: MEC-9S is expressed in ciliated sensory neurons ..... 52

2.2.4 *mec-9* regulates extracellular vesicle biogenesis and release ..... 53

2.2.5 *mec-9* and *pmk-1* act antagonistically in EV biogenesis and release . 55

2.2.6 *mec-9* maintains CEM neuronal morphology ..... 56

2.2.7 *mec-9* regulates ciliary length, positioning, and fasciculation..... 58

2.2.8 **Discussion**..... 61

3 **Appendix** (Unpublished data) ..... 90

3.1 *my2* is a *mec-5* allele ..... 90

3.1.1 *my2* locus on X chromosome ..... 90

3.1.2 Deficiency mapping: *my2* in X:22.9947..24.4738 ..... 90

3.1.3 Whole genome sequencing identified *my2* candidates ..... 91

3.1.4 *mec-5(my2)* ..... 92

3.1.5 *mec-5(+)* rescued the *my2* mutant ..... *93*

3.2 ECM affects LOV-1::GFP localization ..... 94

3.3 ECM regulates CIL-7::GFP localization ..... 94

3.4 *mec-9* does not regulate IL2 branching ..... 95

3.5 *mec-1(e1066)* negatively regulates exopher release ..... 96

3.6 PKD-2 antibody validated ..... 97

3.7 *mec-9* reporters constructed by Knudra ..... 99

3.7.1 *mec-1* and *mec-5* male expression patterns ..... 131

3.7.2 ECM-polycystin mechanisms ..... 132

3.7.3 Electron microscopy of *mec-1* and *mec-5* ..... 132

3.7.4 Male tail electron microscopy ..... 133

3.7.5 *mec-9* long and short isoform expression ..... 133

3.7.6 Amphid neuron activity assays ..... 133

3.7.7 AWA and AFD cilia branching examination ..... 134

3.7.8 Glia cell expression of ECM mutant genes ..... 134

3.7.9 Other genes of interest that may affect polycystin localization ..... 135

3.7.9.1 *mtd-1* ..... 135

3.7.9.2 *del-1* ..... 135
3.7.9.3 ZK550.3 ..... 135
3.7.10 Motor neuron expression and analysis ..... 136
3.7.11 Exopher analysis ..... 136
3.8 Materials and Methods ..... 137
3.8.1 Culture of *C. elegans* nematodes ..... 137
3.8.2 General molecular biology ..... 137
3.8.3 Imaging ..... 138
3.8.4 Transmission Electron Microscopy ..... 139
3.8.5 EV release ..... 139
3.8.6 EV biogenesis ..... 139
3.8.7 Cilia length measurements ..... 140
3.8.8 Antibody staining ..... 140
3.8.9 Response behavior assay ..... 140
3.8.10 Location of vulva assay ..... 141
3.8.11 Male leaving assay ..... 141
3.8.12 Dye filling assays ..... 141
3.8.13 Cloning and rescue ..... 142
3.8.14 Gentle touch assay ..... 142
3.8.15 Temperature sterility ..... 142
3.8.16 Velocity measurements ..... 142
3.8.17 Statistical analysis ..... 143
3.8.18 Ciliary localization and fluorescence intensity ..... 144

3.8.19 Strains..... 144
3.8.19.1 Alleles used ..... 144
3.8.19.2 Transgenic reporters used ..... 145
3.8.19.3 Strains..... 145
4 **Conclusions and Future Directions** ..... 136
4.1 Conclusions ..... 136
4.1.1 *mec-1*, *mec-5* and *mec-9* have broader roles than previously characterized. ..... 136
4.1.2 *mec-9* long and short isoforms have differing expression patterns..... ..... *137*
4.1.3 *mec-9* is necessary for EV biogenesis and release ..... *139*
4.1.4 *mec-9* and *pmk-1* act antagonistically in EV biogenesis and release ..... ..... 139
4.1.5 *mec-9* regulates neuron anatomy and cilia organization ..... *141*
4.1.6 *mec-9* regulates ECM deposition..... *142*
4.2 Future directions ..... 143
4.2.1 MEC-1 and MEC-5 expression profiles in males ..... 143
4.2.2 ECM-Polycystin mechanism studies..... 143
4.2.3 Electron microscopy of Other ECM mutants..... 144
4.2.4 Electron microscopy of male tail ..... 144
4.2.5 *mec-9* long and short translational localization ..... 145
4.2.6 Amphid neuron activity assays ..... 145
4.2.7 AWA and AFD ciliary branching..... 146

*4.2.8* Glial cell expression of *mec-9*, *mec-1*, *mec-5* ..... 146
4.2.9 Other proteins of interest for PKD-2::GFP ciliary localization..... 147
4.2.9.1 MTD-1..... 147
4.2.9.2 DEL-1..... 147
*4.2.9.3* ZK550.3..... 147
4.2.10 Motor neuron expression and analysis ..... 148
4.2.11 Exopher analysis ..... 148
5 **MATERIALS AND METHODS** ..... 149
5.1 Culture of *C. elegans* nematodes ..... 149
5.2 General molecular Biology..... 149
5.3 Imaging..... 150
5.4 Transmission Electron Microscopy ..... 151
5.5 Extracellular vesicle release ..... 151
5.6 EV biogenesis..... 151
5.7 Cilia length measurements ..... 152
5.8 Antibody staining ..... 152
5.9 Response behavior assay..... 152
5.10 Location of vulva assay ..... 153
5.11 Male leaving assay ..... 153
5.12 Dye filling assays..... 154
5.13 Gentle touch assay..... 154
5.14 Cloning and rescue..... 154
5.15 Temperature sensitive sterility ..... 154

5.16 Velocity measurements..... 154

5.17 Ciliary localization and fluorescence intensity..... 155

5.18 Strains used..... 155

6 References ..... 157

**Figures** (Legend on same or previous page)

**CHAPTER 1**

1.1 ECM is necessary for cellular support and interaction ..... 22

1.2 Collagen and elastic fibers are an abundant ECM component ..... 23-24

1.3 Sexual dimorphism in *C. elegans* ..... 25

1.4 *C. elegans* neurons of interest ..... 26-27

1.5 Amphid sensillum, cephalic sensillum, and male tail ray neurons..... 28-29

1.6 Touch receptor neurons and DEG/ENaC proteins ..... 30

1.7 Primary Cilia protrude from cell membrane and contain microtubules..... 31

1.8 Polycystic kidneys are enlarged and dysfunctional ..... 32

1.9 Human and *C. elegans* polycystins ..... 33-34

1.10 PKD-2::GFP localization in *C. elegans* ..... 35

1.11 *mec-9* ECM gene schematics ..... 36-37

1.12 *mec-9* Long and short isoforms and transcriptional reporters ..... 38

1.13 *mec-9*Lp::GFP has expected touch receptor neuron expression pattern .....
..... 39-40

**CHAPTER 2**

2.1 Alleles of *mec-1*, *mec-5* and *mec-9* regulate PKD-2::GFP localization and abundance ..... 67-69

2.2 *mec-1*, *mec-5* and *mec-9* are required for male mating behaviors ..... 72

2.3 *mec-9Sp*::GFP is expressed in ciliated sensory neurons ..... 73-74

2.4 *mec-9(ok2853)* mutants produce excessive ciliary vesicles ..... 75-76

2.5 *mec-9* and *pmk-1* double mutant genetically suppressed single mutant EV biogenesis/release) and PKD-2::GFP ciliary localization phenotypes ..... 77-78

2.6 *mec-9* regulated neuron ciliary and dendritic anatomy ..... 79-80

2.7 *mec-1*, *mec-5*, and *mec-9* mutants are dye filling defective and *mec-9* is necessary for amphid cilia organization and ECM deposition. ..... 82-84

2.8 Model of *mec-9* role at the neuron ..... 85

2.9 Alleles of *mec-1*, *mec-5* and *mec-9* regulate PKD-2::GFP localization and abundance in RnBs ..... 86-87

2.10 *mec-9* regulates PKD1(LOV-1) ..... 88

2.11 *mec-1(e1066)* and *mec-5(e1503)* phasmids are Dyf ..... 89

**CHAPTER 3**

3.1 3.1 Map of deficiency strains used to identify *my2* region ..... 104

3.2 *my2* was in deficiency 13, not in deficiency 4 ..... 105

3.3 Whole genome sequencing identifies *my2* candidates ..... 106

3.4 Locations of *my2* lesions in candidate genes ..... 108-109

3.5 *mec-5(u444)* complements sterility at 25C ..... 110

3.6 *mec-5(e1503)* was severely defective in PKD-2::GFP localization ..... 111

3.7 *my2* is a mec gene ..... 112

3.8 *mec-5(+)* rescues *my2* ciliary localization defect and is cell non-autonomous ..... 113

3.9 MEC-9 regulates localization of both *C. elegans* polycystins..... 114

3.10 MEC-9 regulates LOV-1::GFP ciliary localization: Fluorescence Intensity quantification ..... 115
3.11 *mec-9* regulates CIL-7::GFP localization ..... 116
3.12 MEC-9 regulates CIL-7::GFP localization ..... 117
3.13 *mec-9(ok2853)* has no CIL-7::GFP EV release defect ..... 118-119
3.14 *MEC-9* is not active in IL2 dauer branching ..... 120-121
3.15 Exophers are released from cell body ..... 122
3.16 *mec-1(e1066)* has exopher release ..... 123
3.17 *mec-1(e1066)* release significantly more exophers than WT ..... 124
3.18 Project plan for anti PKD-2 antibody ..... 125
3.19 N terminal and C terminal antibody sites ..... 127
3.20 Anti-PKD-2 antibody in WT male ..... 128
3.21 Anti-PKD-2 in *mec-5(my2)* males ..... 129
3.22 Anti-PKD-2 in *mec-9(ok2853)* ..... 130
3.23 Anti-PKD-2 in *mec-5(my2)* ..... 131
3.24 Anti-PKD-2 in WT hermaphrodite spermatheca ..... 132
3.25 Anti-PKD-2 antibody showed increased, endogenous localization at male specific CEM and RnB cilia ..... 133
3.26 Schematic for *mec-9*L transcriptional reporter ..... 134
3.27 Schematic for *mec-9*S translational reporter ..... 135

**TABLES**

2.1 *mec-1*, *mec-5* and *mec-9* mutants regulate PKD-2::GFP abundance ..... 70-71

2.2 *mec-9* regulated PKD-2::GFP particle abundance and velocity in CEM dendrites ..... 81

2.3 Alleles of *mec-1*, *mec-5* and *mec-9* regulate PKD-2::GFP localization and abundance in RnBs ..... 86-87

3.1 Raw whole-genome sequencing data for *my2* ..... *107*

3.2 Two of twelve epitopes worked in *C. elegans* whole mount immunohistochemistry ..... 126

# CHAPTER 1: INTRODUCTION

## 1.1 **Focus of research: *mec-1*, *mec-5* and *mec-9* ECM genes regulate anatomy and physiology of male specific and amphid organs in *C. elegans*.**

The nematode *Caenorhabditis elegans* (*C. elegans*) is a microscopic roundworm that we have been utilizing to study structures, mechanisms, and diseases that can be found in more complex animals such as humans. I used *C. elegans* as a model of human autosomal dominant polycystic kidney disease (ADPKD) to identify new genes required for polycystin protein localization to antennae-like cellular organelles known as the cilia.

Here I show that the extracellular matrix proteins *mec-1*, *mec-5* and *mec-9* already known to localize and regulate function at non-ciliated touch receptor neurons have broader sites of action and activity. I discovered that proteins in the extracellular matrix (outside of the cell and cilium) regulate the function of proteins inside the cell and cilium. When these extracellular protein-encoding genes are mutated, ciliary length, ciliary receptor localization, and ciliary function are altered; and so is the association between ciliated sensory neurons and surrounding glial cells. *mec-1*, *mec-5* and *mec-9* also regulate anatomy and physiology of male specific and amphid sensory organs in *C. elegans*.

Our findings reveal the promiscuity of ECM components by revealing their activity in ciliated neurons of the worm and broadens the scope of activity of the extracellular matrix proteins named for the touch receptor neuron activity. We also

found ECM proteins contribute to ciliary localization of sensory receptors like PKD-2 which advances the understanding of PKD and expands the options for treatment of ciliopathies. We illustrated that ECM is necessary for the health and well-being of neurons and neural organs. We further propose that ECM regulates aspects of EV biology which builds on the idea that ECM is necessary for extracellular interaction but pushes the envelope enabling us to think of ECM playing a role in extra-organismal communication.

**1.2 Extracellular matrix is necessary for cellular support and interaction**

Extracellular matrix (ECM) is made up of a network of interacting proteins that surround and support cells for mechanosensation, attachment, and signaling (Figure 1.1). Matrix often is thought of as just a physical milieu or surrounding for cells; however, studies show ECM is necessary for tissue morphogenesis and homeostasis throughout the lifespan of an organism. ECM proteins can interact with surrounding cells, and ECM gene mutations can cause anatomical and physiological aberrations. Matrix can interact with and affect human body systems, organs, and tissues such as the integument (layers, anchoring proteins, hemidesmosomes, basement membranes), connective tissues (bone, cartilage), internal organs such as the liver, kidney, and placenta (Bruckner-Tuderman & Bruckner, 1998). ECM is also important in cancer biology in that cells receive signals for growth, proliferation, and migration in response to cues from the environment: tumor cells metastasize by migrating along and through ECM structural proteins (Kain, 2010). The scope of ECM interaction and variety of

interactors is extensive and alterations in ECM quality and quantity contribute to diseases and disorders of various organs and systems.

**1.2.1 Collagen fibers provide strength** Collagens are trimeric, helical ECM proteins made up of three intertwined fibrils of repeating Glycine-X-Y alpha helical peptide chains (X-is often a proline and Y is often hydroxyproline) that intertwine to form collagen fibers (Gordon & Hahn, 2009) (Figure 1.2). Collagens are the "major insoluble fibrous protein in the ECM…and the…single most abundant protein in the animal kingdom (Lodish, 2000)". Collagens provide strength in tissues that require flexibility. There are many categories or "types" of collagens that are determined by molecular composition and structural features of their fibrils (Gordon & Hahn, 2009). ECM disorders are the cause of diseases in the skin, kidneys, and skeletal system. In the skin, hemidesmosome, anchoring fibrils, and basement membranes can lead to diseases like blistering (junctional epidermolysis bullosa) and the skin stretching seen in Marfan syndrome (Reichardt & Prokop, 2011). Genes such as COL4A are implicated Alport syndrome, a genetic disorder that affects the kidneys, hearing, and vision (Bruckner-Tuderman & Bruckner, 1998). Various collagen genes are implicated skeletal disorders such as in brittle bone disease and osteoporosis (Collagen I), osteoarthritis (Collagen II) and rhabdomyosarcoma cells (Collagen XIX) (Bruckner-Tuderman & Bruckner, 1998).

**1.2.2 Adhesive ECM proteins interact and bind** Adhesive ECM proteins are necessary for interaction and binding (Figure 1.1). Collagens have ligand properties and can bind to various receptors (Ricard-Blum, 2011). Other ECM proteins with binding and adhesion properties have been implicated in genetic diseases. Laminin is a large glycoprotein necessary for basement membrane structure and binds to collagen and other matrix proteins. Laminin disorders are found in the above mentioned skin-blistering junctional epidermolysis bullosa and muscular dystrophy (Bruckner-Tuderman & Bruckner, 1998; Colognato & Yurchenco, 2000; Gordon & Hahn, 2009). The glycoprotein, fibrillin and elastin protein are fibrils that are components of elastic fibers, are implicated in Marfan and Williams-Beuren syndrome. Williams-Beuren Syndrome is a disorder with wide ranging expression: intellectual, cardiovascular, facial disabilities, etc. (Bruckner-Tuderman & Bruckner, 1998).

**1.2.3 Extracellular Vesicles are ECM components** ECM is now being explored as a means of diagnosing and possible treatment of disease. Extracellular vesicles (EVs) are submicroscopic, lipid-membrane bound particles that contain myriad components such as nucleic acids and proteins and the mechanism of their release is conserved across many species (Iraci, Leonardi, Gessler, Vega, & Pluchino, 2016). EVs carry proteins such as fibronectin and laminin, which provide communication necessary for altering ECM composition, signaling between ECM and the cells it surrounds, tumor proliferation, and inflammation (Rilla & et.al, 2017). In *C. elegans*, ciliary proteins such as polycystins are EV cargo and affect

male mating behaviors (Wang et al., 2014). mir-34a, a microRNA that regulates the BCL-2 ”cancer gene”, has been found in drug resistant prostate cancer cells and in the EVs released from them, which suggests EVs can be used as a read out of the cells from which they originate (Corcoran, Rani, & O'Driscoll, 2014). This new and cutting edge research on extracellular vesicles has sparked collaborations such as those of the H2020 European Cooperation in Science and Technology (COST) program, European Network on Microvesicles and Exosomes in Health and Disease (ME-HAD), and prompted them and other researchers to begin clinical trials examining the use of EVs as biomarkers, chemotherapeutic carriers in cancer, and cellular regeneration therapies (Fais et al., 2016; Jennifer F Barger, Mohammad A Rahman, Devine Jackson, Mario Acunzo, & S Patrick Nana-Sinkam, 2016). The work presented in this thesis will add to the breadth of knowledge in this emerging ECM and EV field of study.

**1.2.4 ECM in *C. elegans*** *C. elegans* is an excellent model for ECM research. Southern blots (detection of DNA) and screening has been done using *C. elegans* and anywhere from 40-150 unique collagen genes have been identified and classified (Cox, Kramer, & Hirsh, 1984). Mutations in the Type IV basement membrane collagen *emb-9* reveal semi-dominant temperature sensitive embryonic lethality and is necessary for LET-2 collagen protein assembly (Gupta, Graham, & Kramer, 1997). ECM in the cuticle of nematodes is made up of tightly cross-linked collagens and is necessary for maintenance of body shape, as a protective barrier, and for muscular attachment sites (Thein et al., 2009). Specific *C. elegans*

extracellular matrix proteins (MEC-1, MEC-5, and MEC-9) surrounding the touch receptor neurons are essential for mechanosensation and make up the "mantle" around the touch neurons (Du et al., 1996; Gu, Caldwell, & Chalfie, 1996) (Figure 1.6). In this work, I will explore the function and activities of *C. elegans* ECM genes *mec-1, mec-5* and in greater detail, *mec-9*.

**1.3 *Caenorhabditis elegans* is a powerful model organism.** The tiny transparent nematode, *C. elegans*, is an ideal model organism because it is easy to maintain, fertile, transparent, and all the cells and the lineage that generates them have been identified (Figure 1.3). In a lab, *C. elegans* is propagated on small petri dishes, eats bacteria and is sexually mature in two-three days. *C. elegans* is a hermaphrodite species with a life span of approximately 20 days. Hermaphrodites can self-fertilize and produce approximately 300 progeny each, which is ideal for genetic analysis. Because *C. elegans* is transparent, internal structures and fluorescent tagged proteins are easily visualized in living animals using a microscope. *C. elegans* can be readily used for study because all cells (959 somatic in the hermaphrodite) have been identified and mapped including the entire nervous system consisting of hundreds (302 in the hermaphrodite); compared to billions of neurons in the human brain (Riddle, 1997).

*C. elegans* has a compact genome, with a similar number of genes as humans on only six chromosomes rather than 23. The entire genome (about ~20K genes) is

fully mapped, many of which are conserved so this means gene variations can be introduced and studied (Riddle, 1997).

**1.3.1 Hermaphrodites and Males** Hermaphrodites have two “X” chromosomes, whereas males have only one. The species is 99.9% hermaphrodite but there is an occasional male that is produced when there is nondisjunction of the X chromosome. Since we study males, it is necessary to introduce a Him (high incidence of males) mutation (Hodgkin, Horvitz, & Brenner, 1979). This increase in the population has made it possible to notice differences such as mating behaviors and sexual dimorphism in somatic cells (1031), neurons (385), proteins, behavior, and phenotypes in males. Males have 205 male specific cells that form neurons, support cells, muscle, hypodermal, and internal gut cells (Emmons, 2005). The tail is the most obvious means of deciphering the difference in sex because males have wide fan as in contrast to the narrow whip seen in the hermaphrodite tail (Figure 1.3). My work concentrates on the study of how ECM affects nervous system organization and function, particularly in the *C. elegans*.

**1.3.2 *C. elegans* neurons of interest** I will discuss neurons in general and, some specific neurons, in detail in this paper. Neurons are excitatory cells that can receive and send electrical impulses, which enable organisms to communicate internally and interact externally with the environment. Generally, neurons have a soma (cell body), dendrite, and axon. Some sensory neurons in *C. elegans* are ciliated (to be discussed in Section 1.4). Groups of neurons and their supportive

glia may be bundled and bound in sensory organs called sensilla. Specific groups of neurons of interest to be discussed in this work are the amphids, touch neurons (TN), inner labial (IL2), cephalic male (CEM), and Type B ray neurons (RnB) (Figure 1.4).

Amphid sensory organs are found in the bilateral sensilla of the head. The amphid sensilla and its associated sensory neurons are categorized as the "shared" nervous system found in hermaphrodites and males. Each amphid sensillum contains 12 sensory neurons that run from the posterior extension of the nerve ring to the tip of the nose. The distal ends of most of the amphids are located in a glial cell known as the amphid sheath (Ware, Clark, Crossland, & Russell, 1975) (Figure 1.5). The tips (cilia) of eight of these amphid cilia are enclosed by the amphid socket cell, open into a pore in the lateral papillae of the head and are environmentally exposed (Ward, Thomson, White, & Brenner, 1975). The amphids are necessary for chemosensation, dauer entry and exit, and thermosensation (Perkins, Hedgecock, Thomson, & Culotti, 1986; Ward et al., 1975; Ware et al., 1975).

In the male head, CEM cell bodies are located concentrically adjacent to the nerve ring (Figure 1.5). The CEM dendrites extend along the four cephalic sensilla through to the left and right ventral and dorsal papillae where the cilia are environmentally exposed to enable chemotaxis (Sulston, Albertson, & Thomson, 1980). Like the amphids, cephalic sensilla have their own sheath and socket glia.

The cephalic sensillum houses the shared CEP ciliated sensory neuron found in both hermaphrodites and males.

In the male, the nine pairs of male specific RnB neurons are in the tail and the dendrites expand toward the fan of the tail. The nomenclature for the ray neurons is R (ray), n (neuron number 1-9) and B-type to differentiate them from their adjacent A-type neurons. B-type neurons (with the exception of ray 6) have a cilium that protrudes to the environment and sheds extracellular vesicles (Sulston et al., 1980)(Wang et al., 2014). RnB neurons are necessary for male mating behaviors such as mate exploration and response to hermaphrodite (Barrios, Nurrish, & Emmons, 2008). The HOB neuron, also located in the tail at the hook sensillum, are necessary for location of vulva behavior (K. S. Liu & Sternberg, 1995).

Other neurons to note for reference, but not as extensively studied here, are IL2 and touch neurons. The shared six inner labial type 2 (IL2) neuronal cell bodies have environmentally exposed ciliated dendrites that end in each of the papillae in the inner labial sensilla at the nose of the animal (Ward et al., 1975; Ware et al., 1975) (Figure 1.4-5). The IL2 neurons develop extensive arbors in the dauer stage and are necessary for nictation (Schroeder et al., 2013). In reproductively growing animals, the IL2s shed and release ciliary EVs (Wang et al., 2014). The shared non-ciliated, gentle body touch receptor neurons are made up of the AVM, left and right ALM, PVM and left and right PLM (A/P refers to anterior or posterior, L/V refers to lateral or ventral, M refers to a specialized 15-protofilament microtubule

arrangement). The touch neurons are responsible for gentle touch reflex behaviors in that the animal retreats when touched at the head or tail. Gentle touch reflex behaviors are facilitated by degenerin epithelial sodium channels (DEG/ENaC) which are arranged in puncta along the dendrites of the neurons (Chalfie & Sulston, 1981; Emtage et al., 2004) (Figure 1.6).

MEC-4 and MEC-10 are the mechanosensory proteins that constitute the subunits of touch neuron DEG/ENaCs. MEC-2 and MEC-6, DEG/ENaC accessory proteins, act synergistically to increase channel activity and as a linker enabling the channel to interact with microtubules; *mec-12* and *mec-7* encode the specialized touch neuron tubulins (Chelur et al., 2002; M. B. Goodman et al., 2002; R. O'Hagan, Chalfie, & Goodman, 2005; Tavernarakis & Driscoll, 1997). The touch neurons are surrounded by the specialized ECM proteins MEC-1, MEC-5, and MEC-9, which will be later discussed in detail as they are the focus of this work (Figure 1.6).

## 1.4 Cilia and ciliopathies

**1.4.1 Cilia are sensory organelles that interact with ECM** Primary cilia are microscopic, hair like structures that emerge from the surface of many eukaryotic cells (Figure 1.7). Cilia contain a skeleton called an axoneme that is made up of microtubule “bones”. The microtubules emerge from basal bodies and are anchored to the ciliary membrane by “Y-links”. These microtubules are arranged in normally, nine concentric pairs called A-B doublets as they pass through the

cilium. Each tubule in the doublet pair is denoted as A or B. When the microtubules reach the distal ciliary tip, they become A-tubule singlets (M. Silva et al., 2017). Primary cilia function as non-motile sensors, are found on most mammalian cells, and act as signaling organelles that are necessary for tissue growth and development (Satir, Pedersen, & Christensen, 2010). Primary cilia in *C. elegans* are found only on neurons and are necessary for specialized sensory activity (Perkins et al., 1986).

ECM is necessary for cilia formation and activity. In tendons, collagen ECM corrals primary cilia which are lined up in a parallel formation like tendon tissue (Donnelly, Ascenzi, & Farnum, 2010). ECM has been implicated in cilia formation and functionality in *Drosophila* (Marta Andrés, Enrique Turiégano, Martin C Göpfert, Inmaculada Canal, & Laura Torroja, 2014b). Also, ECM proteins such as cadherins and galectins which are known to play a role in cilium retraction and elongation have now been suggested to play a role in cell-to-cell junction signaling via the ECM (Seeger-Nukpezah & Golemis, 2012). Galectin-7 is a beta galactoside-binding protein that localizes to renal primary cilia in a few mammalian species that has been suggested to act as go-between of ciliary function and its surrounding epithelial lining repair (Rondanino et al., 2011). NCBI SmartBLAST Protein software predicts similarity between the EGF repeat domains of the MEC-9 ECM protein and cadherin EGF LAG seven-pass G-type receptor 3 (CELSR3) and these elements are the deleted sequence of *mec-9(ok2853)*, a mutant used in this study.

**1.4.2 Ciliopathies are disorders characterized by abnormal and dysfunctional cilia.** Primary cilia defects lead to disorders referred to as ciliopathies, which cause disease in various body systems such as renal and hepatic cysts, respiratory disorders, polydactyly and skeletal disorders (Davis et al., 2011). More recently, ciliogenesis defects have been noted in mouse models and human patients with Huntington's Disease and Alzheimer's disease (Armato, Chakravarthy, Pacchiana, & Whitfield, 2012; Keryer et al., 2011). Extracellular matrix proteins have been shown to selectively limit protein access to the primary cilia; therefore, further research ECM research in the area of ciliopathies will broaden understanding and ultimately treatment of ciliopathies (Garcia-Gonzalo & Reiter, 2012). Abnormal ECM is observed in ciliopathies such as Bardet-Biedl Syndrome nephronophthisis, and autosomal dominant polycystic kidney disease (ADPKD) (B. Liu, Li, Liu, Dai, & Tao, 2012; Xie et al., 2011).

**1.4.3 ADPKD: ciliopathy caused by PKD protein mutations** ADPKD is a genetic disorder is characterized by the presence of fluid filled cysts which form on and in the kidney's epithelial cell lined renal tubules. These cysts can replace normally functioning renal tissue and result in enlarged, kidneys with many vesicles and end stage renal failure in approximately half of affected patients (Takiar & Caplan, 2011) (Figure 1.8). This ciliopathy affects 1 in ~500 persons regardless of race or gender (Yook et al., 2012). ADPKD can be caused by a mutation in either of the polycystin encoding genes, though most cases (~85%) are caused by PKD1 mutations (Sutters & Germino, 2003). Individuals with mutations in PKD2 often

have a milder presentation and later manifestation of signs and symptoms (Igarashi & Somlo, 2002).

In zebrafish, ciliopathy phenotypes of dorsal axis curvature, hydrocephalus, and pronephronic cyst formation were observed in *pkd1* and *pkd2* knockdowns (Mangos et al., 2010). My studies of the roles of ECM on PKD-2 localization and ciliary structure and function will add to the base of knowledge and may extend further research of this ciliopathy towards the mechanosensory aspect of polycystins and the impact of extracellular matrix on ion channel localization.

**1.4.4 Polycystins are conserved from humans to worms.** Polycystins are evolutionarily conserved and have been studied in many animal models such as human, murine, *Drosophila*, *Xenopus*, and *C. elegans* (Hofherr & Kottgen, 2011). In mammals, the polycystins were once thought to act in a complex as mechanosensors that regulate calcium release into a cell (Nauli et al., 2003). Recent studies show that the polycystins act independently and that rather than calcium, PKD-2 conducts sodium and potassium into the cilium (Liu Xiaowen et al., 2018). The polycystins PKD1 and PKD2 are proteins that may interact via their C terminal domains in cytosol (Hanaoka et al., 2000) (Figure 1.9). A large segment of N-terminal PKD1 extends into the extracellular matrix. This process contains many domains that could act in protein binding and recognition, Ran GTPase, and cell adhesion (Kobe & Kajava, 2001). PKD2 has an often-mutated extracellular domain that is necessary for polycystin channel assembly, stimulation, and gating

(Shen et al., 2016). These two polycystins can be cleaved and have been found to act individually and synergistically in body cells performing myriad functions including acting as ion channels and even in regulation of ECM components (Hanaoka et al., 2000; Mangos et al., 2010).

Polycystins are evolutionarily conserved and found in *C. elegans*, the PKD1 and PKD2 homologs LOV-1 and PKD-2 are necessary for male mating behavior (Barr & Sternberg, 1999) (Figure 1.10). LOV-1 is needed for PKD-2 recruitment to the primary cilium of CEM neurons, putative chemosensors, and eight of the ray neurons located in the male tail (Bae et al., 2006). LOV-1 has a long extracellular C terminal end that has a mucin domain (Barr & Sternberg, 1999). This mucin binding site is made up of glycoproteins that could be explored as a receptor for collagen or other ECM binding.

PKD1 and PKD2 proteins localize to primary cilia of mammalian cells. PKD-1 and PKD-2 are conserved, are also found in primary cilia of *C. elegans* neurons (Figure 1.10) and are necessary for male mating behaviors (Barr & Sternberg, 1999). Literature shows that polycystins can regulate ECM. Extracellular matrix formation and integrity has been shown to be affected and regulated by PKD1 and PKD2 in zebrafish (Mangos et al., 2010). Evidence suggests *pkd1* and *pkd2* mutant zebrafish have abnormal axis curvature because of excess collagens which may have altered notochord structure (Mangos et al., 2010). It is very possible that the

link between collagens and polycystins in zebrafish could be evolutionarily conserved in *C. elegans*.

Given the ancient and evolutionarily conserved role for polycystins in cilia, we use *C. elegans* as a model to study PKD and identify new genes required for polycystin ciliary localization and function. I identified an allele of *mec-5* from a forward genetic screen to identify genes involved in ciliary trafficking of PKD-2::GFP (Bae, Lyman-Gingerich, Barr, & Knobel, 2008). Further investigation revealed *mec-5* cohorts, *mec-1* and *mec-9* also regulate PKD-2::GFP localization. I discovered that the polycystin-ECM relationship is reciprocated: ECMs can regulate polycystin localization and activity. We do not know if the interaction between MEC-1, MEC-5, MEC-9 and the polycystins LOV-1 and PKD-2 is direct or indirect.

## 1.5 MEC ECM PROTEINS: BACKGROUND

**1.5.1 MEC-1, MEC-5, and MEC-9 act as a cohort.** The three ECM genes have an N-terminal signal peptide suggesting they are secreted. MEC-9 was first characterized with MEC-5, a unique collagen (Du et al., 1996) that is strongly expressed during the larval stages in the hermaphrodite ventral seam and hypodermis. MEC-5 collagen has two characteristic Gly-X-Y domains (Du et al., 1996). MEC-5 expression decreases and becomes limited to the head in adult hermaphrodites (Du et al., 1996). *mec-1* and *mec-9* have differing arrangements

of Kunitz and EGF like domains (Figure 1.11). MEC-1 was later characterized and found to have similar EGF and Kunitz protease domains as MEC-9 but arranged differently (Emtage et al., 2004). There are 14 MEC-1 isoforms compared to only two for MEC-9 (WormBase.). The MEC-1 transcriptional reporter is expressed in the hermaphrodite touch receptors and other muscle and gut neurons (Emtage et al., 2004). MEC-1 and MEC-5 localize in puncta along touch receptor neurons via the MEC-4 subunit of the DEG/ENaC ion channel and all three ECM proteins are implicated in DEG/ENaC localization (Emtage et al., 2004).

These three ECM proteins are secreted into the extracellular matrix surrounding touch receptor neurons and *mec-1* and *mec-5* act non-cell autonomously. A *mec-1*(+) construct with a touch neuron specific *mec-18* promoter can rescue the mechanosensory phenotype even though *mec-1* also expresses in non-touch receptor neurons (Emtage et al., 2004). *mec-5*(+) rescue experiments show some *mec-5* mutant phenotypes can be overcome using a muscle-specific *myo-3* promoter (Figure 3.8). All three proteins express in various body cells with changing proteins levels and location in an age dependent manner. The function of these ECM proteins outside the touch receptor neurons is not well understood. *mec-9* has been implicated in FOXO transcription factor activity (Kim et al., 2007) and *mec-1* plays a role amphid and phasmid cilia morphology (Perkins et al., 1986). To my knowledge, little other non-mechanosensory ECM protein activity has been reported, possibly due to sexually dimorphic protein expression and activity. Interestingly, and likely due to the inherent, infrequent occurrence of

males in the *C. elegans* population, male expression pattern of *mec-1*, *mec-5*, or *mec-9* is not reported in the literature.

**1.5.2 *mec-9* is necessary for mechanosensation and transcription factor regulation.** Much of the data presented in this dissertation focuses on *mec-9* because of the penetrant, robust phenotypes and lack of knowledge in the short isoform. *mec-9* transcribes a long and short isoform with differing expression patterns. The long isoform is expressed in the six touch receptor neurons: ALM, AVM, PLM, PVM, and sometimes the PVD (Du et al., 1996). The *mec-9* short transcript is expressed in many more neurons of the head and along the ventral nerve cord in hermaphrodites (Du et al., 1996). *mec-9* is necessary for mechanosensation in *Caenorhabditis elegans* touch receptor neurons (Du et al., 1996), likely as an extracellular attachment point for the MEC-4/MEC-10 components that make up degenerin epithelial sodium (DEG/ENaC) ion channels on touch receptor neurons (Du et al., 1996). MEC-9 is a purported globular ECM protein, is secreted from neurons (and possibly glial cells), and is essential for arrangement of DEG/ENaC ion channels into well-organized puncta along the length of the TRNs (Emtage et al., 2004).

*mec-9* is also essential for the FOXO signaling pathway. DEG/ENaC channels trigger DAF-16/FOXO transcription factor translocation from its diffuse localization in somatic cells (inactive state) into the nucleus (active state) when the animal is subjected to an increase in gravitational force induced by centrifugation. These

signaling responses can cause mechanosensory channels to alter fat accumulation during mechanical stress caused by excessive gravity (Kim et al., 2007). Notably, MEC-9 activities are impacted by *mec-9* lesions found affecting only the long transcript (Du et al., 1996; Emtage et al., 2004).

**1.5.3 MEC-9 has EGF, Kunitz, and glutamic acid rich domains.** Multiple EGF-like domains are often found in extracellular matrix proteins and may be used for calcium dependent protein-protein interactions and mutations in these domains can often result in a decrease in the activity of a protein or large-scale disability (Selander-SunnerhagenSQ, 1992). EGF-like domains are cysteine rich and function in cell growth and differentiation (J. Engel, 1989). Kunitz domains are known for protease inhibition activity and regulate homeostasis, inflammation, cancer progression, tissue remodeling and repair, ion channel activity, and signaling pathways (Shigetomi et al., 2010). Glutamic acid-rich sequences in proteins are negatively charged, unfolded, and disordered, which enables them to function as flexible linkers and/or spacers at membrane channels and facilitate protein-protein interactions (Renu Batra-Safferling et al., 2006).

The MEC-9L isoform has two sets of EGF like domains (seven total), two sets of Kunitz domains (five total), and a glutamic acid rich region at the C terminus (Du et al., 1996) (Figure 1.12). The MEC-9 short isoform begins after the long intron starting with the 10$^{th}$ exon. MEC-9 short contains one set of EGF like domains, one set of Kunitz domains, and a C-terminal glutamic acid rich region (Du et al.,

1996) (Figure 1.12). Each isoform has a hydrophobic N terminus suggestive of a signal sequence (Zhang & Shen, 2016). The long isoform has two calcium binding sites like those identified in blood coagulation factor IX and an arginyl-glycyl-aspartic acid tripeptide (necessary for recognition by integrins on cell surfaces to facilitate adhesion (D'Souza, Ginsberg, & Plow, 1991)) which is not present in the second half of the protein (Du et al., 1996). The fourth Kunitz domain, present in both the short and long isoform, has a methionine residue found in other Kunitz containing proteins specific for inhibition of chymotrypsin proteases (Du et al., 1996).

**1.5.4 *mec-9(ok2853)* deletion interrupts EGF like domains.** *mec-9* short isoform encodes a 502-amino acid protein. *ok2853* is a *mec-9* variation containing a 408-base pair deletion that encodes a 400-base pair, in-frame deletion which perturbs the second set of the EGF like domains found in both isoforms (predicted by APE software) (Barstead et al., 2012) (Figure 1.11 and 1.12). The deleted base pair sequence was blasted against the NCBI database, and gene ontology (GO) terms such as those found in proteins with binding capabilities such as EGF pentraxin, protocadherin and cadherin were represented. Some of the identified molecular GO terms include: ion, chromatin, receptor and cell binding. Further, GO biological terms include signaling, broad range tissue development (including cilia and neuron). GO cellular components include: plasma membrane, ECM, EV, and the lumen of Golgi and lysosomes. An NCBI SmartBLAST of the deleted protein sequence shows similarities to proteins that act in attachment (such as Sushi, von

Willebrand factor type A, EGF and Pentraxin domain-containing protein 1), adhesion and neurite growth (protocadherin and lactadherin), signaling (cadherin), cell migration (SLIT2 and crumbs2), receptors for ligands and enhancers and transcription factor activation. (Notch 1-3, weary, C-type lectin, EGF-like repeat and discoidin-like domain).

**1.5.5 *mec-9* long and short isoforms have differing expression patterns.** *mec-9* Long isoform expression and activity was fully characterized in hermaphrodites but not males (Du et al., 1996). The short isoform was not found to regulate mechanosensation and though expression pattern was examined, expressing neurons were not specifically itemized (Du1996). I examined long and short isoform expression patterns in males using transcriptional markers created by Knudra (Figures 1.12 and 1.13). It has been previously shown that the long isoform is expressed in touch neurons. I confirmed that expression pattern (data not shown) and see that male expression does not differ from hermaphrodite: no expression noted in male specific neurons. Fluorescence imaging showed characteristic neurons extending anteriorly and posteriorly from centrally located TRN cell bodies (Figure 1.13); however, short isoform expression was strikingly different (Figure 2.3) and will be discussed in Chapter 2.

**1.5.6 *MEC-9* short protein localization is not clearly discernable.** *unc-119*+::*mec-9sh*::*MEC-9*sh::GFP was injected into *unc-119* animals and non-Unc animals were recovered. The translational reporter is undetectable by fluorescent

scope in hermaphrodites, males, larva, and embryos at 20$^{o}$C (permissive temperature) and at 25$^{o}$C. There are subtle, low-penetrant, non-significant differences in animals that express the translational marker that are discussed in the future directions section of this paper (Section 4.2.5).

**Figure 1.1 ECM is necessary for cellular support and interaction** This generic cell is surrounded by fibrous, degrading, signaling, and carbon scaffolding matrix proteins. The cell has surface receptor and integrin proteins that facilitate ECM interaction and binding. Image reproduced from Wade 2012 (Wade & Burdick, 2012).

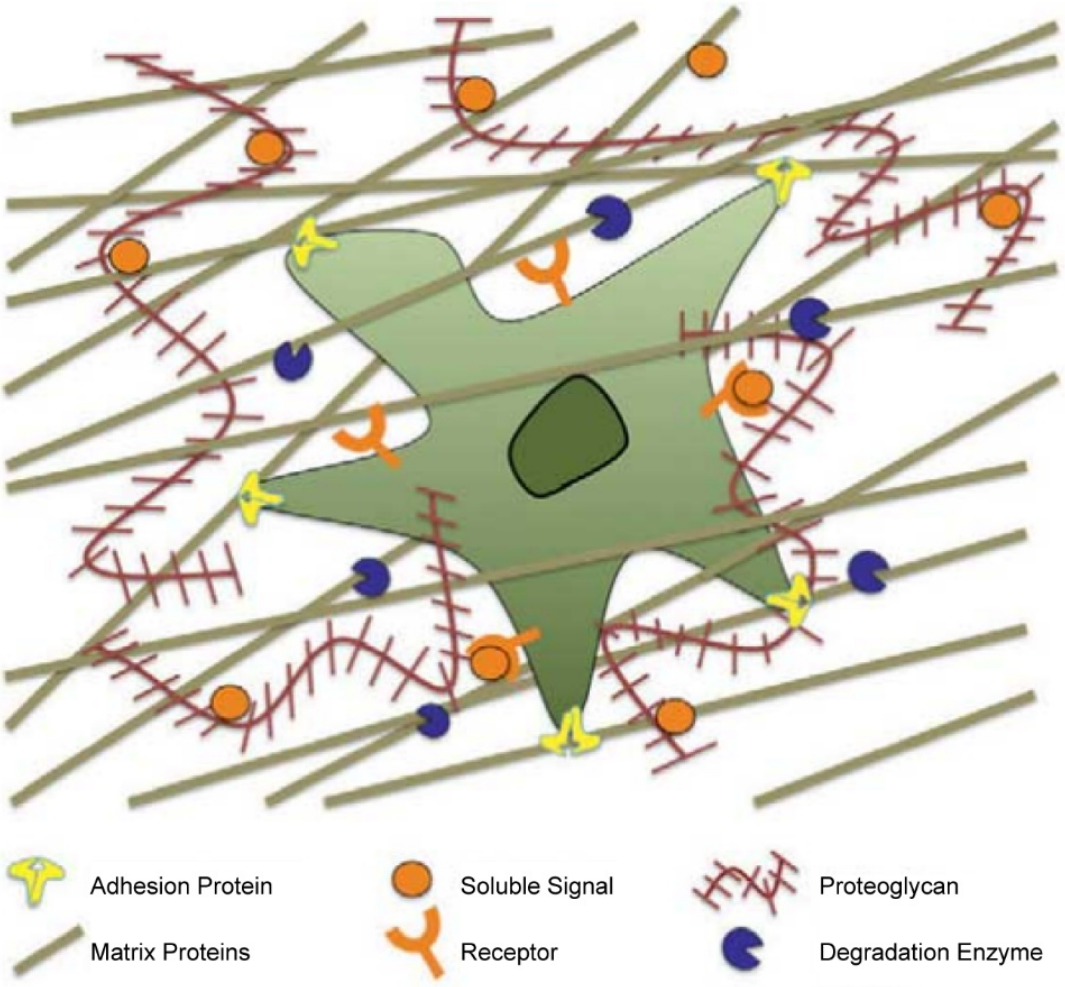

**Figure 1.2 Collagen and elastic fibers are an abundant ECM component.** A. Collagen fibers are made of bundled fibrils. The fibrils are composed of intertwined, triple-alpha helix, peptide chains that consist of glycine-proline-hydroxyproline repeats. Image reproduced from Protocolworld (The collagen molecule.). B. Elastic fibers are made up of elastin and fibrillin ECM proteins. Image reproduced from The Histology Guide (The histology Guide=Connective tissue.). C. Connective tissue contains specialized cells and collagen and elastic fibers. Image reproduced from API Owensboro CTC.(API histology.)

**Figure 1.2 Collagen and elastic fibers are an abundant ECM component.**

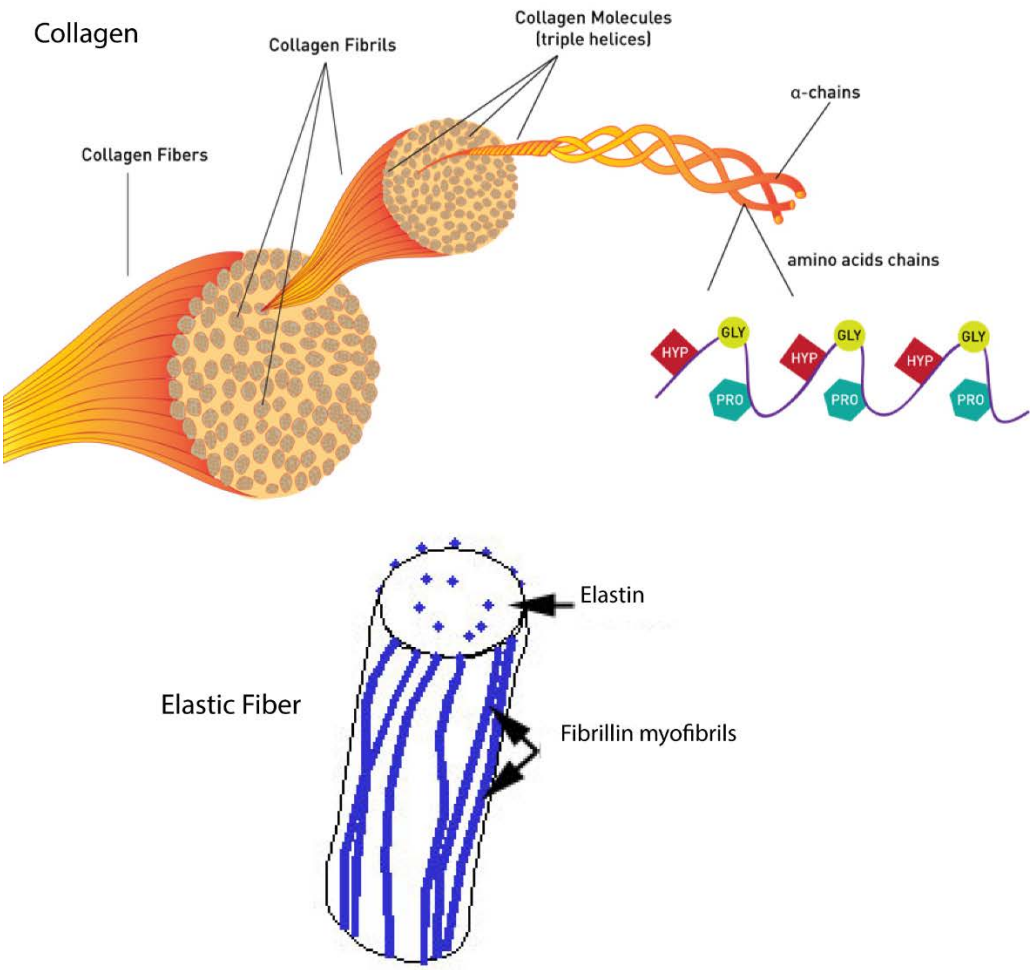

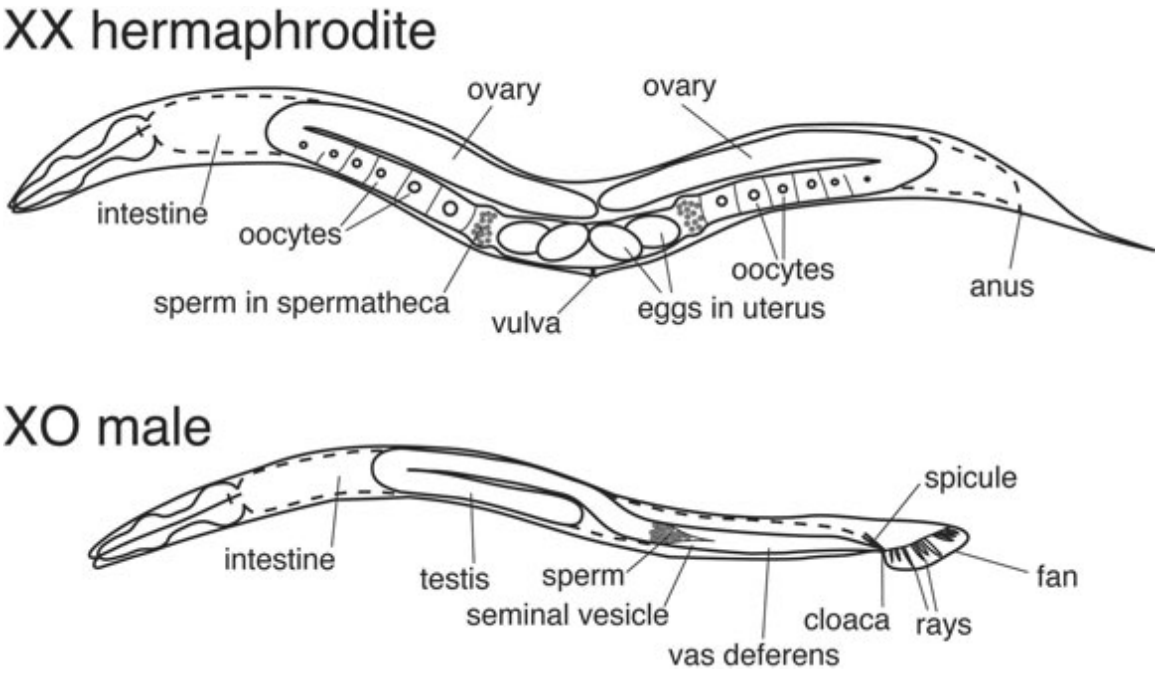


**Figure 1.3 Sexual dimorphism in *Caenorhabiditis elegans*** This figure shows hermaphrodite and male anatomy. Hermaphrodites have two sex chromosomes (XX). Males have one sex chromosome (XO). Hermaphrodites have a feminized body but house both male and female gametes. Males are sexually dimorphic; they have a specialized tail anatomy distinct from the hermaphrodite. Image reproduced from Wormbook Zarkower, D. Somatic sex determination (*WormBook*2005).

**Figure 1.4 *C. elegans* neurons of interest** *C. elegans* male on the left and hermaphrodite on the right. *C. elegans* neurons of interst shown in green. Amphids and inner labial type 2 (IL2) neurons are shared between the male and hermaphrodite nervous system, and male-specific, cephalic male (CEM) neurons are near the nerve ring at the head of the worm. Phasmids neurons, also common in males and hermaphrodites, are in the tail. The ALM, PLML/R, AVML/R and PVM are known as touch receptor neurons (TN) and span the length of the hermaphrodite and male worm. Ray neurons (RnB) are male-specific tail neurons.

**Figure 1.4 *C. elegans* neurons of interest**

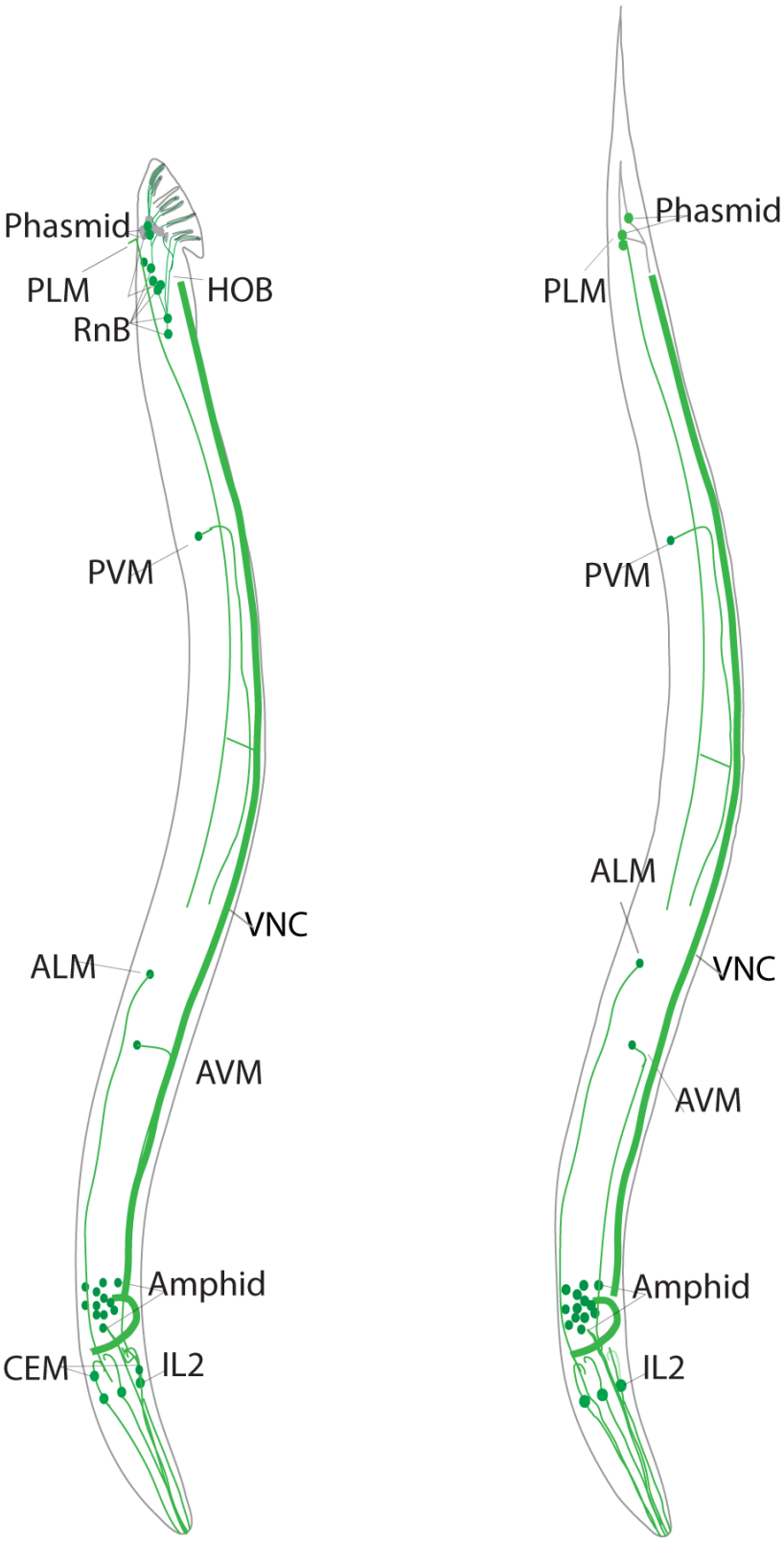

**Figure 1.5 Amphid sensillum, cephalic sensillum, and male tail ray neurons** A. This simplified schematic of the amphid sensillum depict the cilia encased in glia and exposed to the environment. Amphid nomenclature: single cilia denoted as A(amphid) S(single) X; double cilia as AD(X) with X substituted with the chronological alphabetic (A-L) assignation at the end. B. In the cephalic sensillum, CEM and CEP soma and glia are lateral to the pharynx. The CEM and CEP cilia are engulfed by the cephalic sheath and socket glia. The sheath creates a lumen around the ciliary base and ectosomes are stored there until their release from the CEM ciliary pore. Adapted and reproduced from Silva 2017 and Wang 2014 (M. Silva et al., 2017; Wang et al., 2014). C. Ray neuron cell bodies in the tail. Ray dendrites are in the fan of the tail.

**Figure 1.5 Amphid sensillum, cephalic sensillum, and male tail ray neurons**

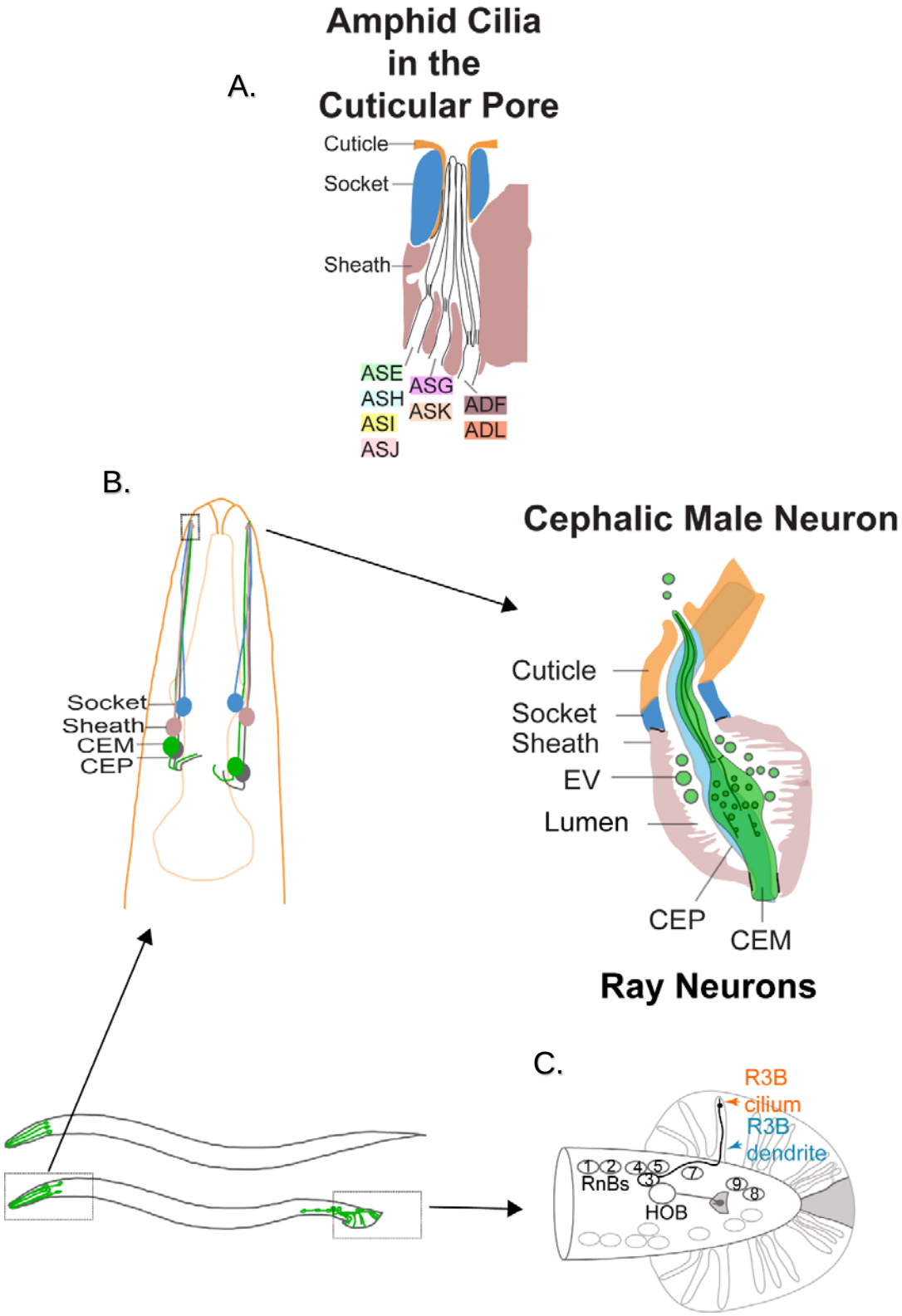

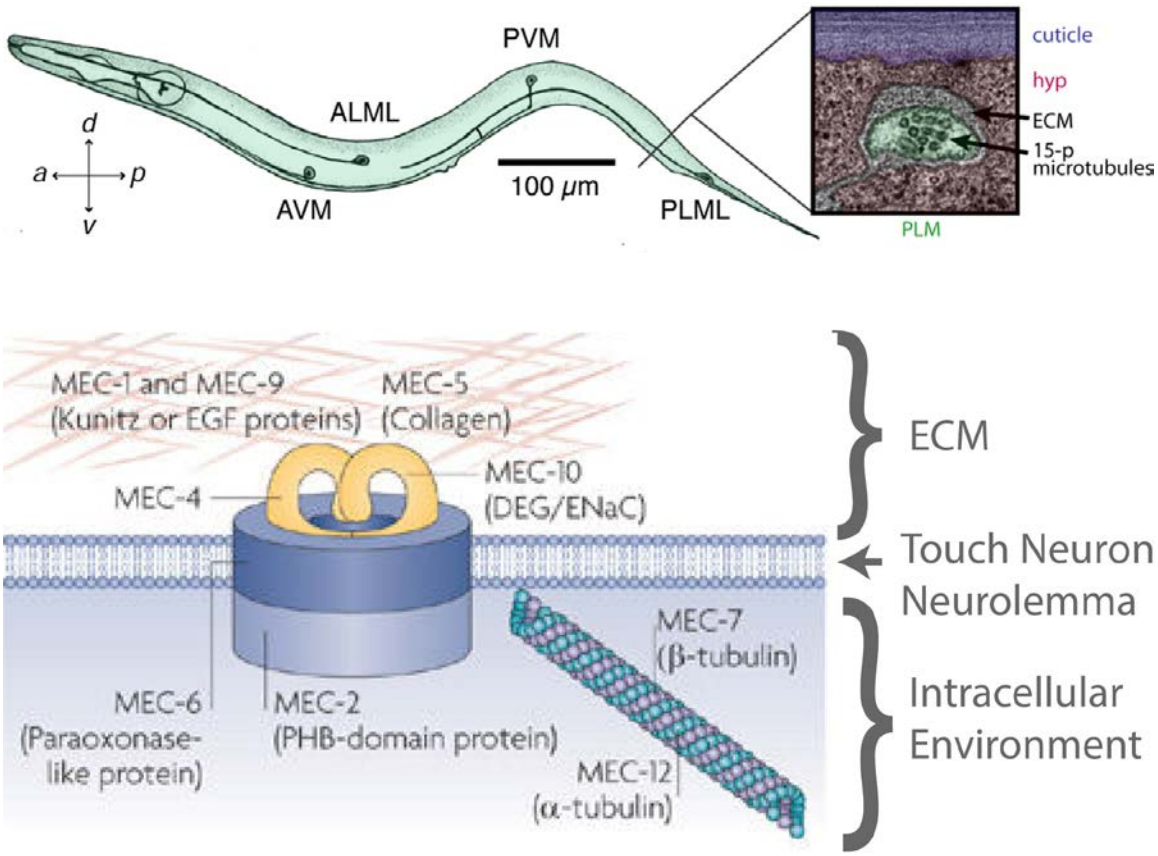


**Figure 1.6 Touch Receptor Neurons and DEG/ENaC proteins** Left and right ALM and PLM, AVM and PVM span the length of the worm and are necessary for touch sensitivity. Wormbook.org (M. Goodman, 2006). B. Proteins that comprise and facilitate mechanosensory DEG/ENaCs (Chalfie, 2009) MEC-4 and MEC-10 are ion channel proteins components. MEC-2 and MEC-2 are accessory proteins that enhance channel activity. MEC-7 and MEC-12 tubulins polymerize to form 15-protofilament microtubules in the touch neurons. MEC-1, MEC-5, and MEC-9 are found in the ECM surrounding the touch neurons.

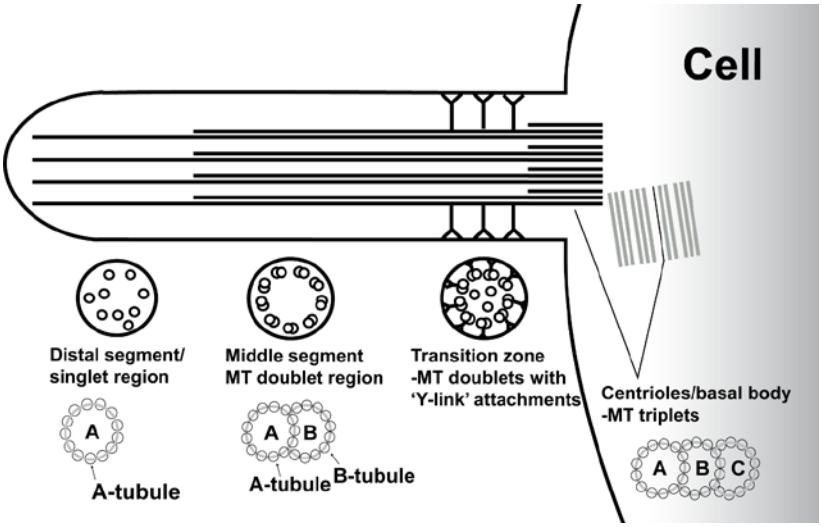


**Figure 1.7 Primary cilia protrude from cell membrane and contain microtubules** Sensory cilia are found on a subset of neurons in *C. elegans*. This schematic of the primary cilium axoneme demarcates three separate regions defined by the microtubular arrangement. Distal segment of the cilium has randomly arranged A-tubule singlets. Middle segment has concentric 9-0 A- and B-tubule doublet arrangement. Transition zone is the most proximal area and has concentric doublets that are attached to the ciliary membrane via "Y-links". The primary cilium emerges from the surface of the cell from the basal body consisting of microtubule triplets. Image by Malan Silva 2017 (Silva, 2017).

**Figure 1.8 Polycystic kidneys are enlarged and dysfunctional** A kidney is normally the size of a human fist but becomes enlarged due to multiple fluid filled sacs in PKD patients. The polycystic kidney undergoes loss of normal anatomy and function. Patients may incur end stage renal disease. Picture reproduced from Sciencedaily.com website. *Credit: Andrew P. Evan, Ph.D., Department of Anatomy and Cell Biology, Indiana University School of Medicine* (Web News Wire 2010).

**Figure 1.9 Human and *C. elegans* polycystins** Human polycystin 1 (PC1) and polycystin 2 (PC2) are shown on top. PC1 is an eleven-transmembrane protein with a large extracellular N-terminus consisting of PKD domains, GPS, REJ, LDL, C-type lectin, WSC, and leucine rich repeats. PC2 is a six-transmembrane protein that may join to PKD1 at their coiled-coiled domains. *C. elegans* polycystins are shown on bottom. *C. elegans* polycystins homologs, LOV-1(PKD1) and PKD-2, are similar in their transmembrane domain structure. LOV-1 has a large extracellular N-terminus, GPS, and Serine threonine rich mucin domains. Scale bar is 200 amino acids. Boxed areas indicate regions homologous to TRPP ion channel proteins. (Abbreviations: LRR: Leucine-Rich Repeat; WSC: cell wall integrity and stress response component; PKD: polycystic kidney disease domain; GPS: GPCR proteolytic site; TM: transmembrane; PLAT: polycystin/lipoxygenase/α-toxin; ST rich: serine-threonine rich.) Image and information reproduced from (R. O'Hagan, Wang, & Barr, 2014).

**Figure 1.9 Human and *C. elegans* polycystins**

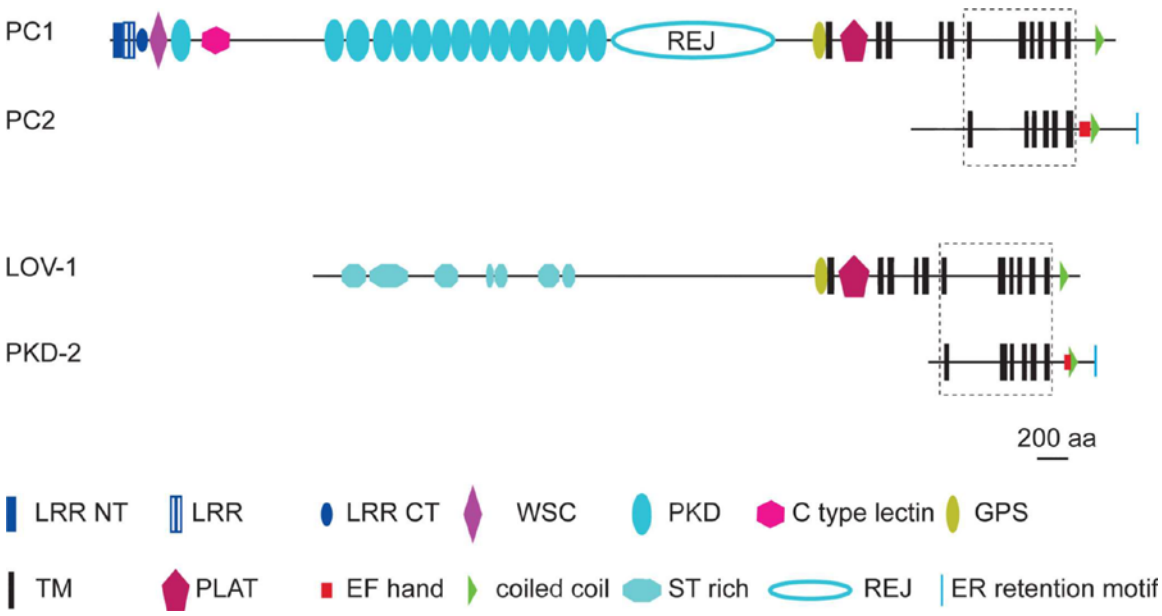

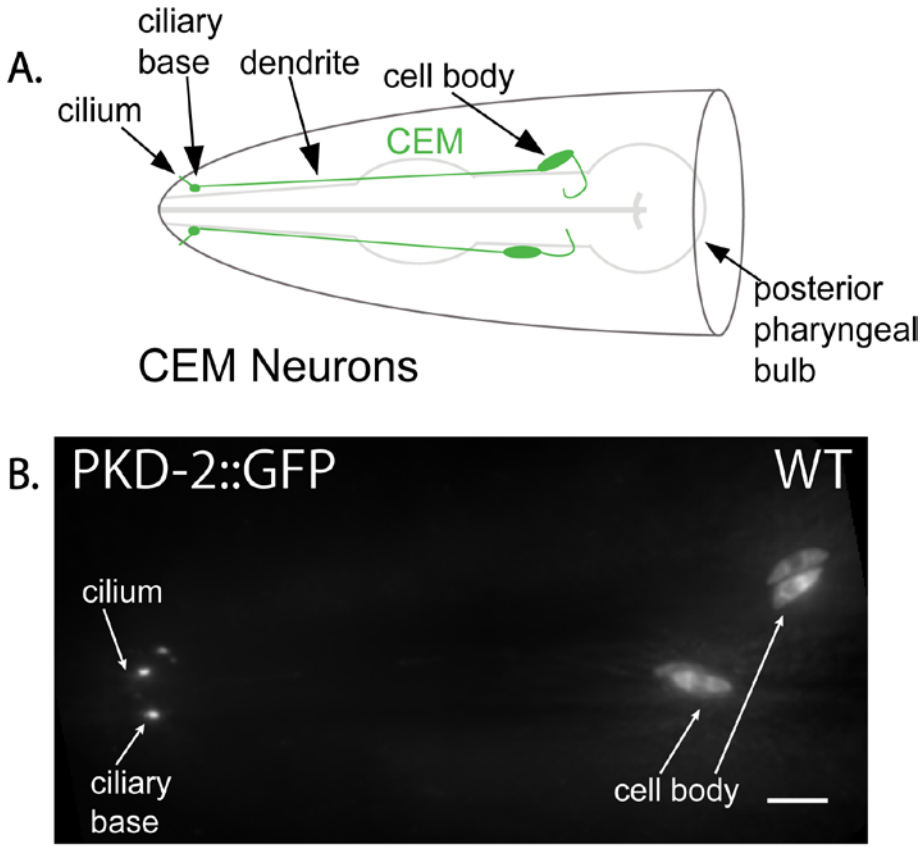


**Figure 1.10 PKD-2::GFP localization in *C. elegans*** Polycystins localize to the soma and cilia (cilia proper and ciliary base) of male specific CEM neurons. Scale bar for all head tail images are 10 microns unless otherwise stated.

**Figure 1.11 *mec-9* ECM gene schematics** The three ECM proteins have an N-terminal signal peptide indicative of secreted proteins. MEC-5 has two Gly-X-Y domains, characteristic of collagens (Du et al., 1996). MEC-1 and MEC-9 have differing arrangements of Kunitz and EGF like domains (Du et al., 1996; Emtage et al., 2004). *mec-1* encodes many isoforms (not shown). *mec-9* encodes a long and short isoform. The *mec-9* short isoform is predicted to use the 9$^{th}$ intron of *mec-9* long as promoter. Black triangles denote alleles with point mutations used in this study. Brackets are deletion mutants. Created by Exon-Intron Graphic marker (Bhatta, ).

**Figure 1.11 *mec-9* ECM gene schematics**

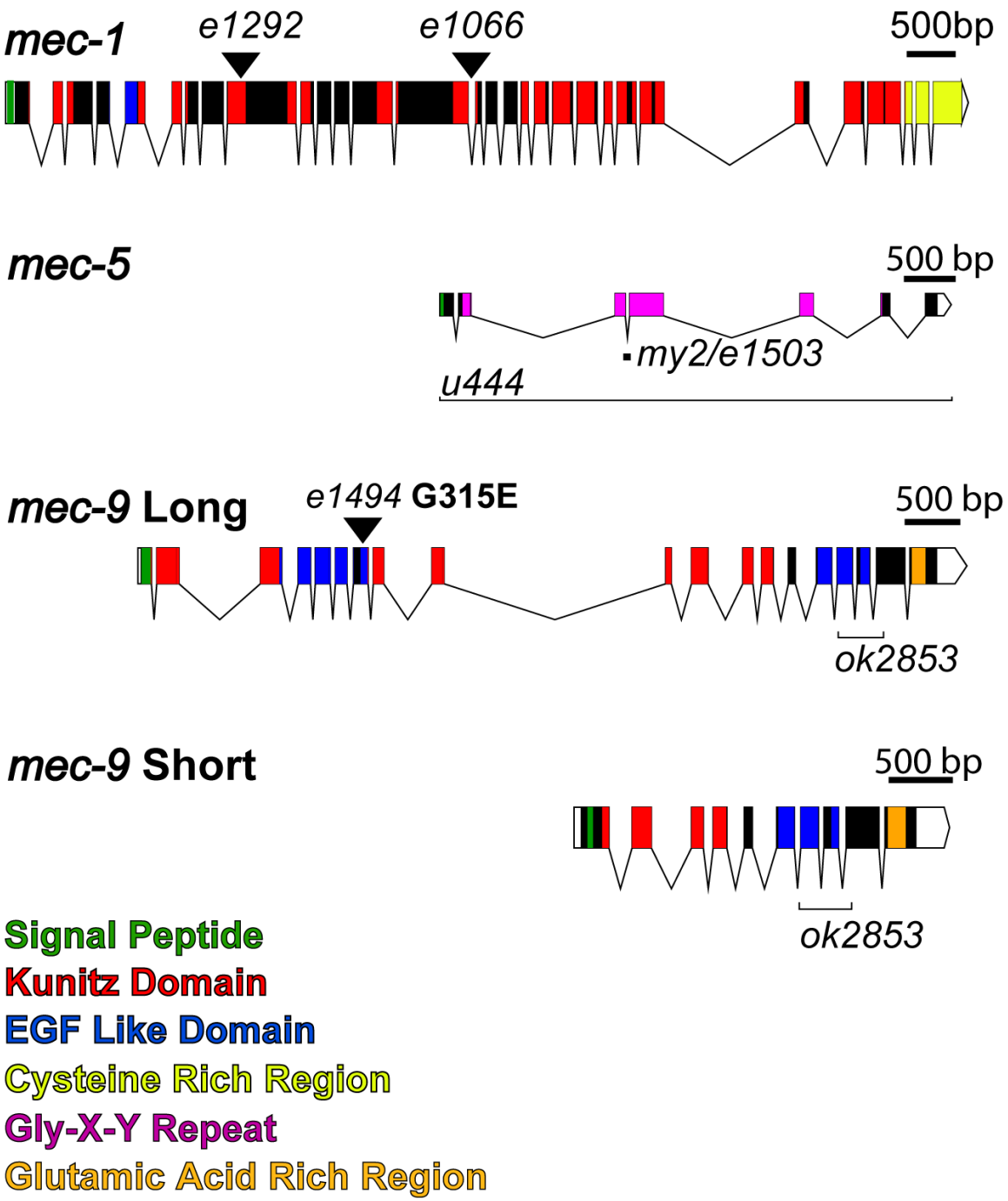

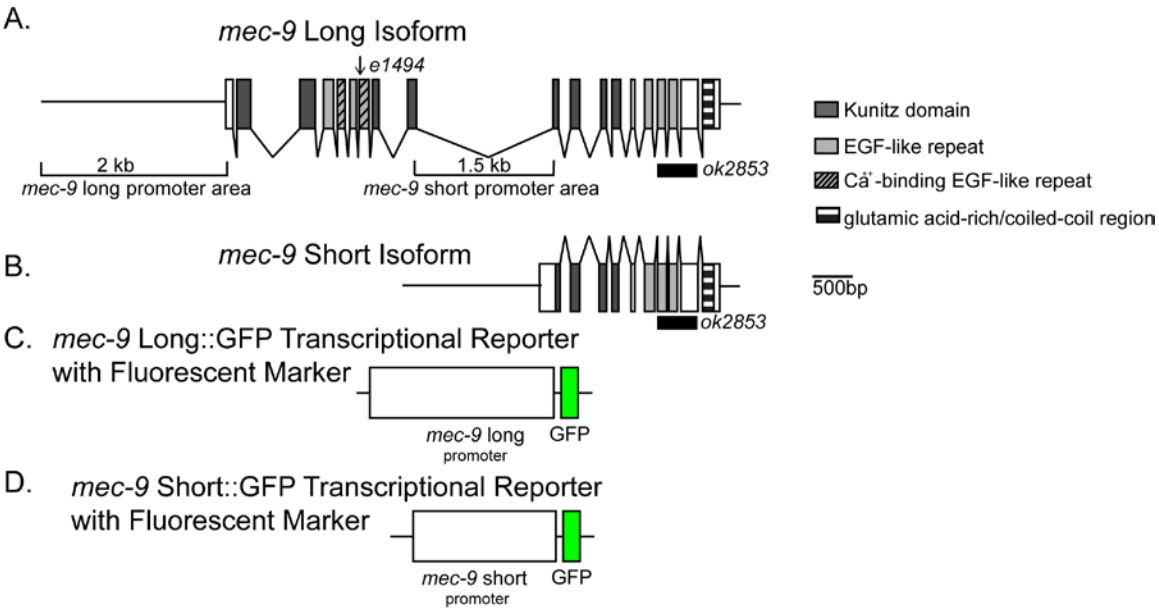


**Figure 1.12 *mec-9* Long and short isoforms and transcriptional reporters** A. *mec-9* long isoform schematic identifying *e1494* point mutation and *ok2853* deletion and the various domains. B. *mec-9* short isoform is the 3' end of *mec*-9 long. Transcriptional markers were constructed by Knudra for long and short isoform promoter areas. C. The *mec-9* long isoform reporter construct consists of 2kb upstream promoter sequence with a C terminal green fluorescent protein tag. D. The *mec-9* short isoform transcriptional reporter is constructed using ~1500 bases of the long 9$^{th}$ intron of the full *mec-9* gene with a C terminal green fluorescent protein tag. Scale bar is 500 base pairs (bp).

**Figure 1.13 *mec-9*Lp::GFP has expected touch receptor neuron expression pattern** (*mec-9* long promoter only) expression in males shows expected touch neuron expression. No expression of transcriptional marker was observed in male-specific neurons of the head (top image) or tail (bottom image). Tail shown to view ventral aspect of worm. Note autofluorescence of fan, spicule, and hook in male tail (bottom image).

**Figure 1.13 *mec-9*Lp::GFP has expected touch receptor neuron expression pattern**

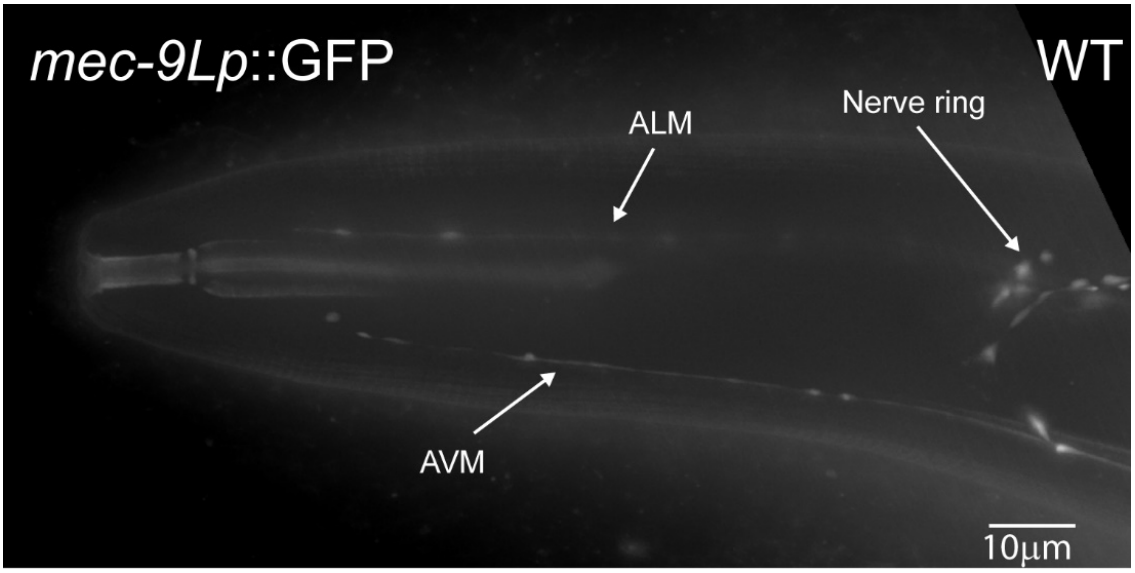


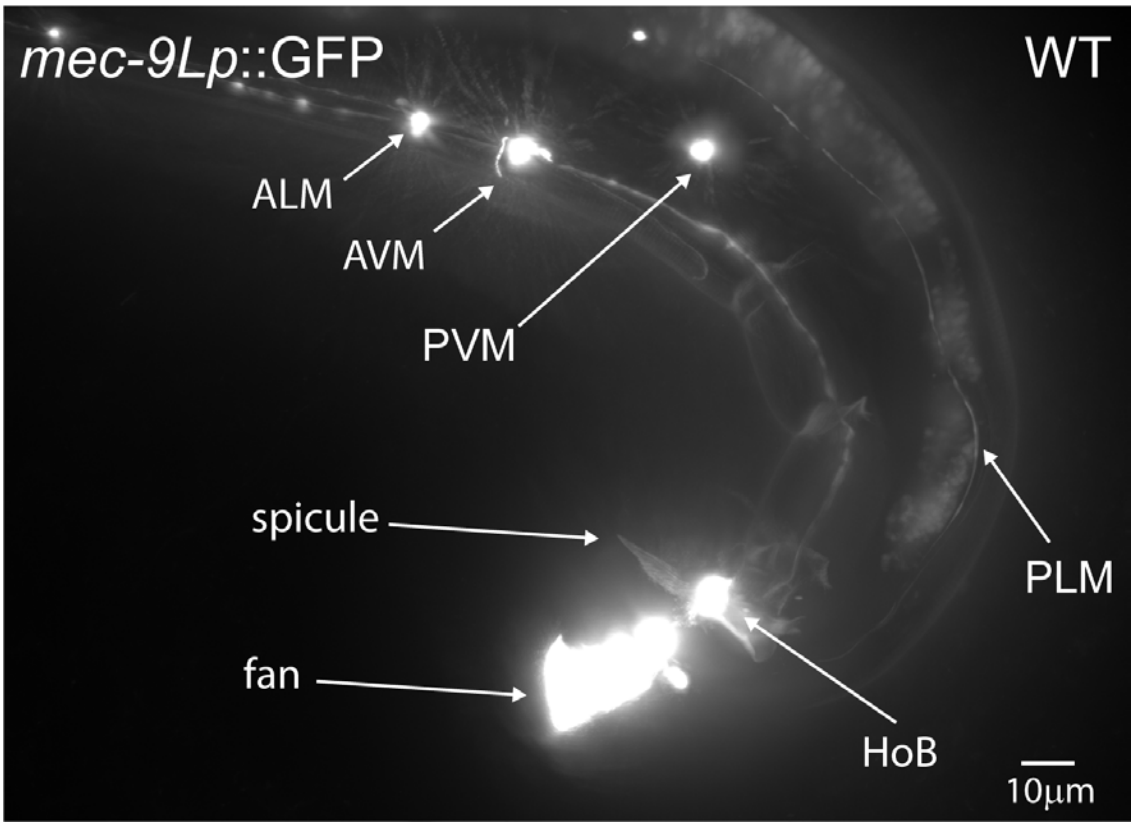

# CHAPTER 2: ECM REGULATES MORPHOGENESIS AND FUNCTION OF CILIATED SENSORY ORGANS

## 2.1 INTRODUCTION

Extracellular matrix (ECM) is made up of a network of interacting proteins such as collagens, laminins, fibrillin, and elastin that surround and support cells for attachment, mechanosensation, and signaling. Studies show these ECM components are necessary for tissue morphogenesis and homeostasis throughout the lifespan of an organism because matrix can interact with and regulate body systems, organs, and tissues such as the integument (layers, anchoring proteins, hemidesmosomes, basement membranes), connective tissues (bone, cartilage), internal organs (liver, kidney, placenta), etc. (Bruckner-Tuderman & Bruckner, 1998) The scope of ECM's interaction and variety of interactors is extensive and alterations in ECM quality and quantity contribute to diseases and disorders of various organs and systems.

*Caenorhabditis elegans* (*C. elegans)* is an excellent model for ECM research. Southern blots (detection of DNA) and screening have been done using *C. elegans* and anywhere from 40-150 unique collagen genes have been identified and classified (Cox et al., 1984) mutations in collagens *emb-9* and *let-2* can cause embryonic lethality (Gupta et al., 1997). *MEC-1*, *MEC-5*, and *MEC-9* are *C. elegans* extracellular matrix proteins, one of which is collagen, that surround the touch receptor neurons and are essential for mechanosensation, touch neuron attachment to the hypodermis, and make up the "mantle" around the touch

neurons (Chen et al., 2013; Du et al., 1996; Gu et al., 1996). Particularly, the EGF domains in MEC-9 are predicted by NCBI SmartBLAST Protein software to have similar structure and maybe similar activity as CELSR3, a cadherin EGF LAG seven-pass G-type receptor 3 transmembrane protein that expresses in glia. CELSR3 has a long N-terminus that extends into the ECM and regulates ciliogenesis, neuronal migration, and formation of neural networks of the central and peripheral nervous system in mice and drosophila (Goffinet & Tissir, 2017). Interestingly, and likely due to the inherent, infrequent occurrence of males in the *C. elegans* population, male expression pattern is not discussed in the literature about any of the three proteins. In this work, I will explore and expand the analysis of the expression, function, and activities of *C. elegans mec-1, mec-5*, *mec-9*.

Primary cilia are microscopic, antenna-like structures that emerge from the surface of many eukaryotic cells and are found at the distal dendrite in a subset of *C. elegans* neurons (M. Silva et al., 2017). These non-motile organelles protrude toward ECM to interact with the external environment of the cell and organism and act as signaling organelles necessary for tissue formation, growth, and activity (Satir et al., 2010). The ECM protein, artichoke, has been implicated in cilia formation and functionality in *Drosophila* (Marta Andrés et al., 2014b). Primary cilia defects lead to disorders referred to as ciliopathies, which cause disease in various body systems such as renal and hepatic cysts, respiratory disorders, polydactyly and skeletal disorders (Davis et al., 2011). More recently, ciliogenesis defects have been noted in mouse models and human patients with Huntington's

Disease and Alzheimer's disease (Armato et al., 2012; Keryer et al., 2011). Abnormal ECM is observed in ciliopathies such as Bardet-Biedl Syndrome, nephronophthisis, and ADPKD (B. Liu et al., 2012; Xie et al., 2011). ECM proteins have been shown to selectively limit protein access to the primary cilia; therefore, further research ECM research in the area of ciliopathies will broaden understanding and ultimately treatment of ciliopathies (Garcia-Gonzalo & Reiter, 2012).

ADPKD is a genetic disorder characterized by the presence of fluid filled cysts which form on and in the kidney's epithelial cell lined renal tubules that can replace normally functioning renal tissue and result in enlarged, polycystic kidneys and end stage renal failure. ADPKD affects 1 in ~500 persons regardless of race or gender and can be caused by a mutation in either of the polycystin encoding genes, PKD1 or PKD2 (Takiar & Caplan, 2011)(Yook et al., 2012) (Sutters & Germino, 2003). Further, it has been shown that dorsal axis curvature, hydrocephalus, and pronephronic cyst formation was observed in zebra fish when polycystin combinations were knocked down, suggesting a role for polycystins as sensors of notochord cell differentiation that affect ECM formation, secretion, and integrity that can be a primary factor in ADPKD (Mangos et al., 2010).

Polycystins are evolutionarily conserved (Hofherr & Kottgen, 2011). A large segment of N-terminal PKD1 extends into the extracellular matrix and contains many domains which could act in protein binding and recognition, Ran GTPase,

and cell adhesion (Kobe & Kajava, 2001). PKD2 has an often-mutated extracellular domain that is necessary for polycystin channel assembly, stimulation, and gating (Shen et al., 2016). These two polycystins can be cleaved and have been found to act individually and synergistically in body cells performing myriad functions including acting as ion channels and even in regulation of ECM components (Hanaoka et al., 2000; Mangos et al., 2010). Polycystins localize to cilia in mammalian cells and the *C. elegans* homologs, LOV-1 and PKD-2, localize to the primary cilia of male specific sensory neurons to regulate male mating behavior (Barr & Sternberg, 1999). We used *C. elegans* as a model to study PKD and identify new genes required for polycystin ciliary localization and function. I identified an allele of *mec-5* from a forward genetic screen to identify genes involved in ciliary trafficking of PKD-2::GFP (Bae et al., 2008). Further investigation revealed its cohorts, *mec-1* and *mec-9* also regulate PKD-2::GFP localization. Here I show ECMs can regulate polycystin localization and activity. Our PKD-2 localization and ECM studies will add to the repository of primary cilium and ADPKD knowledge.

Extracellular vesicles (EV) are submicroscopic, lipid-membrane bound particles that contain myriad components such as nucleic acids and proteins and may now be considered a component of the ECM (Rilla & et.al, 2017). Evidence of their release is conserved across many species (Iraci et al., 2016) and they carry many ECM proteins such as fibronectin and laminin, which provide communication necessary for altering ECM composition, signaling between ECM and the cells it

surrounds, tumor proliferation, and inflammation (Rilla & et.al, 2017). In *C. elegans*, ciliary proteins such as polycystins are EV cargo and affect male mating behaviors (Wang et al., 2014). miR-34a, a microRNA that regulates the BCL-2 ”cancer gene” has been found in drug resistant prostate cancer cells and in the EVs released from them, which suggests EVs can be used as a read out of the cells from which they originate (Corcoran et al., 2014). The work presented in this study will add to the breadth of knowledge in this emerging field of EV study.

Here we used *C. elegans* as a model of autosomal dominant polycystic kidney disease (ADPKD) to identify *mec-1*, *mec-5* and *mec-9* as new genes required for polycystin protein localization to the primary cilia and discovered that proteins in the extracellular matrix (outside of the cell) regulate the movement and activity of proteins inside the cell. When these extracellular proteins are mutated, it also disrupts cell structure, animal behavior, and alters pathways that facilitate community interaction. Here I show that the extracellular matrix proteins MEC-1, MEC-5 and MEC-9, already known to localize and regulate function at non-ciliated touch receptor neurons, have broader sites of action and activity. *mec-1*, *mec-5* and *mec-9* also regulate anatomy, placement, and physiology of male specific and amphid organs in *C. elegans*. These studies are an illustration of how scientists can improve on the current body of knowledge and work together to understand disease and discover treatments.

**2.2 RESULTS:**

### 2.2.1 *mec-1*, *mec-5* and *mec-9* regulate PKD-2::GFP localization.

The *C. elegans* polycystins LOV-1 and PKD-2 localize to cilia and cell bodies of cephalic male-specific (CEM), left and right B-type ray neurons in the tail (RnB; n=neuron 1-9, but not 6), and Hook B (HOB) neurons. (Figure 2.1 A-B, Figures 3.20-3.23 and 2.10 A-B) These male specific neurons are necessary for male mating behaviors (Barr & Sternberg, 1999; Barr et al., 2001). We previously performed a forward genetic screen for genes necessary in PKD-2::GFP localization and identified mutants defective in PKD-2 ciliary receptor localization (the Cil phenotype). *cil-2(my2)* displays abnormally high PKD-2::GFP levels in the CEM cilia and ciliary base and also has abnormal extracellular, extradendritic PKD-2::GFP accumulation along CEM dendrites (Bae et al., 2008). *cil-2(my2)* hermaphrodites also display a temperature sensitive sterility phenotype. The extradendritic PKD-2::GFP accumulation and sterility phenotypes are unique to the *cil-2(my2)* mutant and not the other ten mutants identified in the screen. To clone the gene mutated in the *cil-2(my2)* animals, we used genetic mapping, whole genome sequencing, complementation testing, and rescue experiments of the Cil phenotype to identify *mec-5* (Further discussed in Chapter 3.1).

Expression of the wild-type (WT) *mec-5* genomic region using either the *mec-5* promoter or muscle-specific *myo-3* promoter rescued *cil-2(my2)* defects (Chapter 3.1.5), confirming that *mec-5* was mutated in the *cil-2(my2)* mutant and that *mec-5* acted non-cell autonomously to regulate PKD-2::GFP ciliary localization in male-specific neurons. *mec-5* encodes a collagen protein that is

produced and secreted by hypodermal cells to anchor the degenerin complex in touch receptor neurons to the ECM (WormBase.; Du et al., 1996; Emtage et al., 2004). In these non-ciliated neurons, *mec-5* and the ECM encoding genes *mec-1* and *mec-9* act in concert (Du et al., 1996). We therefore determined whether this MEC-1, MEC-5, and MEC-9 ECM also regulated PKD-2::GFP ciliary localization.

We characterized PKD-2::GFP ciliary localization in two mutant alleles of *mec-1 (e1066* and *e1292), mec-5* (*e1503* and *my2),* and *mec-9* (*e1494* and *ok2853)*. First, we visualized ciliary localization in CEM neurons of WT and mutant males via blind examination. An animal was scored as Cil if CEM cilia, ciliary base, and dendrites in male worms had abnormally increased or mislocalized PKD-2::GFP. Values were reported as percent of animals that are Cil (Figure 2.1 I). In WT, we saw occasional Cil animals (~16% of males). In contrast, *mec-5* males exhibited the most penetrant Cil phenotype: over 60% of *mec-5((my2)* animals and over 70% of *mec-5(e1503)* were Cil (p values < 0.0001). Also, *mec-9(ok2853)* animals had a significantly increased number of Cil males (p=0.008), but *mec-9(e1494)* males were statistically indistinguishable from WT. *mec-1(e1066)* males were also Cil (p= 0.0003), but *mec-1(e1292)* males were similar to WT.

In *mec-1(e1066), mec-5(e1503), mec-5(my2),* and *mec-9(ok2853)* males, we observed abnormally increased PKD-2 localization at CEM cilia, ciliary bases, and occasionally dendrites. (Figures 2.1 C, E, F, and H) The extradendritic accumulation in *mec-1(e1066)*, *mec-5(e1503)* and *mec-9(ok2853)* was

reminiscent of that observed in *mec-5(my2)*. The Cil defect was not observed in *mec-1(e1292)* and was only occasionally seen in *mec-9(e1494)* (Figures 2.1 D and G).

Cil defects were seen in mutants with premature stops and deletions, making it difficult to determine which protein domains were necessary for PKD-2::GFP localization. *mec-1* encodes multiple ECM protein isoforms with multiple disulfide-linked EGF and Kunitz-type protease inhibitor domains (WormBase.; Emtage et al., 2004). The *mec-1* alleles cause gene truncations: *e1292* results in truncation after Kunitz Domain 3 whereas *e1066* truncates after Kunitz Domain 6 (Emtage et al., 2004), both of which remove Kunitz domains but might leave EGF domains intact. *mec-9* encodes two protein isoforms of an ECM protein containing multiple EGF domains, multiple Kunitz domains, and a glutamic acid-rich region (WormBase.; Du et al., 1996). *mec-9* mutations perturb EGF domains: *e1494* is a point mutation in the first set of EGF domains and affects only the *mec-9* long (*mec-9L*) isoform. *ok2853* perturbs the second set of EGF domains via deletions and affects both short and long isoforms (Du et al., 1996). Using whole genome sequencing, we found that both *mec-5* mutants had lesions in the third intron (Chapter 3.1.3 and Figure 3.4). We conclude that some but not all alleles of *mec-1*, *mec-5,* and *mec-9* perturbed PKD-2::GFP localization.

We observed that cilia and ciliary bases appeared brighter in some but not all ECM mutants. We measured highest/maximum fluorescence intensity (FI) of

PKD-2::GFP in CEM neuron cell bodies and cilia (including both cilium and ciliary base) to quantify PKD-2::GFP abundance. FI is a computed measurement of the pixels illuminated in a selected region of interest. *mec-9* mutants had a brighter maximum FI (~1.75x) than WT (Figure 2.1 B and Table 2.1): *mec-9(e1494)* p=0.011 and *mec-9(ok2853)* p<0.0001 (Figure 2.1 J). Our data shows that although *mec-1, mec-5,* and *mec-9* were all necessary for PKD-2 ciliary localization, *mec-9* was also necessary for PKD-2::GFP ciliary abundance.

To test for specificity of ECM components, we examined PKD-2::GFP localization in a hemicentin mutant. Hemicentin is an ECM component required for adhesion between tissues including touch neuron attachment to the epidermis and gonad (B.E. Vogel & E.M. Hedgecock, 2001). Analysis of the hemicentin mutant *him-4(e1267)* revealed no differences in PKD-2::GFP ciliary localization or FI. We conclude that the *mec-9, mec-1,* and *mec-5* ECM genes; but not the *him-4* ECM gene, were necessary for polycystin localization and abundance.

We generated a monoclonal anti-PKD-2 antibody to visualize and measure endogenous PKD-2 localization in WT and ECM gene mutant males and observed similar Cil defects (Figures 3.20 - 3.23). In WT, endogenous PKD-2 was limited to the cell bodies and cilia of CEM head neurons and ray RnB and hook HOB tail neurons. In *mec-9(ok2853)* males, endogenous PKD-2 mislocalized to dendrites and had increased abundance in cilia and cell bodies as shown in FI measurements (Figure 3.23). Endogenous PKD-2 localization was also abnormal

in the ray cilia in *mec-1(e1066)* and *mec-5(e1503)* male tail but not as severely as *mec-9(ok2853)*. We conclude that all three ECM genes regulate the PKD-2 localization pathway with *mec-9* mutants display the most severe Cil defects.

The partner of Polycystin 2 (PKD-2) is Polycystin 1 (LOV-1). We therefore, examined LOV-1 localization in ECM gene mutants. In WT, LOV-1::GFP localizes to the CEM, RnB, and HOB cell bodies and cilia (Barr & Sternberg, 1999). In *mec-9(ok853)* mutants, we observed distal dendritic LOV-1::GFP mislocalization and increased ciliary fluorescence (Figure 2.11). We also observed significantly increased LOV-1::GFP FI in CEMs and RnBs of *mec-5(e1503)* males (data not shown). We conclude that ECM encoding genes *mec-1*, *mec-5*, and *mec-9* regulate polycystin localization in male-specific ciliated sensory neurons.

**2.2.2 *mec-1*, *mec-5* and *mec-9* regulate male mating behaviors.** *pkd-2*, *lov-1*, and the male-specific polycystin expressing neurons are required for the male mating behaviors of mate searching, response to hermaphrodite contact, and location of hermaphrodite vulva (R. O'Hagan et al., 2014). We therefore determined whether the three ECM genes were required for these male sensory behaviors.

*C. elegans* males will leave a food source in search of a mate if no hermaphrodite is present (Barrios et al., 2008). *lov-1* and *pkd-2* mutant males do not leave food to search for a mate. Similarly, *mec-5(e1503)* males were leaving defective (Figure 2A). In contrast, *mec-9(ok2853)* mutants left food more readily

than WT animals (Figure 2.2 A). Hyper-leaving behavior is associated with defects in male-specific and the shared inner labial type 2 IL2 ciliated neurons (Maguire, 2015), suggesting that the *mec-9* mutation may affect other neurons in addition to the polycystin-expressing cells.

When male ray neurons detect contact with a hermaphrodite, males initiate the response behavior by stopping forward locomotion, and initiating backing (Barr & Garcia, 2006). *lov-1* and *pkd-2* mutant males are response defective. *mec-9(ok2853)* and *mec-1(e1066)* mutants had a statistically significant defect in response to hermaphrodite contact, while *mec-5* mutant males displayed normal response behavior (Figure 2.2 B) (Bae et al., 2008). After response, the male scans the hermaphrodite's body for her vulva. *lov-1* and *pkd-2* mutants are location of vulva defective (Lov). Only *mec-9(ok2853)* males displayed the Lov phenotype (Figure 2.2 C).

We previously showed that mate searching, response, and location of vulva do not require MEC-4 and MEC-10, the touch neuron specific degenerin epithelial sodium channel (DEG/ENaC) receptors (Barr & Sternberg, 1999; Barrios et al., 2008). However, *mec-1*, *mec-5*, and *mec-9* ECM genes are required for these male-specific sensory behaviors. We conclude that *mec-1*, *mec-5* and *mec-9* ECMs genes perform activity beyond DEG/ENaC localization and function in touch receptor neurons and are required more broadly for the function of other sensory neurons. Moreover, only *mec-9* was required for all examined male-specific

behaviors suggesting a distinct role in polycystin-expressing male specific neurons.

**2.2.3 *mec-9* long and short isoforms have distinct expression patterns: MEC-9S is expressed in ciliated sensory neurons.** *mec-9* encodes two predicted proteins. The *mec-9* long isoform encodes an 839-amino acid protein with five Kunitz protease inhibitor domains, 7 EGF domains, and a glutamic acid rich/coiled-coiled region (Figure 2.3 A) (Du et al., 1996). The *mec-9* short isoform encodes a 502-amino acid protein with two Kunitz domains, three EGF domains, and a glutamic acid rich/coiled-coiled region (Du et al., 1996) (Figure 2.3 B). Both long and short isoforms encode an N-terminal signal sequence consistent with secreted ECM proteins (Zhang & Shen, 2016). *mec-9*(*ok2853)* is a 408-base pair in-frame deletion that is predicted to remove two of the three EGF like domains in both isoforms (Barstead et al., 2012) (Figure 2.3 A).

Chalfie and colleagues showed *mec-9* long isoform expression in touch receptor neurons and *mec-9* short isoform expression in other neurons in the hermaphrodite nerve ring and ventral cord (Du et al., 1996). We examined long and short isoform expression patterns in males using transcriptional reporters (Figure 2.3 C and D). We find that *mec-9Lp::GFP* (long isoform transcriptional reporter) was expressed only in the shared touch receptor neurons (found in both males and hermaphrodites) and not male-specific neurons (Figure 1.14). However, *mec-9Sp*::GFP (short isoform transcriptional reporter) was expressed in

polycystin-expressing CEM, RnB, and HOB male-specific as well as shared ciliated sensory neurons found in both males and hermaphrodites (Figures 2.3 D-I).

*mec-9Sp*::GFP was expressed in the amphid neurons in the head and phasmid in the tail that take up the lipophilic fluorescent dye DiI (Figures 2.3 H'' and I''). *mec-9Sp*::GFP was coexpressed with the kinesin-3 gene *klp-6* transcriptional reporter in the shared IL2 neurons and male-specific CEM neurons in the head and RnB and HOB neurons in the tail (Figure 2.3 F-G). These 27 *klp-6* expressing neurons are called extracellular vesicle releasing neurons (EVNs) based on their ability to shed and release ciliary EVs (Wang et al., 2015).

**2.2.4 *mec-9* regulates extracellular vesicle biogenesis and release.** EVs are shed and released from male specific IL2, CEM, and RnB neurons (Wang et al., 2014) all of which expressed *mec-9Sp*::GFP. To determine if *mec-9* regulates EV biogenesis, we counted PKD-2::GFP containing EVs that were shed and released into the media from the male head and tail. WT adult males released an average of 26 PKD-2::GFP carrying EVs from the CEM neurons compared to 78 EVs in *mec-9* mutants ($p=0.0008$): a threefold increase (Figure 2.4 C). The EV hypersecretion phenotype of *mec-9* mutants contrasts other previously described EV hyposecretion mutants that are deficient in EV release (Maguire, 2015; R. e. a. O'Hagan, 2017; M. Silva et al., 2017; Wang et al., 2014).

Next, we used transmission electron microscopy (TEM) to more closely examine the ultrastructure of the male cephalic organs containing EVs in ECM and lumenal spaces (Wang et al., 2014). In WT, EVs are shed from the ciliary base of the CEM neuron and occupy a lumenal space formed by the glial support cells (Figure 2.4 E). In *mec-9* mutants, we observed three striking defects. First, in the *mec-9* cephalic lumen we observed an immense accumulation of EVs that ranged in diameter from 45nm to 226nm (Figure 2.4 F). Second, we saw an increase in the volume of the glial lumen occupied by the EVs. The 2D area of the *mec-9* mutant lumen was massively extended, perhaps due to EV hypersecretion and increased EV storage (Figure 2.4 F). Eight WT and 12 *mec-9* cephalic sensilla were compared and revealed increased occurrences and larger diameters of lumenal spaces surrounding cilia and distal dendrites. The enlarged EV containing lumen is a phenotype observed in mutants that shed but do not environmentally release EV (R. e. a. O'Hagan, 2017; M. Silva et al., 2017; Wang et al., 2014).

Finally, *mec-9* cephalic sensilla were filled remarkable light and dark matrix filled vesicles, themselves also containing EVs. For example, the lightly shaded vesicle shown here was 506 nm in diameter and contained smaller vesicles ranging in diameter from 40-90 nm (Figure 2.4 F). Dark matrix vesicles found at the level of the distal CEM dendrite were 898 and 1056 nm in diameter and contained vesicles that ranged from 51-171 nm (Figure 2.4 G). For both abnormal EV and matrix-filled vesicle phenotypes in *mec-9,* we observed vesicles in the lumenal spaces surround the ciliary transition zone (TZ) and distal dendrite (Figure 2.4 G); a phenomenon not previously described in any of our other EV biogenesis

mutants. We propose that the *mec-9* and likely the *mec-5* extradendritic PKD-2::GFP ciliary localization (Cil) phenotype may correlate to extra-dendritic accumulation of the abnormal EVs in the ECM surrounding the CEM dendrite.

**2.2.5 *mec-9* and *pmk-1* act antagonistically in EV biogenesis and release.** We wondered if the EV hypersecretion and excessive EV storage phenotypes seen in *mec-9* mutants were due to abnormal EV biogenesis or to defects in neuronal integrity. To test the former possibility, we examined genetic interactions with a positive regulator of EV shedding and release – the p38 MAPK *pmk-1*. We previously showed that *pmk-1* mutants do not accumulate EVs in the cephalic lumen and release fewer PKD-2::GFP labeled EV from ray neurons into the environment (Wang et al., 2015). In contrast, *mec-9* mutants exhibit the opposite phenotypes: hypersecretion and excessive release of cephalic EVs. In a *mec-9(ok2853); pmk-1(km25)* double mutant we see that EV release from ray neurons is restored to WT levels, suggesting that *mec-9* and *pmk-1* may act antagonistically, with *mec-9* as a negative regulator, *pmk-1* as a positive regulator (Figure 2.5 B). We see similar results in CEMs: WT and the *mec-9(ok2853); pmk-1(km25)* double mutant release comparable numbers of PKD-2::GFP labeled EVs (Figure 2.5 A). Further, PKD-2::GFP fluorescence intensity (FI) and blind study of ciliary localization was analyzed and although the *mec-9* and *pmk*-1 single mutants exhibit an increase of PKD-2::GFP at the ciliary base, the ciliary localization phenotype and increased ciliary FI is ameliorated in the double mutant (Figure 2.5

C). We conclude that MEC-9 is a negative regulator of EV biogenesis, with the mutant shedding and releasing excessive amounts of EVs.

**2.2.6 *mec-9* maintains CEM neuronal morphology.** The ECM encoding genes *mec-1*, *mec-5*, and *mec-9* regulate touch receptor neuron attachment and integrity (C. Chen et al., 2013; Chun-Liang Pan, Chiu-Ying Peng, Chun-Hao Chen, & Steven McIntire, 2011). We showed that PKD-2::GFP accumulated in extradendritic spaces in *mec-5* and *mec-9* mutants in CEM neurons (Figures 2.1 E, F, and H). We therefore examined CEM neuronal morphology using a soluble GFP reporter. In WT and *mec-9* CEMs, *pkd-2p*::GFP expressed and localized throughout the neuron in the cell body, dendrite, and cilium (Figure 2.6 B). We did not observe extradendritic accumulation of soluble GFP in *mec-9* mutant, therefore the neurons are not fragile or leaky. However, *mec-9* mutant dendrites appeared brighter and more irregular than WT (Figure 2.6 C).

To determine if there were differences in the dendritic morphology of WT and *mec-9* mutants, we traced each of four CEM dendrites with line profile tool available in ImageJ imaging software and compared FI peaks from the CEM cilium to cell body. These peaks represent dendritic varicosities and the example shown is indicative of the increased number and size of the varicosities in the *mec-9* mutant compared to WT (Figure 2.6 D). WT animals averaged 30.6 varicosities per animal, whereas *mec-9* mutant animals average 36 varicosities ($p = 0.0211$) (Figure 2.6 E).

We defined gross varicosities as those that are noticeably larger than normally observed and measure this phenomenon by blind investigation and FI. Blind study comparison showed that WT averaged 3.7 gross varicosities per animal and *mec-9* mutants averaged almost double (7 gross varicosities per animal) ($p=0.0007$; Figure 2.6 F) The FI of the peaks/varicosities in WT were measured and normalized to 100. In comparison, *mec-9* mutant animals' varicosities averaged 159% of WT intensity ($p<0.0001$; Figure 2.6 G). We concluded that the ECM gene *mec-9* was important for CEM dendritic morphology.

To determine if defects in dendritic morphology impacted protein transport in CEMs, we measured the number and velocity of PKD::GFP particles in time lapse videos. First, we measured and calculated the number of anterograde and retrograde particles moving along the dendrite. WT animals have an average of 82.66 ±5.199 anterograde and retrograde particles/µm. *mec-9(ok2853)* mutants have significantly fewer: 63.97 ±2.976 particles/µm.

Table 2). Next, we measured anterograde and retrograde PKD-2::GFP particle velocity. In WT, PKD-2::GFP puncta moved at an anterograde velocity of 0.82 µm/s (± 0.007 SEM) and overall retrograde velocity of 0.76 µm/s (± 0.006 SEM) (Table 2). In *mec-9(ok2853)*, PKD-2::GFP anterograde and retrograde velocities were significantly slower than WT (Table 2). Combined, these results

indicate that the MEC-9 ECM component may also regulate the neuronal cytoskeleton and transport.

**2.2.7 *mec-9* regulates ciliary length, positioning, and fasciculation.** Given that *mec-9S* was expressed in many ciliated sensory neurons, we used transmission electron microscopy (TEM) to examine ultrastructure of sensory organs in the head of fixed age-matched young adult WT and *mec-9* males (Figure 2.6 A). The head contains four cephalic sensilla, six inner labial sensilla, and two amphid sensilla, each of which performs distinct sensory functions in the worm.

In the male, the cephalic sensillum possesses the cephalic male CEM neuron and the sex-shared CEP neuron. We viewed the CEM in cross section and measured from the ciliary transition zone to the ciliary tip and found WT CEM cilia to be ~2100nm in length (Figure 2.6 A). In *mec-9* mutants, the CEM neurons were 1.2-1.5 times longer than WT. CEP cilia length was not significantly different between WT and *mec-9* mutant animals.

The inner labial sensilla house the IL1 and IL2 neurons. WT dorsal and ventral IL2 cilia averaged 1155 nm and the lateral IL2s averaged 1085 nm (Figure 2.6 A). In the *mec-9(ok2853)* mutant, dorsal and ventral IL2 cilia were about 2x longer than WT and the *mec-9(ok2853)* mutant lateral IL2s were ~1.3 times longer than WT (Figure 2.6 A). IL1 ciliary lengths were similar in WT and *mec-9*, consistent with *mec-9S* expression in IL2 but not IL1 neurons.

*mec-9S* was also expressed in the dye-filling amphid sensory neurons that are housed in bilateral amphid sensilla (Figure 2.2 H-I). Dye filling assays assess ciliary integrity: WT animals dye fill whereas ciliary mutants are dye filling defective (Dyf). *mec-1(e1066)* have a slight Dyf phenotype (Perkins et al., 1986). We first determined whether *mec-5* and *mec-9* mutants had dye filling defects. *mec-1(e1066)*, *mec-5(e1503)*, and *mec-9(ok2853)* had subtle amphid Dyf defects with 1-4 cells of 12 not filling (Figure 2.7 A). *mec-1(e1066)* and *mec-5(e1503)* phasmids are Dyf, with 1-2 out of four cells not filling (Figure 2.11). These data are consistent with *mec-1*, *mec-5*, and *mec-9* ECM genes being required for shared amphid ciliated sensory neurons.

We proceeded to examine amphid sensilla ultrastructure using TEM. In WT, 10 amphid cilia are enclosed in a pore of the bilateral papilla at the worm nose and surrounded by the cuticle (Figures 2.7 B and 2.7 D). *mec-9* worms exhibited a misshapen cuticular pore encapsulating only the ASE cilium (Figure 2.7 C). In the WT amphid channel, ten cilia are present in their invariant and precise arrangement (Figures 2.7 D and 2.7 G). In *mec-9* mutants, we observed only cilia from the ASE, ASG, ASH, ASI, ASJ, and ASK (the single ciliated amphids) in the more proximal amphid channel; ADF and ADL (the double ciliated neurons) were displaced in an adjacent, aberrant electron dense space (Figure 2.7 I). We conclude that *mec-9* was necessary for cilia alignment and placement in amphid sensilla.

*mec-9shp*::GFP was expressed in ADL and ADF. We measured ciliary lengths in these double ciliated amphid neurons from the bifurcation at the transition zone to ciliary tip. In contrast to the longer CEM and IL2 cilia in *mec-9* mutants, the cilia of the ADL and ADF amphid neurons were significantly shorter than WT by ~1.5x (Figure 2.6 A). We also measured single ciliated amphid axonemes and found the ASI cilia significantly than WT (Figure 2.6 A). These amphid cilia length defects may contribute to dye filling defects observed in *mec-9* mutants (Figure 2.7 A). Not only were *mec-9* amphid cilia shorter and misplaced, *mec-9* mutant amphid transition zones were disorganized and abnormally dispersed along the anterior-posterior axis (compare WT in Figure 2.7 F to *mec-9* in Figure 2.7 I), suggesting that the *mec-9* ECM component is necessary for regulating dendritic fasciculation and/or transition zone placement.

Perkins et. al. described the presence of dark matrix vesicles in the space between the amphid cilia and sheath in WT animals (Perkins et al., 1986). In *mec-9(ok2853)* mutants, we noticed a substantial increase in electron dense extracellular spaces that we identified as large matrix filled vesicles (Figure 2.7 H). We also noticed that *mec-9* mutants had excessive matrix filled spaces in the amphid neuron sheath surrounding the amphid neurons that decouples cilia from glia (Figures 2.7 H). Because of these spaces, there is a dysmorphic amphid socket and sheath in *mec-9* mutant animals, which may contribute to the disorganization of the amphid channel neurons (Figures 2.7 G-I). We conclude that *mec-9* regulates ECM deposition in amphid and cephalic sensilla (Figure 2.4 G).

## 2.3 Discussion

ECM is important for neuronal anatomy and organization of the brain and nervous system (Gardiner, 2011). For example, the ECM glycoprotein Reelin is necessary for migration of neocortical radial cells in the mammalian brain (Franco, Martinez-Garay, Gil-Sanz, Harkins-Perry, & Müller, 2011). In *C. elegans*, ECM components *dex-1* and *dyf-7* regulate amphid dendritic extension, which can affect cilia placement (Heiman & Shaham, 2009). Mutations in the RNA splicing gene *mec-8* or ECM component *mec-1* mutants cause ciliary fasciculation defects likely due to interruptions in adhesion proteins (Perkins et al., 1986). The ECM gene *mec-9* is expressed in the *C. elegans* nervous system where it provides mechanical support to multiple cell types including non-ciliated touch receptor neurons (Figure 2.3 F-I) and ciliated sensory neurons.

*mec-9* encodes two isoforms (Figure 2.3 A and B). The *mec-9* long isoform is expressed in touch receptor neurons (Figure 1.14 and (Du et al., 1996)). Here, we show that the *mec-9* short isoform is expressed in the shared and male-specific ciliated nervous system. In amphid and phasmid sensory organs, *mec-9* mutants are dye filling defective, which reflects abnormalities in stereotypical ciliary positioning and fasciculation. In cephalic sensory organs of males, *mec-9* mutants display distended extracellular spaces that contain excessive amounts of ciliary EVs and longer cilia. In CEM neurons, *mec-9* is also required for dendritic integrity, with *mec-9* mutant dendrites showing varicosities and waves as opposed to more

linear trajectories. This abnormal dendritic morphology is typically observed in the nervous system of aged animals, and these age-dependent defects are accelerated by mutations that disrupt neuronal excitability or mechanosensation, including the *mec-1*, *mec-5*, and *mec-9* ECM genes (Chun-Liang Pan et al., 2011). Further studies are needed to ascertain if MEC-9 protein physically restrains the dendrite or attaches to the ciliary or dendrite membrane to properly position the neuron. *However,* it is clear that MEC-9 and the ECM support the development and function of the *C. elegans* sensory nervous system.

ECM and cilia share an intimate association. In aortic valves, primary cilia are restricted to ECM zones (Toomer et al., 2017). Chondrocytes have cilia embedded in ECM (Ruhlen, 2014). In umbilical cord mesenchyme, ECM regulates ciliary orientation (Nandadasa, Nelson, & Apte, 2015). ECM regulates ciliogenesis and organogenesis of Kupffer's vesicle, the zebrafish equivalent of the mammalian embryonic node (Compagnon et al., 2014; Hochgreb-Hägele, Yin, Koo, Bronner, & Stainier, 2013). In *Drosophila*, the ECM protein artichoke is required for morphogenesis of ciliated organs (Marta Andrés et al., 2014a). The ECM gene spacemaker/Eyes shut/RP25 is necessary for ciliary pocket morphology and photoreceptor survival (Yu et al., 2016), with mutations causing photoreceptor degeneration in retinitis pigmentosa patients (Barragan et al., 2008).

ECM influences ciliary length in multicellular animals. Here we show that ECM regulates ciliary length in a cell-type specific manner in *C. elegans*. In amphid channel neurons, *mec-9* is a positive regulator, with *mec-9* mutants having shorter

cilia. Conversely, in EV-releasing IL2 and CEM neurons, *mec-9* is a negative regulator of ciliary length, with *mec-9* mutants having significantly longer cilia. In mammalian skin, ECM component laminin-511 and its receptor integrin-b1 are required for primary cilia formation (Gao et al., 2008). In mouse embryonic fibroblast 3T3-L1 cells, type 1 collagen promotes primary ciliary growth by repressing the HDAC6-autophagy pathway (Xu Q, Liu X, Liu W, Hayashi T, Yamato M, Fujisaki H, Hattori S, Tashiro SI, Onodera S, Ikejima T., 2018). In zebrafish Kupffers Vesicle, laminin-1 is a positive regulator of ciliary length (Hochgreb-Hägele et al., 2013). The mechanisms by which ECM controls ciliary length are largely unknown. A positive or negative feedback loop may act cell autonomously (between the ciliated cell and the ECM secreted by the cell itself) or non-autonomously (between the ciliated cell and ECM secreted by neighboring cells).

EVs are components of the ECM and EVs themselves may carry ECM proteins as cargo (Rilla & et.al, 2017). Here we show that *mec-9* mutants display dramatic increases in EV shedding and release (Figure 2.4 C) and abnormal dark/ light matrix vesicles containing EVs (Figure 2.4 G), suggesting that the MEC-9 ECM component negatively regulates both EV shedding and release. We do not understand how ECM regulates EV biogenesis. However, genetic analysis revealed that *mec-9* and the p38 MAPK *pmk-1* act antagonistically in EV biogenesis and release. *pmk-1* mutants are defective in EV shedding and EV release (Wang et al., 2015). Interestingly, *pmk-1* suppresses the *mec-9* EV

hypersecretion phenotype and *mec-9* suppresses *pmk-1* EV hyposecretion (Figure 2.5), suggesting that these genes act in opposing pathways that control EV biogenesis. An intriguing possibility is that MEC-9/ECM and *pmk-1* kinase regulate the same target(s) such as a cell surface ECM receptor. In mice, CELSR3 (cadherin EGF LAG seven-pass G-type receptor 3) has MEC-9 EGF domains in its N-terminal ectodomain and CELSR3 interacts with a kinase that regulates extension and guidance of sensory neurons (Goffinet & Tissir, 2017)**.** Mice deficient in CELSR2 and CELSR3 are defective in ependymal cilia development and develop hydrocephalus, a ciliopathy phenotype (Tissir et al). The ligand(s) that activates CELSR2 and CELSR3 are not known.

The CELSR family is categorized as adhesion GPCRs (Liebscher I, 2016). Adhesion GPCRs (aGPCRs) contain a large N-terminal ectodomain that contains a tetherized agonist *Stachel* sequence (reviewed by Liebscher and Schöneberg 2016). Removal or structural changes to the N-terminal ectodomain exposes the *Stachel* sequence which in turn activates the GPCR (Liebscher and Schöneberg 2016). Proposed mechanisms of Stachel release and activation of aGPCR signaling include mechanical stress and binding of ECM proteins to the N-terminus (Liebscher et al., 2014; Liebscher, Monk, & Schöneberg, 2015; Rong Luo et al., 2014; Scholz N, Monk KR, Kittel RJ, Langenhan T., 2016).

The polycystin-1 family, while an 11-transmembrane spanning receptor class, has features similar to an aGPCR (F. B. Engel & Cazorla-Vazquez, 2018). The function of the polycystins remains an enigma, even thirty years after the

cloning of PKD1 and PKD2 (Ma M, Gallagher AR, Somlo S, 2017). Based on their ciliary localization, the polycystins were thought to be ciliary mechanosensors, but this model was disproven by the Clapham lab (Markus Delling, Paul G DeCaen, Julia F Doerner, Sebastien Febvay, & David E Clapham, 2013; Paul G DeCaen, Markus Delling, Thuy N Vien, & David E Clapham, 2013). In mice, an ECM receptor integrin signaling pathway is essential for the development of ADPKD (Lee, Boctor, Barisoni, & Gusella, 2015). Inactivation of integrin-b1 or integrin-linked kinase inhibits cystogenesis in *Pkd1* mutant mice (Lee et al., 2015; Raman A, Reif GA, Dai Y, Khanna A, Li X, Astleford L, Parnell SC, Calvet JP, Wallace DP, 2017). In zebrafish, pkd2 deficiency causes increased collagen synthesis via upregulated protein secretion and downregulation of this secretory pathway rescues cystogenesis (Le Corre, Eyre, & Drummond, 2014). Ciliogenesis genes are required for cystogenesis in pkd1 or pkd2 mutant mice (Ming Ma, Xin Tian, Peter Igarashi, Gregory J Pazour, & Stefan Somlo, 2013). Primary cilia from cysts of Pkd1 or Pkd2 conditional knockout mice are longer than controls while precystic *pkd1* and *pkd2* ciliary lengths are comparable to control (Liu Xiaowen et al., 2018). Combined, these studies reflect the close but poorly understood association between ECM, cilia, and the polycystins.

An intriguing possibility is that the ECM itself acts in permissive fashion to allow cell-type specific instructive ligand activation and signaling, a mechanism used by adhesion GPCRs. Our data are consistent with this possibility and reveal the promiscuity of ECM components in nervous system of the worm. We found

ECM proteins contribute to ciliary localization of sensory receptors like PKD-2 which advances the understanding, to consequently expand the options for treatment of ciliopathies like PKD. Notably, abnormal ECM is implicated in the pathogenesis of ADPKD (Calvet, 1993). Renal fibrosis observed in PKD is characterized by excessive deposition of ECM proteins (Drummond, 2011; Song CJ, Zimmerman KA, Henke SJ, Yoder BK, 2017). Here we also illustrated that ECM is necessary for the health and well-being of neurons and neural organs. We further propose that ECM regulates EV biogenesis and shedding, which builds on the idea that ECM is necessary for extracellular interaction but pushes the envelope enabling us to think of ECM playing a role in extra-organismal communication.

**Figure 2.1 Alleles of *mec-1*, *mec-5* and *mec-9* regulate PKD-2::GFP localization and abundance.** (B-H) Images were compiled from a 630x maximum intensity Z-series obtained by fluorescent microscope. Scale bar is 10 µm A. Schematic of WT Cephalic male neurons in the head of a male (green). B. A lateral view of WT PKD-2::GFP (translational reporter). GFP localized to CEM cell bodies and cilia. C-D. Lateral view of PKD-2::GFP in *mec-1* mutant alleles. C. Increased PKD-2::GFP at *mec-1(e1066)* CEM cilia and ciliary base. D. *mec-1(e1292)* was indistinguishable from WT. E-F. *mec-5* PKD-2::GFP ciliary localization. Extra-dendritic and increased ciliary PKD-2::GFP observed in *mec-5(e1503)* and *mec-5(my2)* male CEMs. G-H. PKD-2 localization in *mec-9* mutant males. G. Increased PKD-2::GFP at the *mec-9(e1494)* CEM ciliary base. H. Extra-dendritic and increased PKD-2::GFP at the *mec-9(ok2853)* CEM ciliary base. I. Graph of the fraction of PKD-2::GFP mislocalization in CEM neurons of wild type and mutant males via blind examination. An animal was scored as “Cil” (ciliary localization defective) if CEM cilia, ciliary base, and dendrites in male worms had abnormally increased or mislocalized PKD-2::GFP. Values were reported as fraction of animals that are Cil. Significance was determined by Kruskal Wallace test with Dunn’s multiple comparisons test performed to compare groups. In WT, we observed occasional Cil animals (~16% of males). *mec-1*, *mec-5* and *mec-9* all had mutant alleles that mislocalized PKD-2::GFP. J. Ratio (cilium/cell body) of maximum intensity showed that pKD-2::GFP abundance in CEM cilia is increased in comparison with the cell bodies only in *mec-9* ECM gene mutants; however, mec-*1* and *mec-5* alleles also affected PKD-2 abundance (Table 2.1). Background

measurements were subtracted from cilium and cell body values for standardization of images and we expressed the measurements in ratio of cilia to cell body FI. Significance was measured by Kruskal-Wallace test, comparisons made using Dunn's multiple comparisons. Wild type animal values were normalized to 100. The *mec-9* mutants had a brighter maximum FI (~1.75x) than WT (Figure 1J): *mec-9(e1494)* $p=0.011$ and *mec-9(ok2853)* $p<0.0001$ (Figure 1J).

**Figure 2.1 Alleles of *mec-1*, *mec-5* and *mec-9* regulate PKD-2::GFP localization and abundance.**

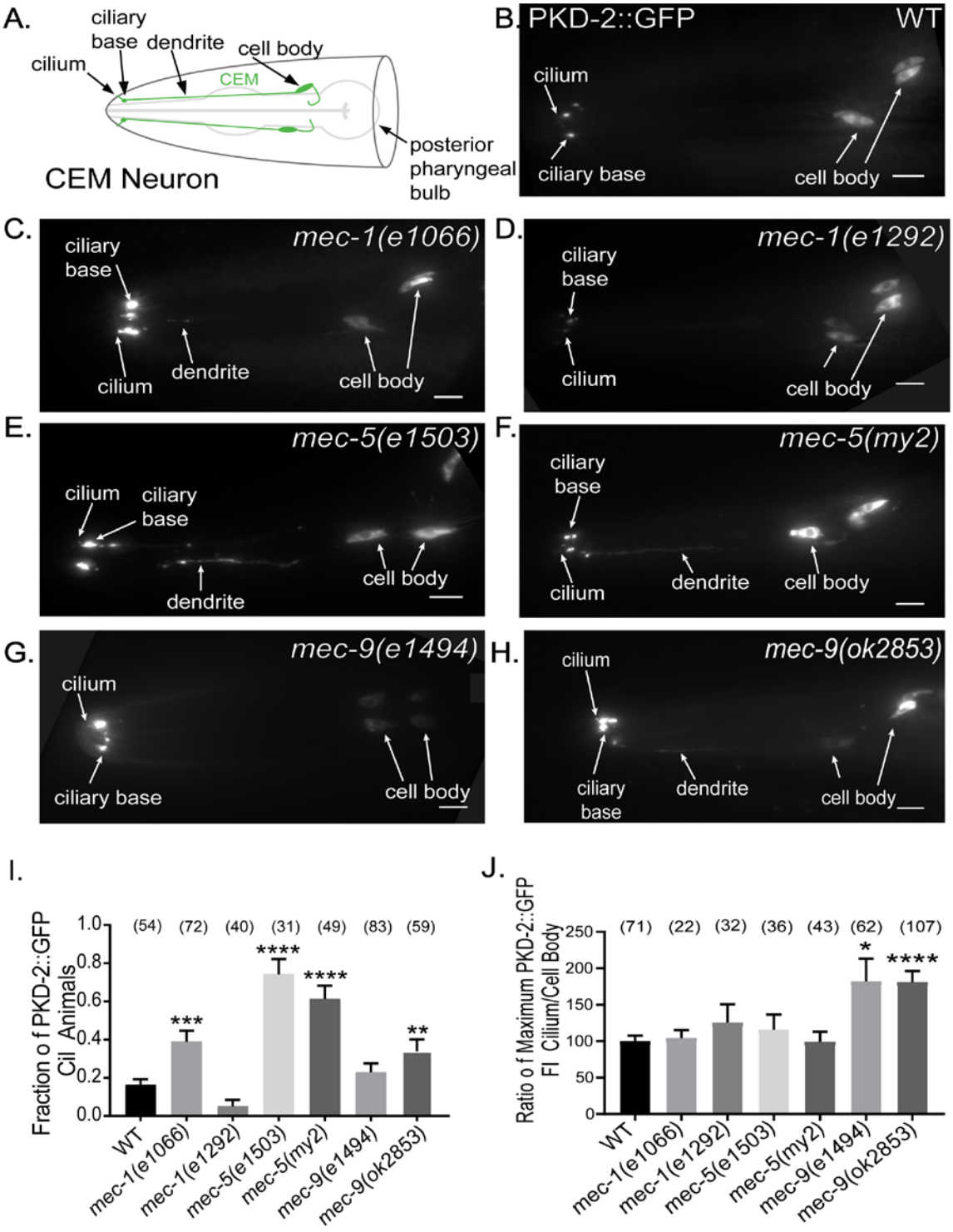

**Table 2.1 *mec-1*, *mec-5* and *mec-9* mutants regulate PKD-2::GFP abundance.** Ratio (Ex-cilium/cell body or that which is specified in Table 2.1) of maximum or mean fluorescence intensity (as specified in table) showed that PKD-2::GFP abundance in *mec-1*, *mec-5* and *mec-9* mutants are variable. For example (cilium/cell body) of maximum intensity showed that PKD-2::GFP abundance in CEM cilia is increased in comparison with the cell bodies only in *mec-9* ECM gene mutants; however, *mec-1* and *mec-5* alleles also affected PKD-2 abundance. Background measurements were subtracted from cilium and cell body values for standardization of images and we expressed the measurements in ratio of cilia to cell body FI. Significance was measured by Kruskal-Wallace test, comparisons made using Dunn's multiple comparisons. Wild type animal values were normalized to 100. The *mec-9* mutants had the brightest maximum FI when compared than WT *p<0.05, **p<0.01, ***p<0.001, ****p<0.0001.

**Table 2.1 *mec-1*, *mec-5* and *mec-9* mutants regulate PKD-2::GFP abundance**

(Increased, Decreased, *=p value)

| WT n=54 | Cil=cilium CB=cell body Den=dendrite BG=background | *mec-1 (e1066) n=72* | *mec-5 (e1503) n=31* | *mec-9 (ok2853) n=59* |
|---|---|---|---|---|
| FI/cell body FI | Cil/CB mean | ↓ * | ns | ↑ **** |
| | Cil/CB max | ↓ * | ns | ↑ ** |
| | Den/CB mean | ↓ * | ↑ * | ↓ **** |
| | Den/CB max | ↑ * | ↑ ** | ns |
| FI-background | Cil-BG mean | ns | ns | ↑ **** |
| | Cil-BG max | ns | ns | ↑ **** |
| | Den-BG mean | ns | ns | ↑ **** |
| | Den-BG max | ↑ *** | ns | ↓ **** |
| | CB-BG mean | ↑ * | ↓ * | ↑ **** |
| | CB-BG max | ns | ↓ **** | ↑ **** |

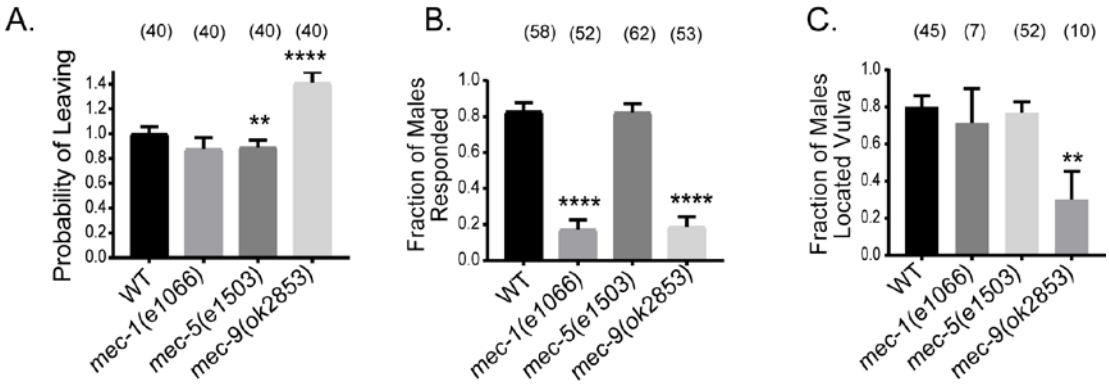


**Figure 2.2 *mec-1*, *mec-5* and *mec-9* are required for male mating behaviors.** **(**A-C) *mec-1(e1066)* males were response defective, *mec-5(e1503)* males were leaving assay defective, *mec-9(ok2853)* males were defective in all three measured mating behaviors. A. Leaving assay measured the probability of males leaving food to search for a mate. WT values normalized to 1. *mec-5(e1503)* males were leaving assay defective when compared to WT. *mec-9(ok2853)* males left food more readily than WT. B. *mec-1(e1066)* and *mec-9(ok2853)* males were defective in responding to hermaphrodite contact. C. *mec-9(ok2853)* males were location of vulva defective. Significances determined by Kruskal-Wallis test (Mann-Whitney test for WT vs. *mec-5(e1503)* only); p values compared by Dunn's multiple comparisons test. ** p<.01; **** p<0.0001.

**Figure 2.3 *mec-9Sp*::GFP is expressed in ciliated sensory neurons.** (A-B.) *mec-9* long and short transcripts. A. *mec-9* long isoform encodes a secreted ECM protein that as 5 Kunitz domains, 7 EGF repeats, and a glutamic acid-rich/coiled-coil region (Du et al., 1996). *e1494* is a point mutation in the first set of EGF domains and *ok2853* perturbs the second set of EGF domains via base pair deletions. B. *mec-9* short transcript is 502 aa (Du et al., 1996): promoter for the *mec-9* short transcript located in *mec-9* long 9th intron, 53 short isoform specific amino acids encoded, and then the 450 3' *mec-9* long amino acids. C. We used the 2kb upstream sequence with a C terminal GFP tag to construct *mec-9Lp*::GFP transcriptional reporter. D. We used the 1.5kb *mec-9* long intron 9 sequence with a C terminal GFP tag to construct *mec-9Sp*::GFP transcriptional reporter. E. Ciliated sensory neurons expressed *mec-9Sp*::GFP: CEMs, IL2, amphids, RnB, HOB, phasmids. Male (top), hermaphrodite (bottom). Ventral nerve cord (non-ciliated neurons) expression also observed and shown. (F-G.) *mec-9Sp*::GFP coexpressed with the kinesin-3 gene, *klp-6* transcriptional reporter. *klp-6* transcriptional reporter expressed in male-specific CEM and IL2 neurons in the head and RnB and HOB male-specific neurons in the male tail. F. Lateral view of male head. *mec-9Sp*::GFP expressed in CEMs and IL2 neurons. G. Lateral view of male tail. *mec-9Sp*::GFP expressed in HOB and RnB neurons. (H-I.) *mec-9Sp*::GFP coexpressed with DiI. DiI is a lipophilic dye taken up by amphids and phasmids. Hermaphrodite shown here. H. *mec-9Sp*::GFP expresses in amphids in the hermaphrodite (and male-not shown) head. I. *mec-9Sp*::GFP expresses in phasmids.

**Figure 2.3 *mec-9Sp*::GFP is expressed in ciliated sensory neurons.**

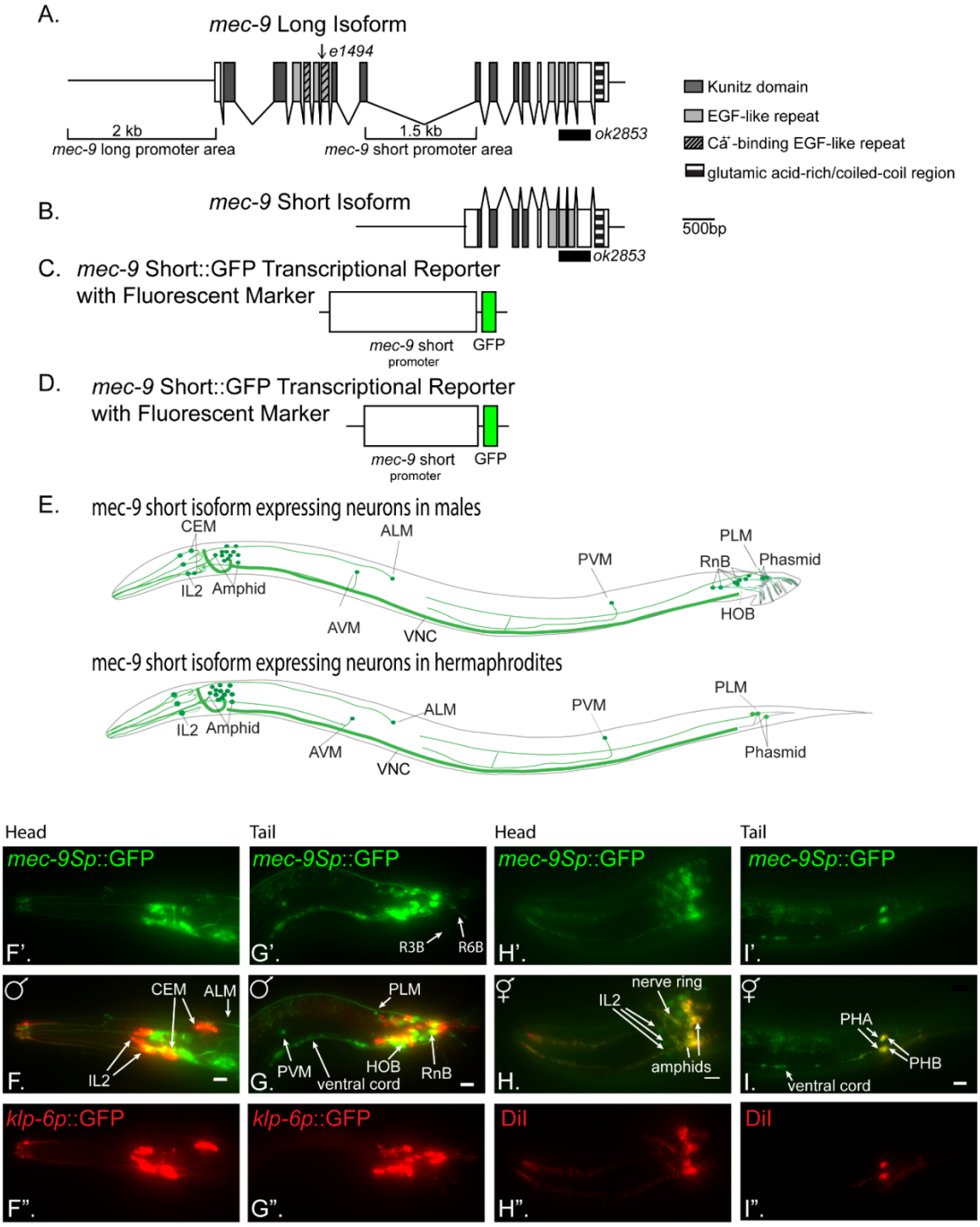

**Figure 2.4 *mec-9(ok2853)* mutants produce excessive ciliary vesicles**. (A-B) Head images of WT and *mec-9(ok2853)* mutant males show EVs were released. Image brightness was increased and inset was magnified to visualize EVs. Scale bars 10µm B. *mec-9(ok2853)* males produced significantly more PKD-2::GFP tagged EVs than WT (A.). C. *mec-9(ok2853)* released significantly more PKD-2::GFP-tagged EVs. Significance determined by Mann-Whitney test; ***p<0.001 D. Schematics of WT and mec-9 mutant CEM sensilla. In WT, EVs are released from cilium and are stored in lumen of the sheath glial cell. Dashed lines (E, F, and G) denotes cross section level observed in images 4E, F, and G. *mec-9(ok2853)* mutants store and release excess EVs and contain dark and light matrix vesicles that contain EVs. (E-F.) Cross section of the cephalic sensillum at the level of the transition zone in WT and *mec-9(ok2853)* males. CEM neurons shaded green, CEP neurons shaded blue. Scale bars 500 nm E. Two EVs (arrows) observed in WT; one in the lumen and one in CEM cilium. F. *mec-9(ok2853)* had a distended lumen with a significant increase of EVs and a lightly shaded matrix filled vesicle itself containing EVs. G. Dark electron-dense matrix filled vesicles contained EVs. These vesicles were located at the level of the distal dendrite (See dotted line marked G in Figure 2.4 D).

**Figure 2.4 *mec-9(ok2853)* mutants produce excessive ciliary vesicles**.

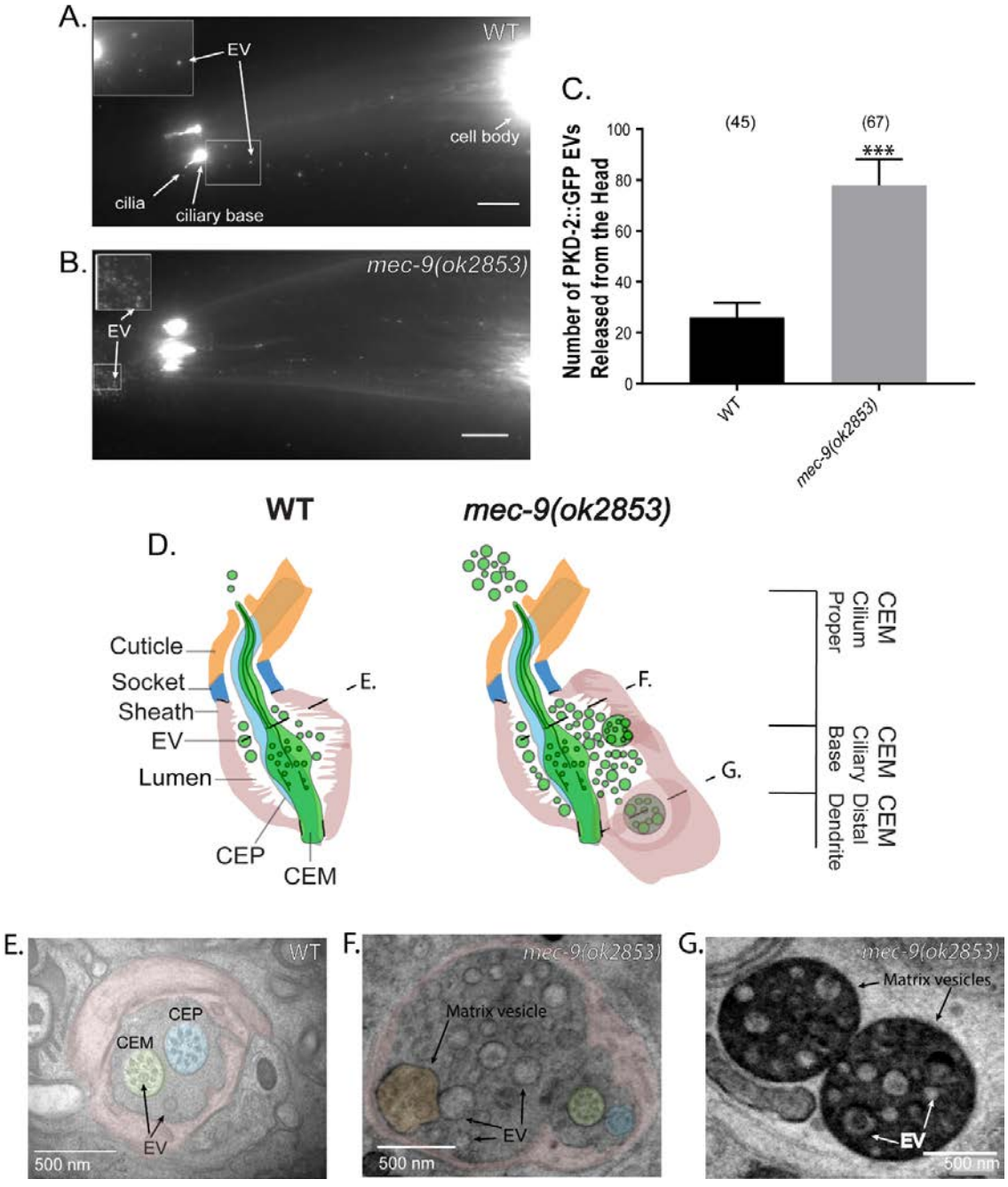

**Figure 2.5 *mec-9* and *pmk-1* double mutant genetically suppressed single mutant EV biogenesis/release) and PKD-2::GFP ciliary localization phenotypes.** A. The p38 MAPK *pmk-1* mutant males, previously shown to be defective in RnB EV release (Wang et al., 2015), suppressed the *mec-9(ok2853)* abnormal EV hypersecretion in the head. B. *mec-9* suppressed the *pmk-1* RnB EV release defect. C. *mec-9;pmk-1* double mutant suppressed PKD-2::GFP Cil defect observed in both *mec-9* and *pmk-1* single mutant males. Significance was determined by Kruskal-Wallace test and Dunn's multiple comparisons test. *p<0.05, **p<0.01, ***p<0.001, ****p<0.0001.

**Figure 2.5 *mec-9* and *pmk-1* double mutant genetically suppressed single mutant EV biogenesis/release and PKD-2::GFP ciliary localization phenotypes.**

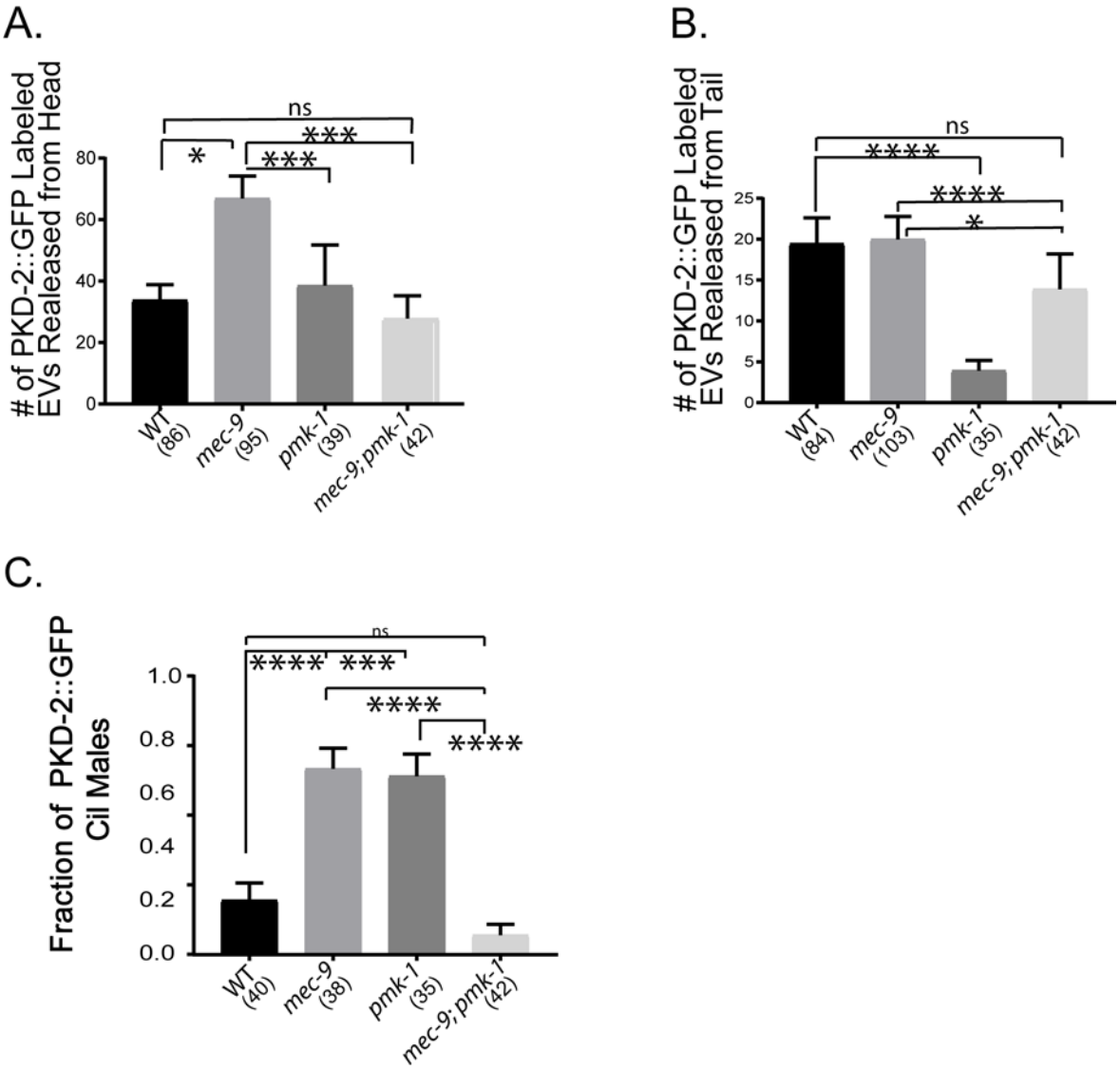

**Figure 2.6 *mec-9* regulated neuron ciliary and dendritic anatomy** *mec-9* regulated cephalic male, inner labial, and amphid neuron cilia length and maintained CEM neuronal integrity. A. Amphid, double ciliated (ADL, ADF), amphid single ciliated (ASE, ASG, ASI, ASJ, ASK), cephalic (CEP) and male-specific CEM (ventral and dorsal), and inner labial (IL2) neurons were measured using serial sectioned electron micrographs (each layer~70 nm). Lengths were determined by counting number of 70 nm layers from transition zone to ciliary tip of each cilium. WT amphid cilia were longer than those in *mec-9(ok2853)* mutants. WT CEM, CEP and IL2 ilia were shorter than *mec-9(ok2853)* cilia. Significance measured by Kruskal-Wallace test and Dunn comparisons test. *p<0.05, **p<0.01 (B-D.) *mec-9* maintained dendritic integrity. Images are maximum intensity Z-stacks of WT and *mec-9(ok2853)* males that expressed *pkd-2* transcriptional green fluorescent reporters. Images were brightened to observe dendritic morphology. Scale bars are 10 µm B. Varicosities were observed in WT male CEMs, examples denoted by arrows. C. *mec-9* mutant males have more varicosities. Large, “gross” varicosities denoted by arrows. D. A line plot of WT (black) and *mec-9(ok2853)* (red) dendritic fluorescent intensity disclosed increased number of varicosities (E.), increased gross varicosities (F.), and that varicosities had a greater fluorescence. FI measured here using transcriptional reporter which allows for observation of neuron morphology only, not protein abundance measurements. (G.). Total varicosities and gross varicosities measured by blind study. Significance measured by Mann-Whitney test. Varicosity Fluorescence (G) normalized to 100. *p<0.05, ***p<0.001, ****p<0.0001

**Figure 2.6 *mec-9* regulated neuron ciliary and dendritic anatomy**

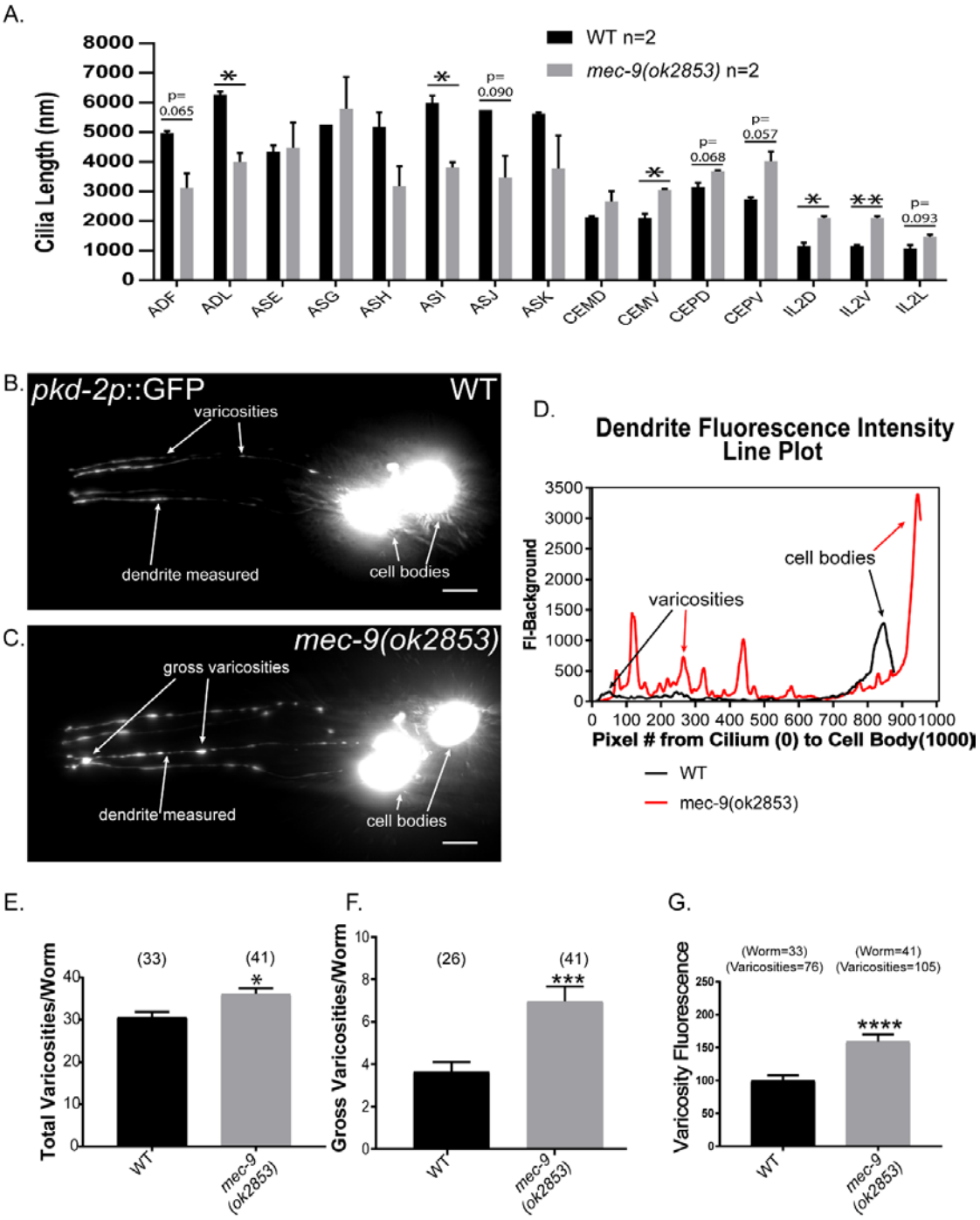

**Table 2.2 *mec-9* regulated PKD-2::GFP particle abundance and velocity in CEM dendrites**

| | Mean ± SEM | n | N | p value | Diff. from WT |
|---|---|---|---|---|---|
| **Total particles/µm** | | | | | |
| WT | 82.66 ± 5.199 | 48 | 18 | | |
| *mec-9(ok2853)* | 63.97 ± 2.976 | 83 | 23 | 0.0241 | -18.68 ± 5.559 |
| **Anterograde Velocity** | | | | | |
| WT | 0.8215 ± 0.007 | 4654 | 18 | | |
| *mec-9(ok2853)* | 0.7496 ± 0.005 | 4765 | 23 | <0.0001 | -0.07186 ± 0.009 |
| **Retrograde Velocity** | | | | | |
| WT | -0.7607 ± 0.006 | 4971 | 18 | | |
| *mec-9(ok2853)* | -0.6551 ± 0.004 | 5019 | 23 | <0.0001 | -0.1056 ± 0.008 |

**Table 2.2 *mec-9* regulated PKD-2::GFP particle abundance and velocity in CEM dendrites** The number and velocity of PKD::GFP particles was measured using time lapse fluorescent videos. The average number of anterograde and retrograde PKD-2:GFP particles moving along the dendrite are reported here in particles/µm. *mec-9(ok2853)* mutants have significantly fewer particles than WT. Anterograde and retrograde PKD-2::GFP particles velocities were measured in microns per second along the CEM dendrite. *mec-9(ok2853)* mutant PKD-2::GFP overall dendritic anterograde and retrograde particle velocity was slower than WT. Time lapse video speed: 300 ms. Significance measured using Mann-Whitney test for particle number and velocities.

**Figure 2.7 *mec-1*, *mec-5*, and *mec-9* mutants are dye filling defective and mec-9 is necessary for amphid cilia organization and ECM deposition.** A. Number of amphid neurons out of 12 that filled with dye. (B-C) Schematics of WT and *mec-9(ok853)* amphid sensory organ (not all neurons shown). Proximal and medial sections of WT amphid cilia were in the sheath. Distal cilia were surrounded by socket and inverted cuticle with cilia tips exposed to the environment. Dashed lines (D, E, and F) denote levels of cross sections shown in Figures 8 D-F. C. *mec-9(ok2853)* amphid cilia were short and displaced with few ciliary tips exposed to the environment. Dashed lines (G, H, and I) denote levels of cross sections shown in Figures 8 G-I. D. Left amphid channel pore with ten cilia at level of singlet microtubules. WT double ciliated amphids were found dorsally and ventrally in the pore with the ADF (medial) and ADL (lateral). The WT single ciliated amphids are found in the center two rows of amphids. The top row of single ciliated neurons from medial to lateral are the ASE, ASH, and ASG. The bottom row:: ASI, ASJ, and ASK. WT left and right (not shown) amphids are mirror images of each other. D' is schematic of D. Neurons are labeled by final amphid letter. E. WT middle segment contained 10 cilia with microtubules arranged concentrically in axonemes. E' is a schematic of E. F. We observed the transition zones of most WT amphid cilia at this level and they were embedded within the amphid sheath. G. Only one out of ten cilia was visible in *mec-9* mutant channel pore. Socket and sheath had abnormal morphology as compared to WT. H. *mec-9* mutant middle segment: six out of ten cilia were visible in the lumen and there was increased matrix. *mec-9* mutant amphids were abnormally arranged in three rows of two

cilia. The top row: ASG and ASH, the second row: ASK and ASE, and the bottom row: ASI and ASJ, all of which are single ciliated amphids. Increased numbers of matrix filled vesicles were observed. I. The double ciliated amphids (ADFs and ADLs) were in adjacent, aberrant electron dense spaces. Scale bars 200 nm.

**Figure 2.7 *mec-1*, *mec-5*, and *mec-9* mutants are dye filling defective and mec-9 is necessary for amphid cilia organization and ECM deposition.**

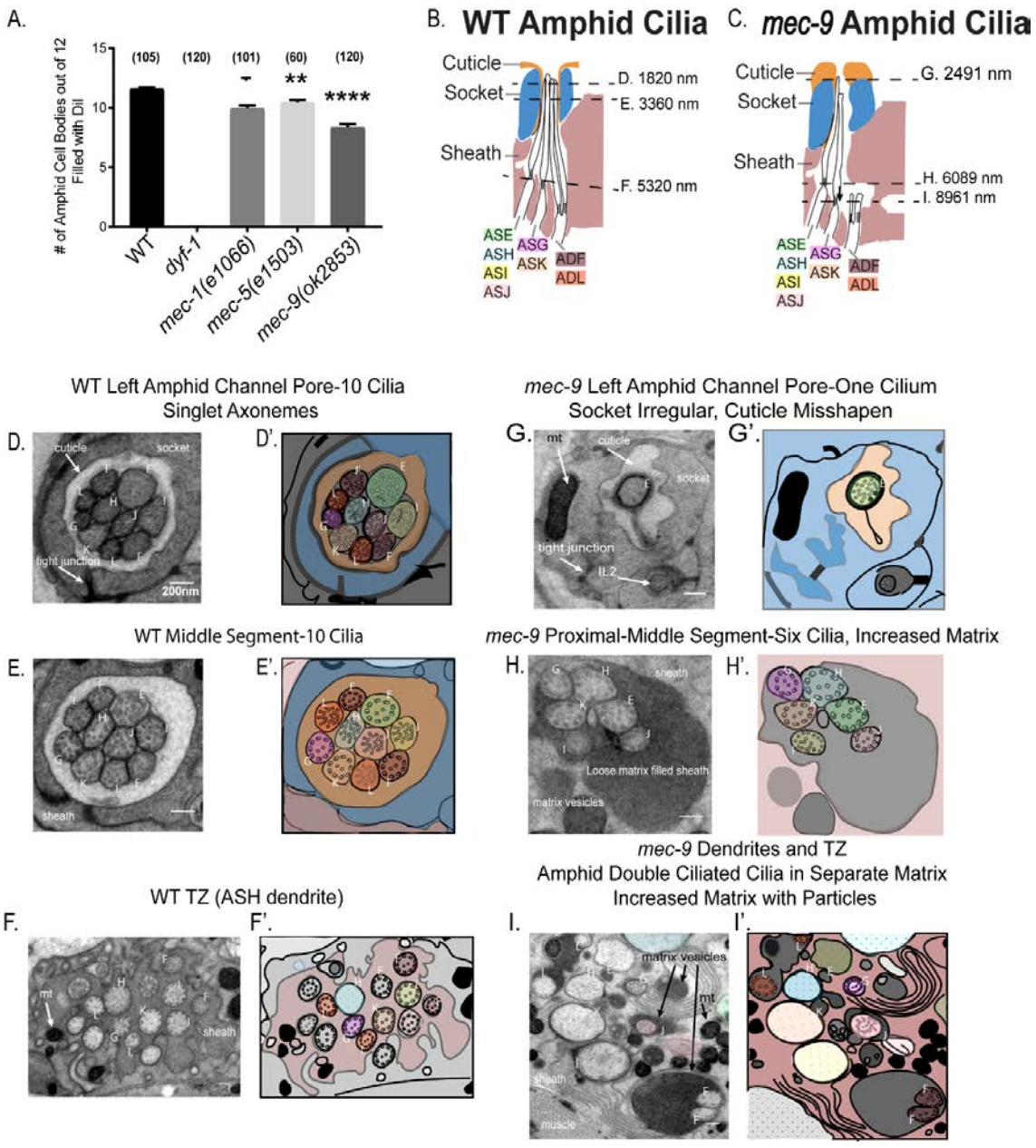

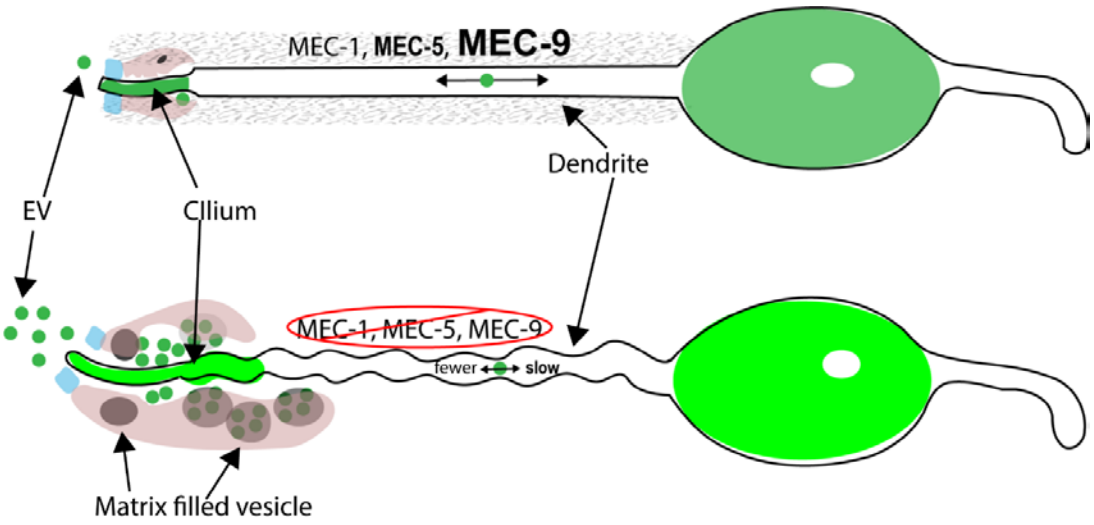


**Figure 2.8 Model of *mec-9* role at the neuron.** *mec-1*, *mec-5*, and *mec-9* regulate PKD-2::GFP localization and male mating behaviors. *mec-9* regulates neuron anatomy, such as dendritic integrity, cilia length and organization, and matrix deposition. *mec-9* also is necessary for PKD-2::GFP dendritic trafficking: there are fewer and slower moving PKD-2::GFP particles in *mec-9* mutants. *mec-9* negatively regulates EV biogenesis, storage, and release.

**Figure 2.9 and Table 3 Alleles of *mec-1*, *mec-5* and *mec-9* regulate PKD-2::GFP localization and abundance in RnBs.** A. Schematic of WT RnBs and HoB male neurons in the tail of a male (green). (B-E) Images were compiled from a 630x maximum intensity Z-series obtained by fluorescent microscope. Scale bar is 10 µm. B. A ventral view of WT PKD-2::GFP (translational reporter). GFP localized to RnB and HOB cell bodies and cilia. Dorsal view of *mec-1(e1066)* here showed Increased PKD-2::GFP at RnB cilia and ciliary base but overall there is decreased FI (Table 3). D. *mec-5(e1503)* PKD-2::GFP ciliary localization showed Increased PKD-2::GFP at RnB cilia and ciliary base but overall there no statistical difference from WT (Table 3). E. There was increased PKD-2::GFP at *mec-9(ok2853)* at RnB cilia and ciliary base and a significant increase in FI (Table 3). Table 3. Ratio (Ex-cilium/cell body or specified in table) of maximum or mean intensity showed that PKD-2::GFP abundance in RnB cilia is generally increased in only in *mec-9* ECM gene mutants; however, observed FI variability suggested *mec-1* and *mec-5* alleles also affected PKD-2 abundance (Table 3). Background measurements were subtracted from cilium and cell body values for standardization of images and we expressed the measurements in ratio of cilia to cell body FI. Significance was measured by Kruskal-Wallace test, comparisons made using Dunn's multiple comparisons. *p<0.05, **p<0.01, ***p<0.001, ****p<0.0001.

**Figure 2.9 and Table 3 Alleles of *mec-1*, *mec-5* and *mec-9* regulate PKD-2::GFP localization and abundance in RnBs.**

A.

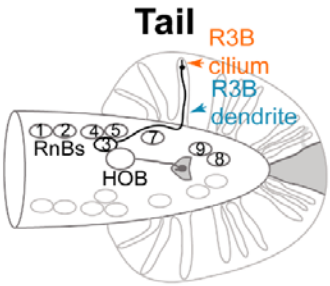


B.

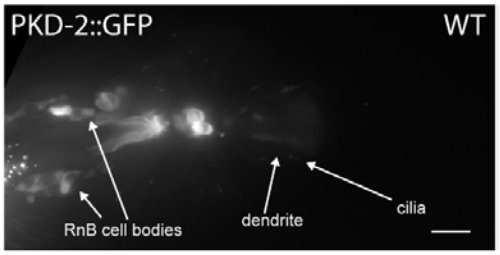


C.

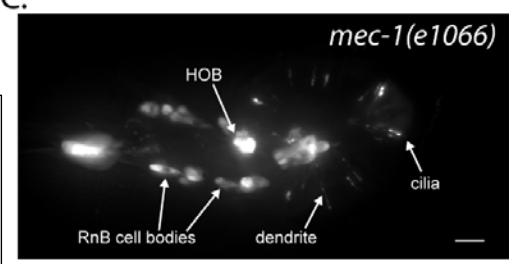


D.

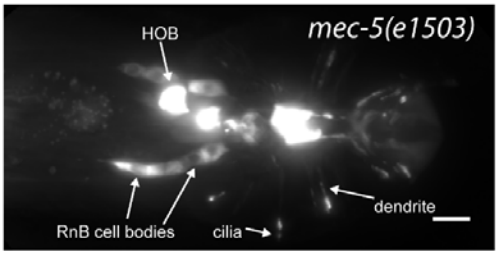


E.

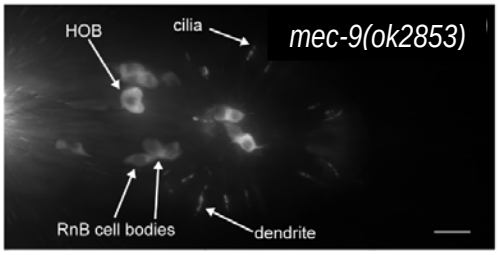


**Table 3 ECM Mutant Analyses of RnB PKD-2::GFP Fluorescence Intensity**

(Increased, Decreased, *p value)

| Cil=cilium CB=cell body Den=dendrite BG=background | *mec-1 (e1066)* | *mec-5 (e1503)* | *mec-9 (ok2853)* |
|---|---|---|---|
| Cil/CB mean | ns | ns | ns |
| Cil/CB max | ↓ ** | ns | ↑ * |
| Den/CB mean | ↓ * | ↑ * | ↓ * |
| Den/CB max | ns | ns | ns |
| Cil-BG mean | ns | ns | ↑ * |
| Cil-BG max | ↓ * | ↓ **** | ↑ *** |
| Den-BG mean | ns | ns | ns |
| Den-BG max | ns | ns | ↑ ** |
| CB-BG mean | ns | ns | ↑ * |
| CB-BG max | ns | ns | ↑ ** |

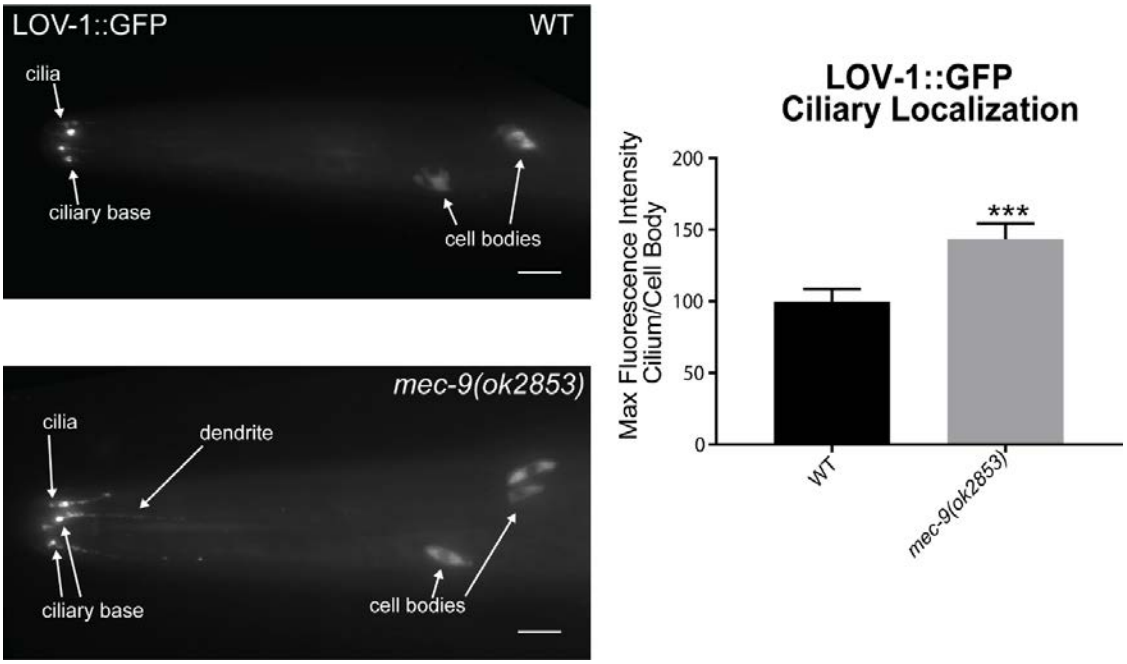


**Figure 2.10 *mec-9* regulates PKD1(LOV-1).** The partner of Polycystin 2 (PKD-2) is Polycystin 1 (LOV-1). In WT, LOV-1::GFP localizes to the CEM, RnB, and HOB cell bodies and cilia. In *mec-9(ok853)* mutants, we observed distal dendritic LOV-1::GFP mislocalization and increased ciliary fluorescence. Significance measured by Mann-Whitney test. ***p<0.001. Scale bar is 10 µm.

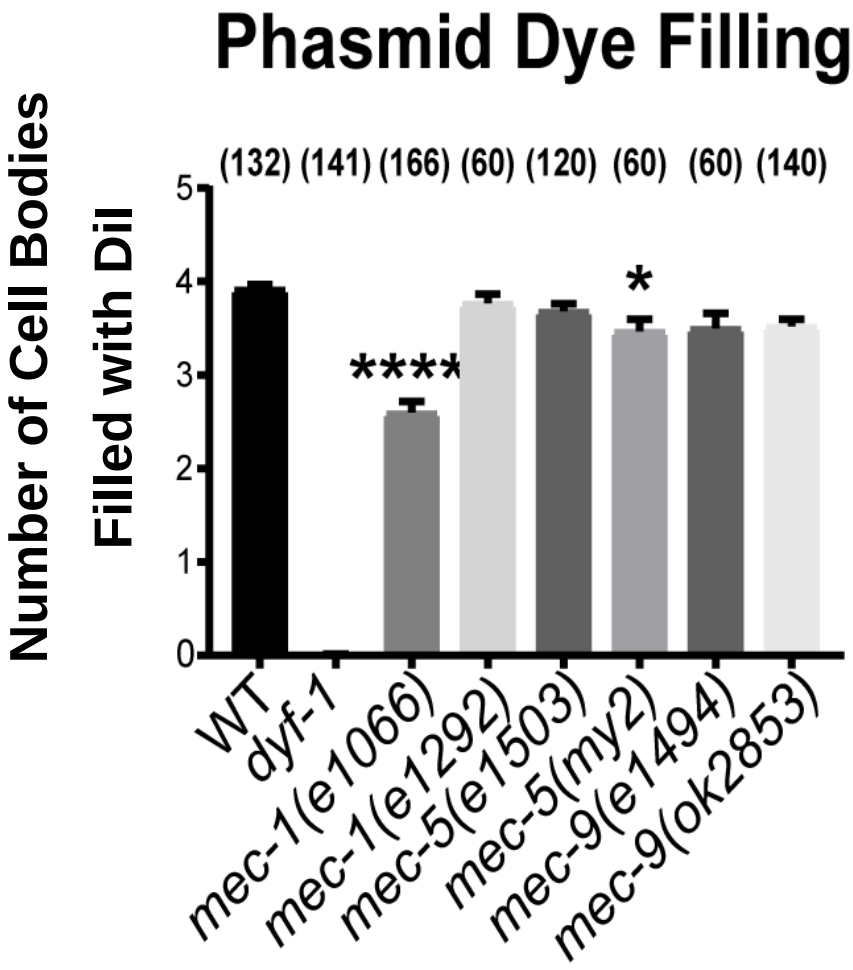


**Figure 2.11 *mec-1(e1066)* and *mec-5(e1503)* phasmids are Dyf.** In *mec-1(e1066)* and *mec-5(e1503)*, one-two out of four phasmid cells do not fill. Significance measured by Kruskal-Wallace test with Dunn comparisons. ****=<0.0001, *p<0.05.

## CHAPTER 3: APPENDIX (UNPUBLISHED DATA)

### 3.1 *my2* is a *mec-5* allele

**3.1.1. *my2* locus on X chromosome** *cil-2(my2)* was a mutant isolated from in a screen to identify new genes important in ciliary localization of PKD-2::GFP (Bae et al., 2008). Initial characterizations and efforts to identify this mutant were done by Karla Knobel. Dr. Knobel noted the puncta or “vesicles” in the medial to distal aspect of the male specific CEM dendrites and speculated that they may extracellular (unpublished data). She also noted *cil-2(my2)* hermaphrodites are sterile at 25$^{o}$C. Two-factor, three-factor, single nucleotide polymorphism (SNP), and deficiency mapping indicated that the *my2* gene locus is on linkage group (chromosome) X, near and likely to the right of *unc-3* (Fay, 2006a; Fay, 2006b; Fay & Bender, 2008; Sigurdson, Spanier, & Herman, 1984). *unc-3* is at genetic position X:21.32 +/- 0.015 cM and genomic position X:14773538..14783564.

**3.1.2. Deficiency mapping: *my2* in X:22.9947..24.4738** Precise deficiency mapping near and to the right of *unc-3* further isolated locus to a genetic position between 22.9947-24.4738 on LGX. (Figure 3.1) *mnDf4* complemented the *my2* hermaphrodite temperature sensitive sterile phenotype. *mnDf13* failed to complement *my2* (Figure 3.2). Therefore, I used the end of *mnDf4* as the probable *my2* locus beginning boundary (22.9947). The end of *mnDf13* was used as the probable *my2* locus end boundary (24.4738).

**3.1.3 Whole genome sequencing identified *my2* candidates.** The *my2* strain was outcrossed to Bristol (N2) three times and then sent to the Hobart lab for whole-genome-sequencing. *my2* specific lesions were identified using one-step whole-genome-sequencing and SNP mapping analysis (Doitsidou, Poole, Sarin, Bigelow, & Hobert, 2010). Whole genome sequencing identified genomic lesions in X:22.9947..24.4738 (Table 3.1 and Figure 3.3 and 3.4). Lesions of interest were identified in *mec-5*, *let-2*, *crb-1*, and *tps-1* genes. Complementation analyses for temperature sensitivity and examination of PKD-2::GFP ciliary localization in the CEM of males were performed in animals containing various alleles of these four genes (Figures 3.5 and 3.6).

LET-2 is an alpha-2 Type IV basement membrane collagen that interacts with a mechanosensory ion channel component, UNC-105 (Benjamin D. Williams & Robert H. Waterston, 1994; Jingdong Liu, Bertold Schrank, & Robert H. Waterston, 1996). The lesion identified here was at genomic position X:16382321 and was a missense, point mutation that changed a cytosine to an adenine causing an amino acid change: GGA->AGA [Gly->Arg] (Table 3.1 and Figure 3.4).

CRB-1 is a homolog of Drosophila Crumbs polarity protein and it is a transmembrane protein that regulates positioning of the adherens junctional protein DLG-1 and helps anchor the gut epithelium (Benjamin D. Williams & Robert H. Waterston, 1994; Lockwood, Lynch, & Hardin, 2008; Waaijers, De Amil Da Costa Jacob Ramalho, Joao, Koorman, Kruse, & Boxem, 2015). The lesion

identified here was at genomic position X:17406984 and was a missense, point mutation that changed a cytosine to a thymine. This changed the corresponding amino acid: CGC->TGC [Arg->Cys] (Table 3.1 and Figure 3.4).

TPS-1, trehalose 6-Phosphate Synthase, is an enzyme necessary for sugar synthesis and is implicated in aging and protein homeostasis (Depuydt, Shanmugam, Rasulova, Dhondt, & Braeckman, 2016; Honda, Tanaka, & Honda, 2010). The lesion identified here was at genomic position X:17473197 and was a missense, point mutation that changed a guanine to an adenine. This caused a change in amino acid: CGC->TGC [Arg->Cys] (Table 3.1 and Figure 3.4).

**3.1.4 *mec-5(my2)*** Whole-genome sequencing identified three lesions in the third intron of *mec-5* at genomic positions X:15945743, 15945744, and 15945755. These lesions are all non-genic, point mutations (Table 3.1 and Figure 3.4). The first two lesions changed guanines to thymines. The last lesion changed an adenine to a thymine. We did not know why these non-coding lesions affected PKD-2::GFP ciliary localization. Possible explanations could be that the mutations may have affected regulatory elements that altered *mec-5* splice sites or gene expression (Chorev & Carmel, 2012).

Several data supported *my2* as an allele of *mec-5.* First, the *mec-5(e1503)* allele had a similar ciliary localization defect than the previously unknown *my2* mutant (Figure 3.6). However, the *mec-5(u444)* null allele did not affect ciliary localization.

Second, gentle touch assays revealed that *my2* has the characteristic mechanosensory defect seen in Mec mutants (Chalfie & Sulston, 1981) (Figure 3.7). Third, the presence of the temperature sensitivity phenotype lends support to *my2* as a *mec-5* allele because a separate circadian rhythm study lists *mec-5* in a catalog of genes that have fluctuating expression levels in response to shifting temperature within 24 hour periods (Rachel Jones, 2010). *mec-5(u444)* has a significant temperature sensitivity sterility phenotype, though *mec-5(e1503)* was able to produce offspring (Figure 3.2). The variability in the TS phenotype could be attributed to *mec-5* allelic alterations, but more study must be done here to fully understand these differences.

**3.1.5 *mec-5(+)* rescued the *my2* mutant** We hypothesized that the *my2* PKD-2::GFP ciliary localization defects were caused by mutations in the *mec-5* gene. To test this, we cloned the *mec-5* gene using two constructs using pPD95.75 YFP plasmids from Brian Coblitz-Chalfie Lab (BstBI restriction enzyme was used to remove the yellow fluorescent protein-YFP). One construct was *mec-5p::*MEC-5, the other was *myo-3p*::MEC-5. *mec-5* expresses in the head and at the touch neurons in hermaphrodites (Du et al., 1996; Emtage et al., 2004). *myo-3* encodes a minor isoform of myosin heavy chain and expresses in body, gut and vulva muscle in the hermaphrodite and diagonal male tail muscles (Joseph P. Ardizzi & Henry F. Epstein, 1987). We used these two constructs to see if the *mec-5(+)* gene could rescue the ciliary localization phenotype and if the gene acted cell autonomously. Constructs with both the endogenous (*mec-5p::*MEC-5) and

heterologous (*myo-3p*::MEC-5) promoter were injected into *my2* hermaphrodites at a 20 ng/ul concentration and rescued the ciliary localization phenotype. All five lines of *my2* animals injected with *mec-5p::*MEC-5 and five out of six lines injected with *myo-3p*::MEC-5 showed rescue of the PKD-2::GFP ciliary localization defect (Figure 3.8). This data indicated that *my2* was an allele of *mec-5* and that *mec-5* acted non-cell autonomously.

**3.2 ECM affects LOV-1::GFP localization** The *C. elegans* polycystins LOV-1 and PKD-2 are necessary for male mating behaviors. *mec-9* regulates PKD-2::GFP localization, mate searching, response, and vulva location (Figures 2.2 A-C), so I determined if *mec-9* was necessary for LOV-1::GFP localization as well. There was increased LOV-1::GFP and fluorescence intensity in *mec-9(ok2853)* mutants (Figures 3.9-10). It may be that *mec-9* genetically interacts with *lov-1* and/or *pkd-2* or it is intriguing to speculate that MEC-9 may directly interact with the long, extracellular N terminus of LOV-1 or PKD-2 through its short extracellular loops.

**3.3 ECM regulates CIL-7::GFP localization** In addition to polycystin localization defects, we found that *mec-9* mutants also were defective in localizing CIL-7::GFP tagged EV cargo (Figures 3.11-12). CIL-7 is a myristoylated protein that is expressed in CEM neurons and regulates EV biogenesis and release (Maguire et al., 2015). Interestingly *mec-9(ok2853)* exhibited no defect in CIL-7::GFP tagged EV release, suggesting there are different mechanisms involved in EV cargo sorting (Figure 3.13).

**3.4 MEC-9 does not regulate dauer IL2 branching** ECM mutants display dendritic ciliary localization and varicosity phenotypes in the CEM neurons. IL2 neurons arborize (branch) when animals are stressed and enter the alternate developmental, dauer stage. KPC-1, a proprotein convertase, regulates this activity in IL2, PVD, and FLP neurons (Schroeder et al., 2013). Like MEC-1 and MEC-9, KPC-1 has a proteinase inhibitor domain. Since *mec-9(ok2853)* IL2 neurons have longer cilia, I wondered if their IL2 dendrites functioned normally in dauers. As seen via the transcriptional *klp-6p::*GFP reporter, *mec-9* dauers display WT dendritic arborization and exhibit secondary, tertiary, and quaternary branching, unlike the *kpc-1* mutants (Figure 3.14). There is no observable dauer branching phenotype in *mec-9(ok2853)* mutants. *mec-9* regulates dendritic integrity in CEM neurons but our results indicated that *mec-9* does not function in the IL2 dauer branching pathway. Dauer branching analysis performed by Dr. Nate Schroeder. Scale bar 10 µm.

**3.5 *mec-1(e1066)* negatively regulates exopher release** Cells must regulate their contents to maintain homeostasis. This was the original hypothesis for extracellular vesicles, especially apoptotic bodies (a subset of EVs) (Kalra, Drummen, & Mathivanan, 2016). Recent discovery by the Driscoll lab shows that *C. elegans* neurons prepare and release large exophers (up to the size of the cell body) containing cellular contents, protein aggregates, and organelles. This phenomenon is increased in during cellular stresses such as decreased chaperone or autophagy activity and mitochondrial stress (Ilija Melentijevic et al., 2017).

In a previous study, exopher-genesis and jettison was noted by bright concentration of fluorescent protein at the eventual extrusion end of the cell. (Figure 3.15) Ilija Melentijevic of Driscoll Lab used mCherry2 as a reporter for exopher detection as it is general knowledge that this marker aggregates. However, he noted that this phenomenon was not completely penetrant. In the 2017 report, exophers were detected in 23% in ALM touch neurons of 2-day-old adults at time of imaging (Figure 3.15). However, exophers were not found at all in PLM neurons.

I detected an increase in exopher production with PKD-2::GFP tagged cargo at the CEM neuron in the *mec-1(e1066)* mutant. In WT males, exophers were only occasionally observed: less than once per animal (Figure 3.17). In *mec-1* males, PKD-2::GFP-labeled exophers were observed (Figures 3.16-17). Exopher presence is often accompanied by a PKD-2::GFP ciliary localization defect. This is interesting because though *mec-9* and *mec-1* have similar Kunitz protease domains, MEC-1 has an overwhelming number of these Kunitz domains: MEC-9 short has three, MEC-9 long has five, MEC-1 has fifteen. These domains could be useful for maintaining protein homeostasis. We conclude that MEC-*1* acted in the exopher pathway and additional study could determine MEC-1 exopher release mechanisms.

**3.6 PKD-2 ab validated** Abmart® was used to construct monoclonal anti-PKD-2 antibodies to address the possibility that ciliary localization defects may be due to overexpression with PKD-2::GFP reporter (Figure 3.18). Twelve epitopes were validated by ELISA at Abmart (Table 3.2). I performed antibody staining with all epitopes, imaged each line, and observed fluorescence in two of the twelve peptide sequences. One epitope tagged the PKD-2 N terminus and two clones fluoresced at appropriate male specific neurons (Figure 3.19). Clone C111 is an N terminal PKD-2 antibody that tags aggregates in CEM cell bodies (Figure 3.20, 3.22 and 3.25) in a similar manner as seen in PKD-2::GFP localization in *lov-1(sy583)* mutants (Bae et al., 2006). Clone C295 is an N terminal PKD-2 antibody that fluoresces in the entire cell body (Figure 3.21). One epitope tagged the C terminal

end of the PKD-2 protein (Figure 3.19) and only clone, C103 exhibited similar fluorescence as the non-aggregating C295 and appeared to tag sperm (Figure 3.24). The PKD-2 antibody labeled expected areas of the CEM neuron (Figures 3.20-3.25) and there is anti-PKD-2 expression even without presence of PKD-2::GFP, indicating that this antibody recognizes endogenous PKD-2 (Figure 3.25). Anti-LOV-1 expression was difficult to detect in these ECM mutants, though rigorously and repeatedly attempted.

The following is correspondence from Abmart that explains formation of anti-PKD-2:

> **Antigen Design Report (edited correspondence from Abmart-changes for clarity in parentheses)**
>
> The (PKD-2) sequence you submitted was subject to a rigorous analysis by our scientists using a proprietary algorithm. This method (named SEAL™) aims to identify fragments of your protein that would most likely yield monoclonal antibodies. After a careful examination of structure, sequence and numerous other factors, we have designed 12 peptide antigens optimized for immunization.
>
> Each of your antibodies will be tested before mailing to verify an ELISA titer above 100,000 to 1. Your final package will arrive with 6-20 antibodies raised against different epitopes of the same protein. The resultant choice of antibodies would greatly increase your chance of success in any specific application.

**3.7 *mec-9* reporters constructed by Knudra** Knudra Transgenics constructed and injected DNA into animals to create a total of three constructs: two transcriptional (Figures 1.13 and 3.26) and one translational (Figure 3.27) extrachromosomal arrays for visualization of *mec-9* expression and MEC-9 localization. Knudra used the *tbb-2* 3' UTR in a plasmid when constructing these transcriptional reporters because the *tbb-2* 3' UTR drives expression in all cell types (Merritt, Rasoloson, Ko, & Seydoux, 2008). Knudra plasmid constructs also contain an *unc-119*$^{+}$-selection-cassette. *unc-119* worms are injected and non-uncoordinated, crawling F1 animals that carry reporter are selected and individually plated.

The following inset text is direct written communication from Knudra describing the scope and progress of the construction and injections of these three reporters. Notice difficulty in construction of translation reporter (Project 3). This reporter did not fluoresce.

> **PROJECT 1: *MEC-9* LONG ISOFORM TRANSCRIPTIONAL REPORTER**
> **DVOR01 Extrachromosomal Array service: *mec-9*Lp::GFP::*tbb-2* transgene**
> **DNA Construction**
> pNU1415 - DVOR01 - *mec-9*L::GFP::*tbb-2* extrachromosomal array
> Project component complete.
> **Transgenic Injections and Capture**
> NU1415 - DVOR01 - extrachromosomal array injections and screening
> **SCOPE:** Project component objective is to generate an extrachromosomal array-harboring animal, as part of the DVOR01 project at Knudra. Transgenesis requires 1 client-specific plasmid pNU1415. The plasmid contains *mec-9*L::GFP::*tbb-2* and the *unc-119*-rescue selection cassette. The DNA mix is injected into gonads of 3 sets of 10x in the *unc-119* background strain. Injected animals are screened for crawling transgenics

in F2 populations to select germline transmitting arrays. Populations from singled F2 are chunked to save copy. Copy is sent to client.
**PROGRESS:** Oligos in design.
**PROGRESS:** Oligos received and used for PCR. PCR amplification parts were used in a Gibson ligation and transformation resulting in six colonies. These were screened by RE digest and gave the expected banding pattern Two candidates were sent for sequencing and one was confirmed to be correct. Project component complete.
**PROGRESS:** Completion of the plasmid has activated this project. We are preparing the plasmid to create an injection mix.
**PROGRESS:** Injections were performed. Four plates were identified as having crawlers in the F1 generation. We are now waiting to see if the arrays are heritable in the F2 generation.
**PROGRESS:** One line confirmed and being prepped to send.
**PROGRESS:** One line sent. Project complete.

**PROJECT 2: *MEC-9* SHORT TRANSCRIPTIONAL REPORTER**
**DVOR02 Extrachromosomal Array service: *mec-9*Sp::GFP::*tbb-2* transgene**
**DNA Construction**
pNU1416 - DVOR02 - *mec-9*Sp::GFP::*tbb-2* extrachromosomal array
Project component complete.
**Transgenic Injections and Screening**
NU1416 - DVOR02 - extrachromosomal array injections and screening
**SCOPE:** Project component objective is to generate an extrachromosomal array-harboring animal, as part of the DVOR02 project at Knudra. Transgenesis requires 1 client-specific plasmid pNU1416. The plasmid contains *mec-9*Sp::GFP::*tbb-2* and the *unc-119*-rescue selection cassette. The DNA mix is injected into gonads of 3 sets of 10x in the *unc-119* background strain. Injected animals are screened for crawling transgenics in F2 populations to select germline transmitting arrays. Populations from singled F2 are chunked to save copy. Copy is sent to client.
**PROGRESS:** Oligos in design.
**PROGRESS:** Oligos received and used for PCR. PCR amplification parts were used in a Gibson ligation and transformation resulting in 8 colonies. Four of these were screened by RE digest and three gave the expected banding pattern Two candidates were sent for sequencing and both were confirmed to be correct. Project component complete.
**PROGRESS:** Completion of the plasmid has activated this project. We are preparing the plasmid to create an injection mix.
**PROGRESS:** Injections were performed. Five plates were identified as having crawlers in the F1 generation. We are now waiting to see if the arrays are heritable in the F2 generation.

**PROGRESS:** One line confirmed and being prepped to send.
**PROGRESS:** One line sent. Project complete.

**Project 3: *mec-9* short translational reporter**

**DVOR03 Extrachromosomal Array service: *mec-9*Sp::GFP::*MEC-9*S::*mec-9*utr transgene**

DNA Construction

pNUXXX_1 - DVOR03 - *mec-9*Sp::GFP::*MEC-9*::*mec-9*utr extrachromosomal array

**SCOPE:**

Project component objective is to create the extrachromosomal array, where GFP::*MEC-9*S is expressed under the *mec-9*S promoter. This project requires a transgenesis plasmid for creating the extrachromosomal array, *mec-9*S::GFP::*MEC-9*S::*mec-9*utr, as part of the DVOR03 project at Knudra. Project is assembled from 2 parts. Part 1 is a plasmid backbone and *mec-9*p::GFP as PCR amplified material. Part 2 is 3kb of *MEC-9*S::*mec-9*utr as PCR amplified material. Final plasmid is assembled by Gibson ligation technique. Transformant DNA is screened by RE digest for proper size. Candidates are confirmed by DNA sequencing of appropriate coding regions.

Transgenic Injections

NUXX1 - DVOR03 - extrachromosomal array injections

SCOPE:

Project component objective is to generate an extrachromosomal array-harboring animal, as part of the DVOR03 project at Knudra. Transgenesis requires 1 client-specific plasmid pNUXXX. The DNA mix is injected into gonads of 3 sets of 10x in the *unc-119* background strain.

Transgenic Capture

NUXX1 - DVOR03 - *mec-9*Sp::GFP::*MEC-9*S extrachromosomal array

**SCOPE:**

Project component objective is to perform screening as part of the DVOR03 project at Knudra. Transgenesis requires 1 plasmid. The plasmid contains *mec-9*Sp::GFP::*MEC-9*S::*mec-9*utr and the *unc-119*-rescue selection cassette. Injected animals are screened for crawling transgenics in F2 populations to select germline transmitting arrays. Populations from singled F2 are chunked to save copy. Copy is sent to client.

**PROGRESS:**

Requires completion of DNA component before start.

**PROGRESS:**

We redesigned the oligos and used special amplification conditions to generate a PCR product. The products were used in a Gibson ligation and transformation. Colonies were tested by RE digest for the correct banding pattern. 2 plasmids were sent for sequencing and came back as correct. Project component complete.

**PROGRESS:**

An injection mix was made, and injections were performed. Screening begins next week.

**PROGRESS:**
Screening identified 2 candidates. These appear to be stable array lines, but we are waiting one more generation to confirm that the array is transmissible.
**PROGRESS:**
Our two candidates did not confirm as stable arrays. We have repeated the injections and screening begins later this week.
**PROGRESS:**
From the second injections, again we did not get stable array lines. For both injection sets we were able to observe transgenic animals, but unable to isolate heritable lines. Do you think there could be a toxicity issue? In the second injection set, we reduced the plasmid from 15ng/ul to 10ng/ul, but this did not result in any stable crawling lines. Do you think *mec-9* overexpression could have an effect on movement?
**PROGRESS:**
We rescreened the latest injections and identified 2 stable lines with low heritability. We are now working to clean these animals and examine them for GFP expression.

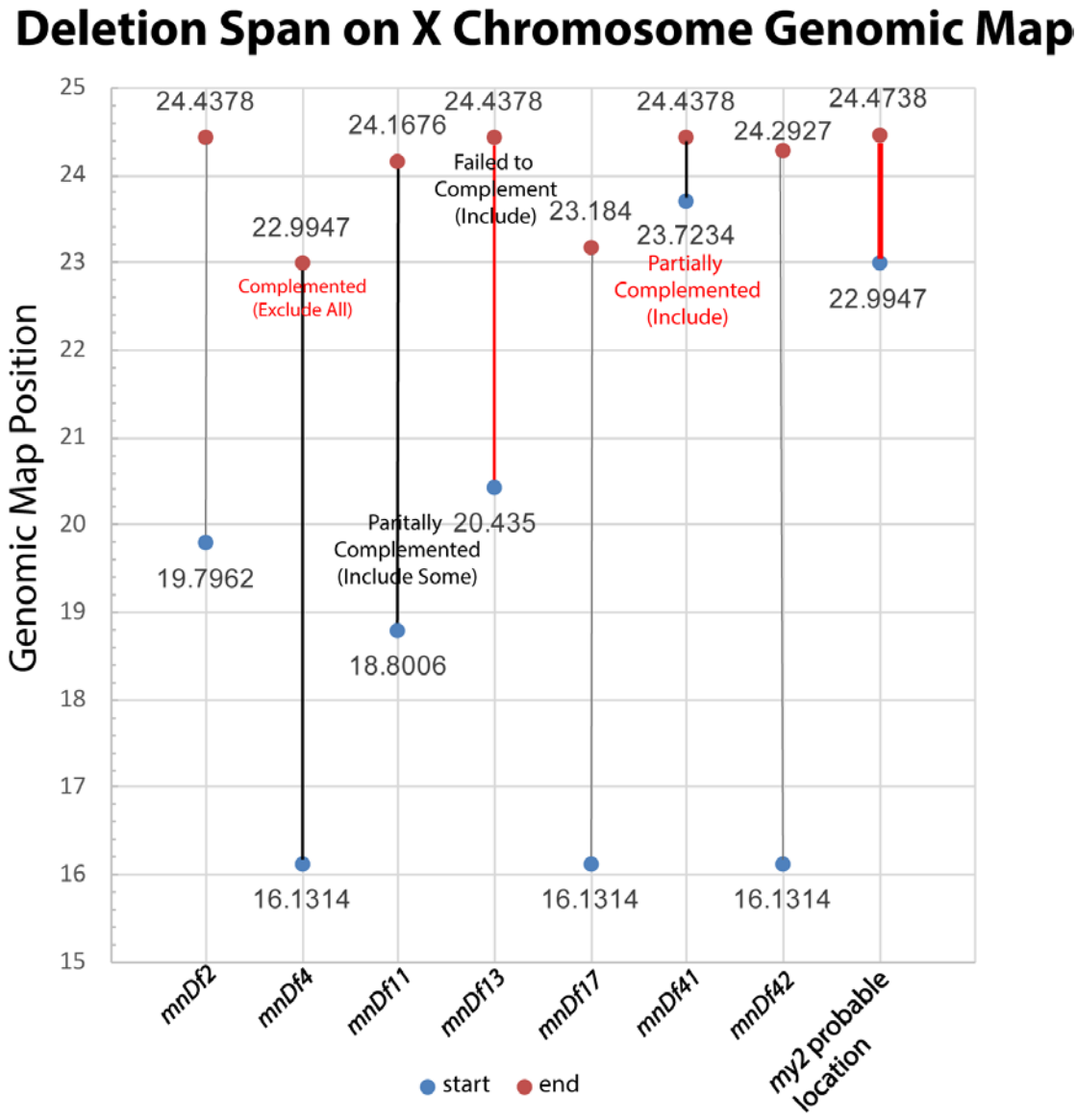


**Figure 3.1 Map of deficiency strains used to identify *my2* region** Strains in grey and black complemented the temperature sensitivity sterility phenotype of *my2* hermaphrodites. (Figure 3.2) End of *mnDf4* used as start boundary for possible *my2* locus. End of *mnDf13* used as end boundary of possible *my2* locus

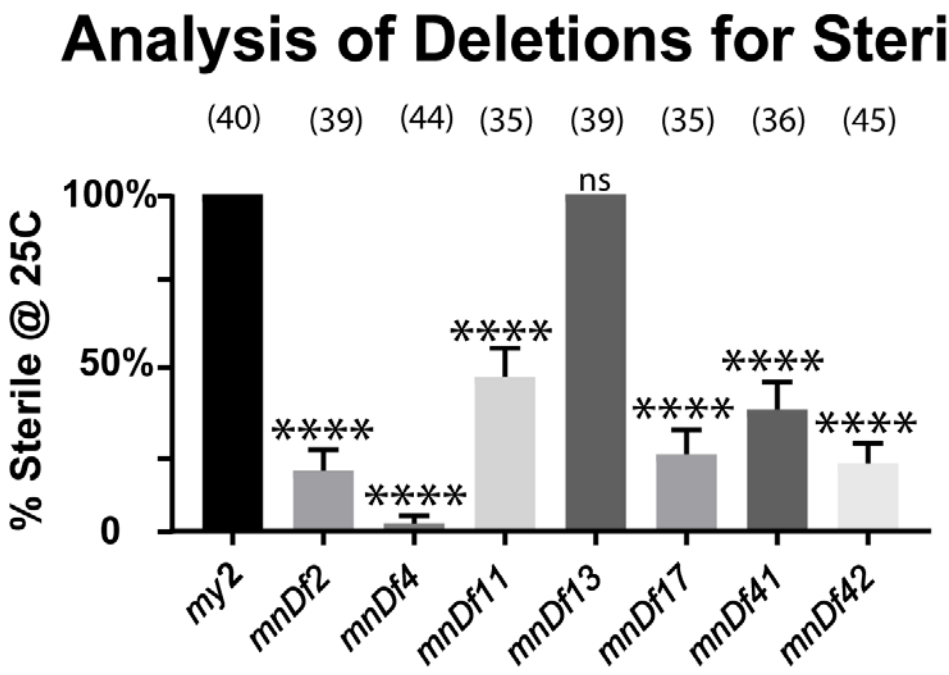


**Figure 3.2 *my2* was in deficiency 13, not in deficiency 4** Deficiency mapping and complementation analysis supported probable location of *my2* between 22.9947-24.4738 on genomic map. *mnDf11*, *mnDf13,* and *mnDf41* more similarly phenocopied (failed to complement) the *my2* 25C sterility. *mnDf4* complemented *my2*, so that area was excluded as a possibility. Significances determined by Kruskal-Wallis test; p values compared by Dunn's multiple comparisons test. ****p<0.0001; ns=not significant.

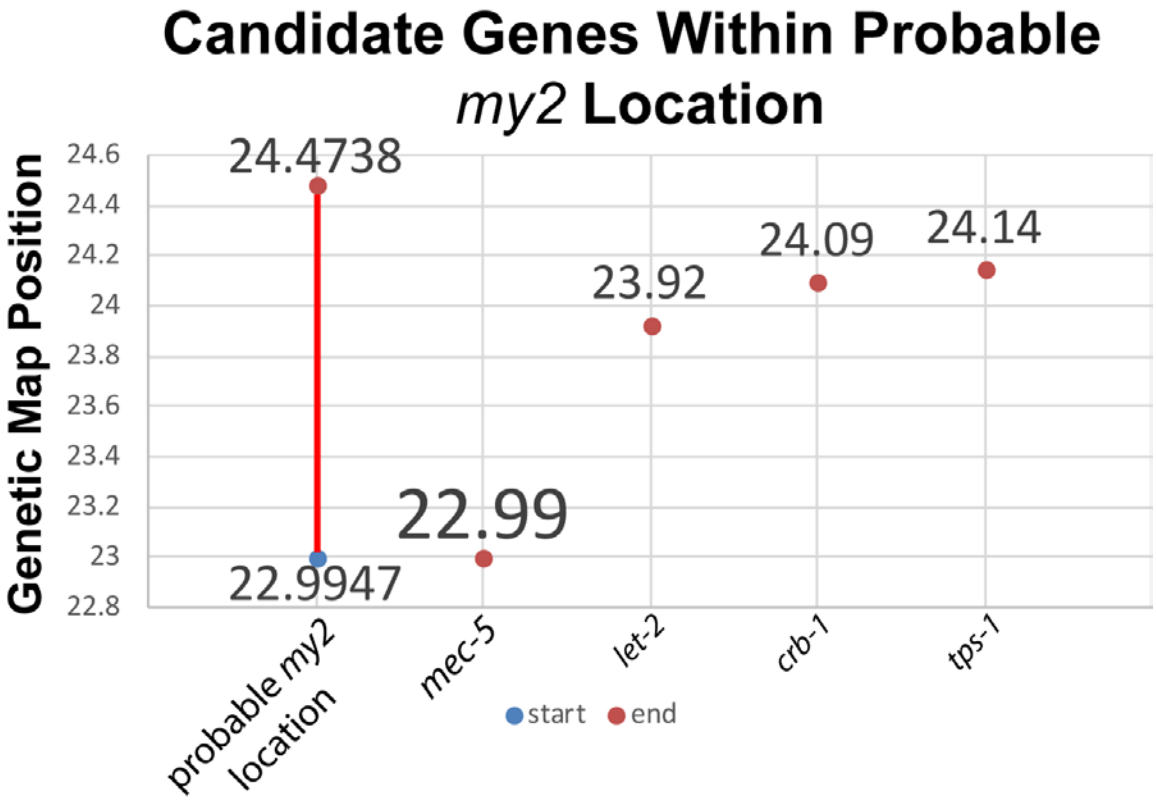


**Figure 3.3 Whole genome sequencing identifies *my2* candidates** Identification and genetic map location of genes with lesions in *cil-2(my2)*. Alleles of these genes tested for temperature sensitivity and ciliary localization (Figures A.4—5).

Table 3.1

| length | per locus 5way conservation | reference base | sample base | consensus score | sequencing depth | variant type | class | description | parent features | gene |
|---|---|---|---|---|---|---|---|---|---|---|
| 1 | 1 | C | T | 36 | 16 | point | missense | GGA->AGA[Gly->Arg] | F01G12.5a,F01G12.5b.1, F01G12.5b.2 | *let-2* |
| 1 | 0 | C | T | 34 | 21 | point | missense | GGA->GAA[Gly->Glu] | F11C7.4 | *crb-1* |
| 1 | 0.07 | G | A | 8 | 8 | point | missense | CGC->TGC[Arg->Cys] | ZK54.2a,ZK54.2b.1, ZK54.2b.2,ZK54.2b.3 | *tps-1* |
| 1 | 0 | G | T | 29 | 11 | point | nongenic | 1815 into | E03G2.3 | *mec-5* |
| 1 | 0 | G | T | 31 | 11 | point | nongenic | 1816 into | E03G2.3 | *mec-5* |
| 1 | 0 | A | T | 31 | 11 | point | nongenic | 1827 into | E03G2.3 | *mec-5* |

**Table 3.1 Raw whole-genome sequencing data for *my2*** Partial data from Hobert Lab showing the *my2* vs WT variants within X:22.9947-24.4738, the area of interest we determined from deficiency mapping. The length (Column 1 heading) refers to number of bases. Reference base is the base in WT, sample base is the base in *my2.* Consensus score is an algorhithmic value used to determine if the change seen can be considered a “real” mutaion: should be ≥3. Sequencing depth is the number of times it was sequenced from the different fragments in the sample: should be >3. Variant type describes the type of genetic differenc: ex-point, deletion, etc. Class is the type of mutation. Description is the location relevant to the gene. Parent feature is the gene number and gene name is given if gene has been previously characterized. All descriptions and explanations garnered through direct contact with Dr. Richard Poole in the Hobart Lab (Columbia University).

**Figure 3.4 Locations of *my2* lesions in candidate genes** These are schematics of genes that have lesions in *my2* within the 22.9947-24.4738 genetic map positions, an area identified by deficiency mapping (Figure 3.1). *let-2, tps-1,* and *crb-1* lesions are missense, point mutations in coding areas. The three lesions in *mec-5* (denoted by black box) are point mutations in the non-coding third intron (see Figure 1.11 for other known *mec-5* alleles used in this study). Red stars indicate sites of point mutations. Scale bars represent 500 bases. Domain information for *let-2*(ZK54.2a), *crb-1*(F11C7.4) and *mec-5*(E03G2.3) from Uniprot (Nucleic acids research.2018). Domain information for *tps-1*(ZK542.b.1) from *e!ensemble* (Daniel R. Zerbino, et al, 2018).

**Figure 3.4 Locations of *my2* lesions in candidate genes**

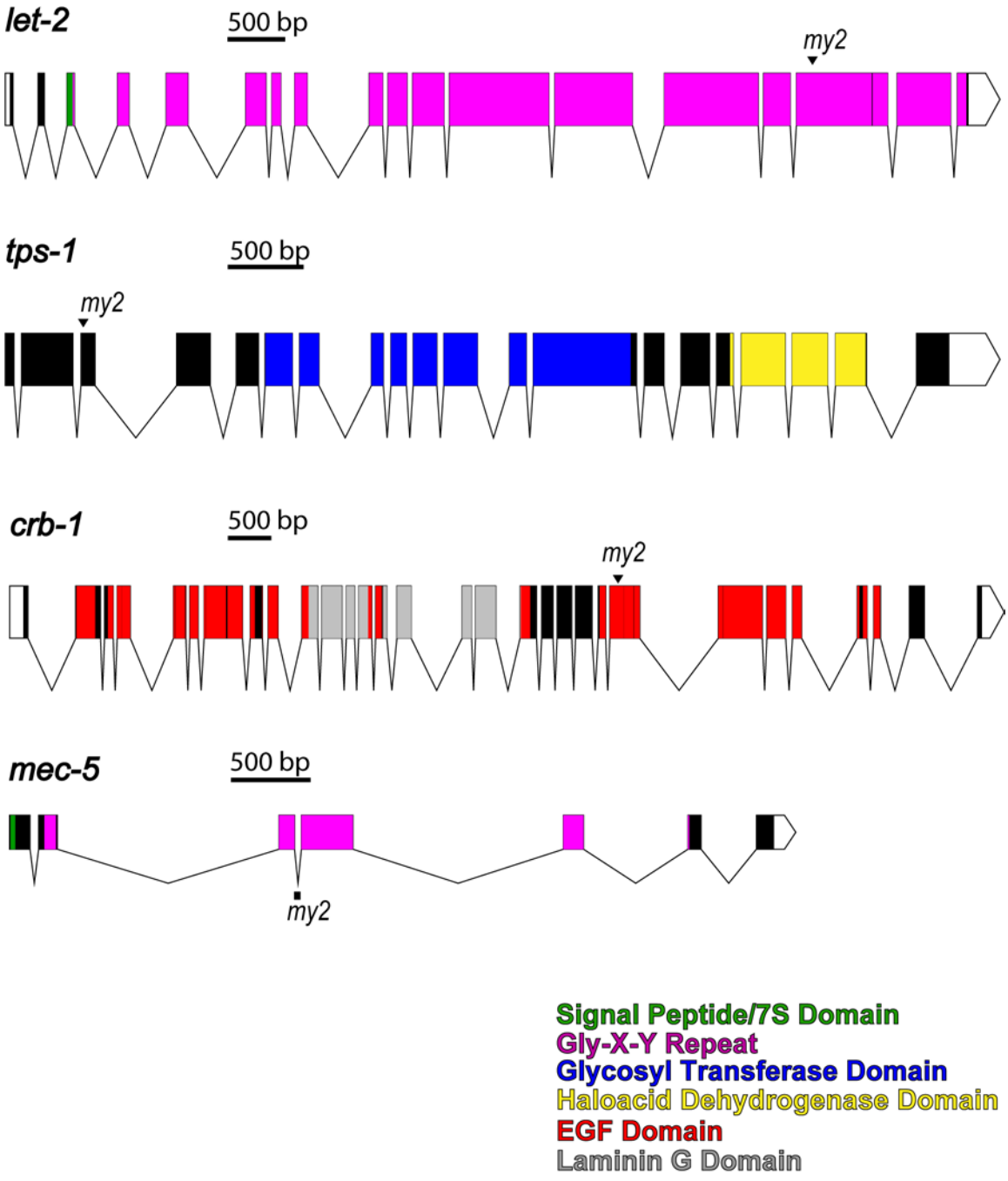

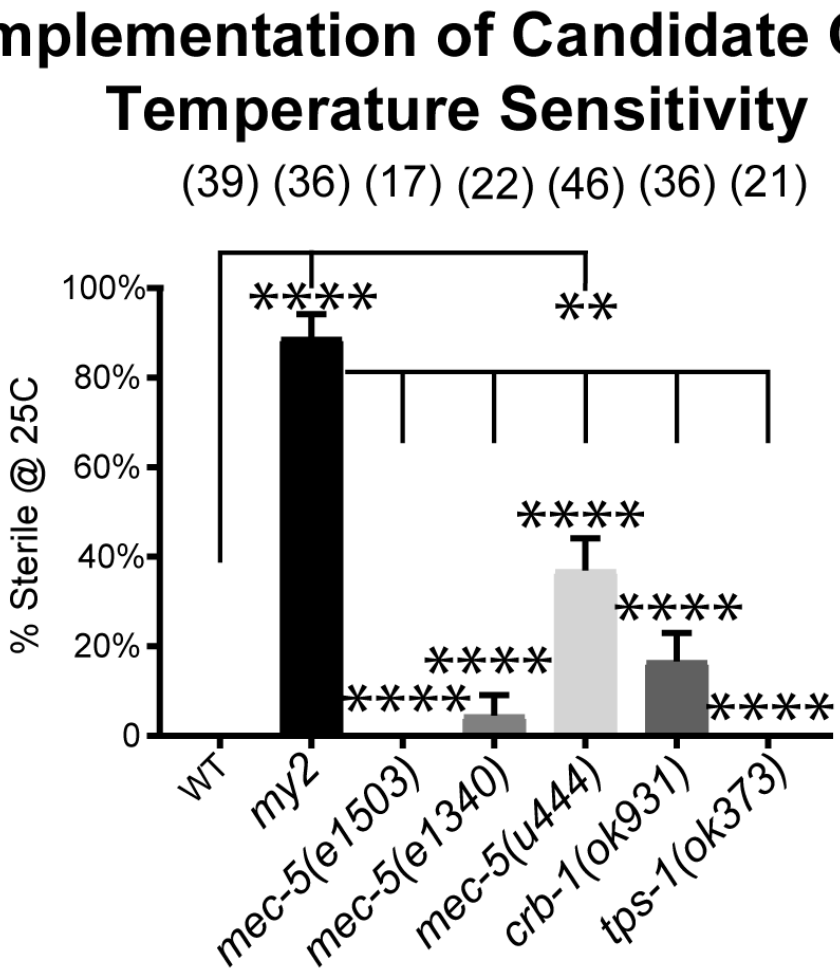


**Figure 3.5 *mec-5(u444)* complements sterility at 25C.** Two of three *mec-5* alleles complement sterility at 25C. *mec-5(u444),* the *mec-5* null allele does not fully complement *my2* sterility at 25C. *mec-5(e1503)* and the other candidate *my2* genes complemented temperature sensitive Ste. *my2* temperature sensitive sterility and PKD-2::GFP ciliary localization defect may not be linked. Significance measured by Kruskal-Wallace test, comparisons made using Dunn's multiple comparisons. **p<0.01; ****p<0.0001.

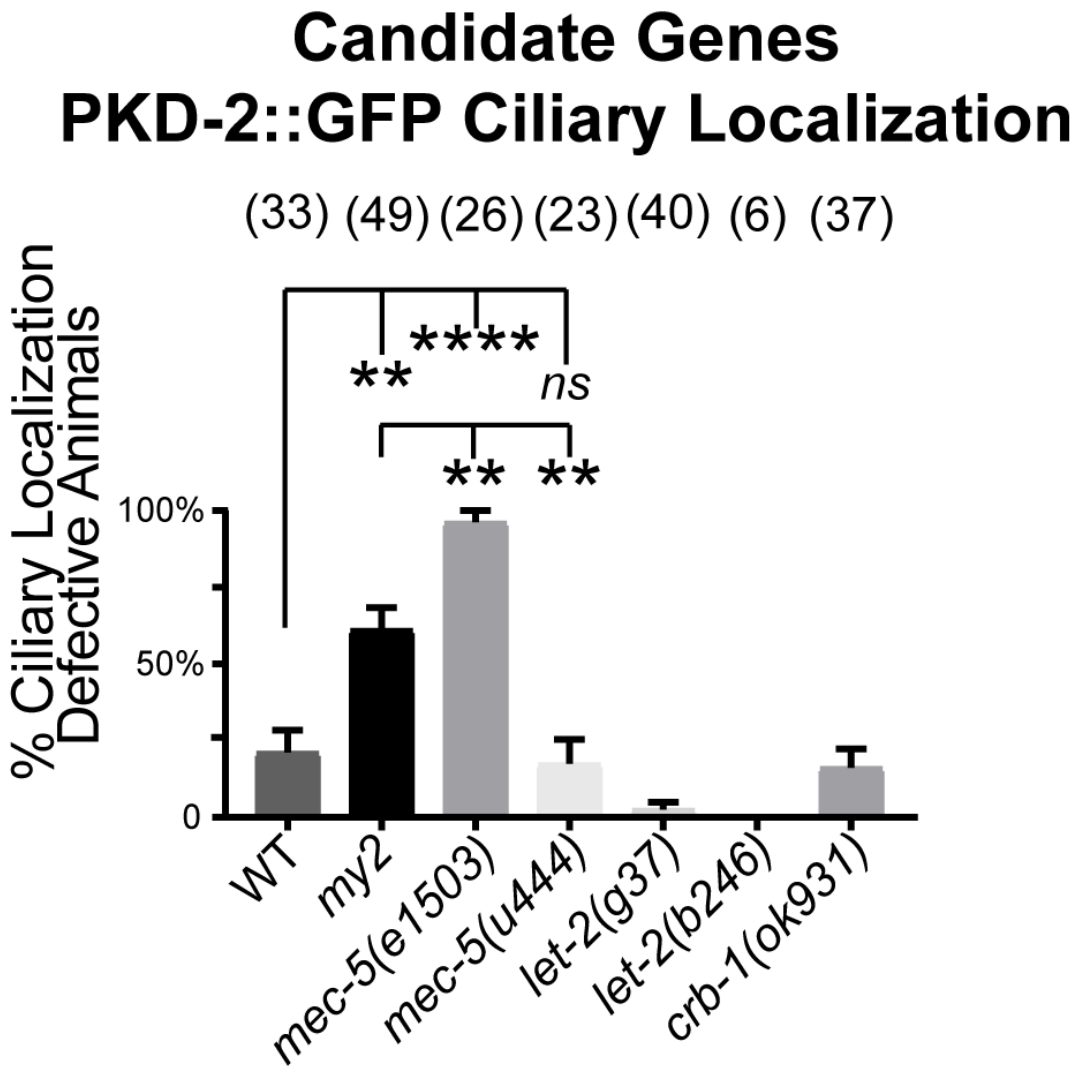


**Figure 3.6 *mec-5(e1503)* was severely defective in PKD-2::GFP localization.** Whole genome sequencing identified four candidate genes with lesions in the determined "probable *my2* location". *mec-5* alleles presented with marked ciliary localization defects. *mec-5(ok3313)* animals were difficult to maintain and therefore were not further characterized. *let-2* alleles were not tested for sterility; *let-2* is already known to be lethal at 25C. Significance measured by Kruskal-Wallace test, comparisons made using Dunn's multiple comparisons. **p<0.01; ****p<0.0001.

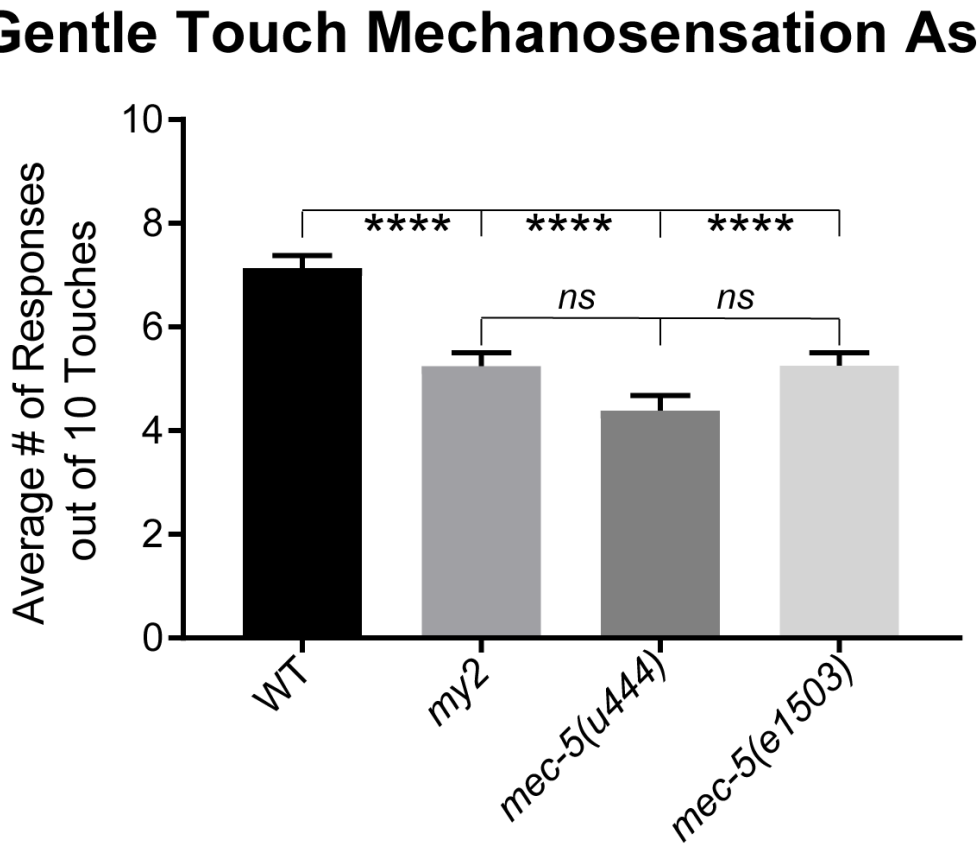


**Figure 3.7 *my2* is a mec gene** *my2* is gentle touch defective, characteristic of the Mec mutants. *mec-5(u444)* is the null mutant. Significance measured by Kruskal-Wallace test, comparisons made using Dunn's multiple comparisons. n=90 worms for each allele ****p<0.0001.

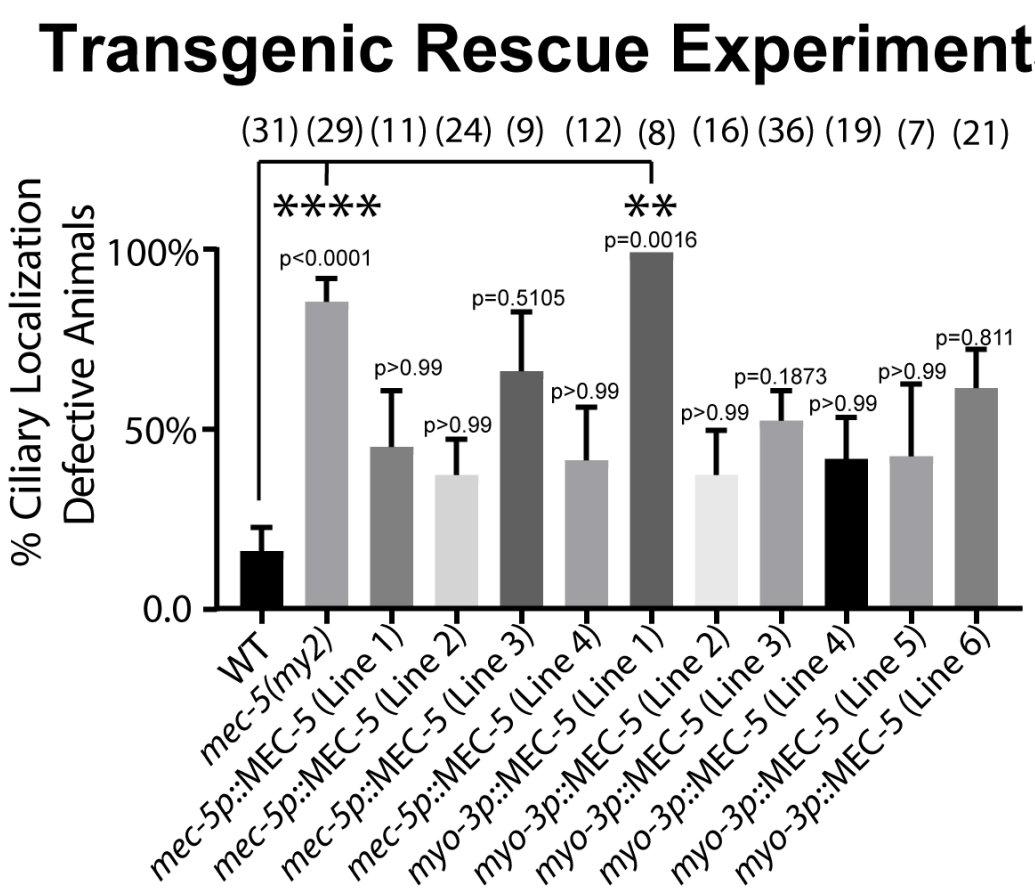


**Figure 3.8 *mec-5(+)* rescues *my2* ciliary localization defect and is cell non-autonomous** *mec-5p::*MEC-5 and *myo-3p::*MEC-5 constructs can rescue PKD-2::GFP ciliary localization in nine out of ten transgenic lines. Significance measured by Kruskal-Wallace and Dunn's multiple comparisons tests. P values shown are compared to WT value. **p<0.01, ****p<0.0001.

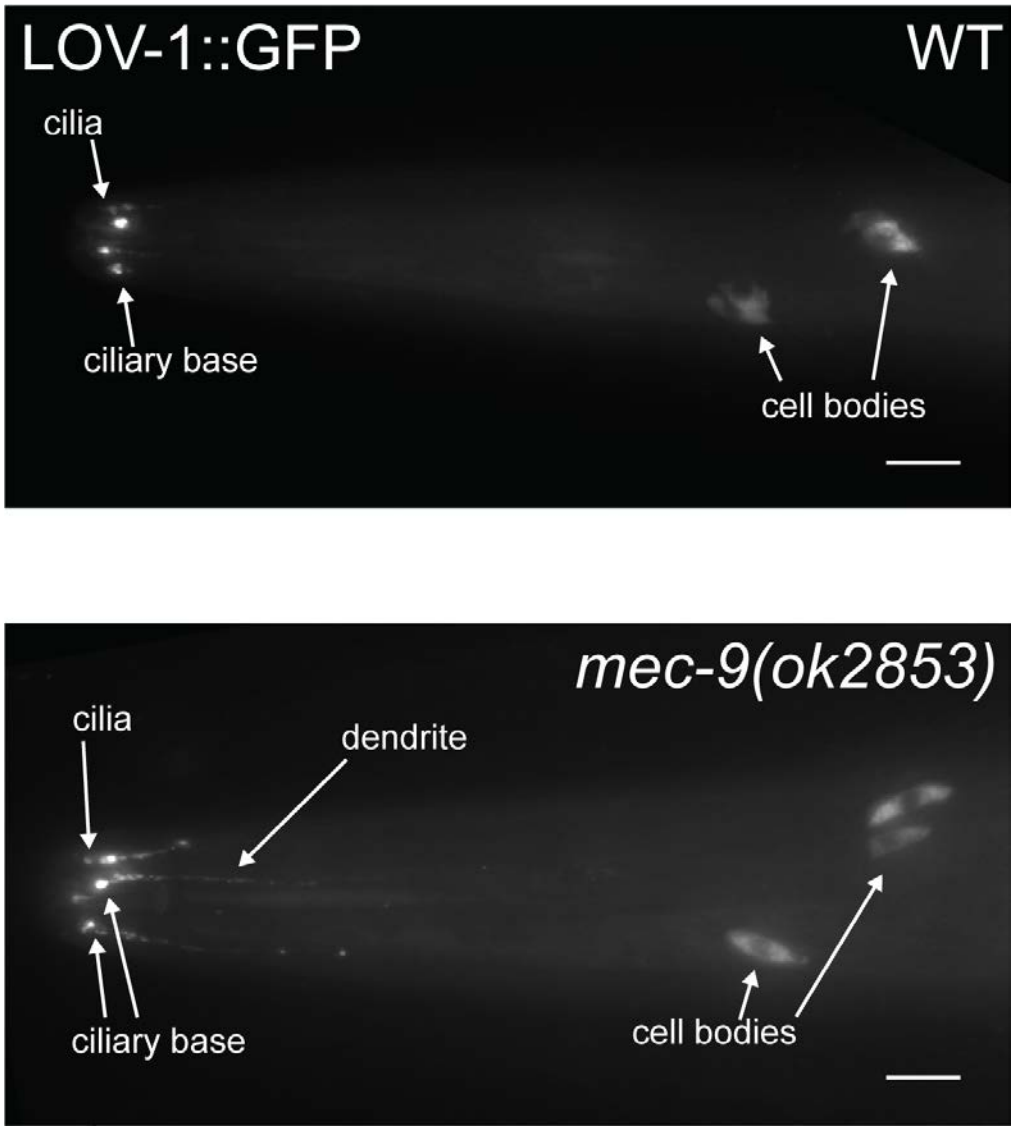


**Figure 3.9 MEC-9 regulates localization of both *C. elegans* polycystins** LOV-1::GFP mislocalizes to CEM distal dendrites in mutant animals. Scale bar is 10 µm.

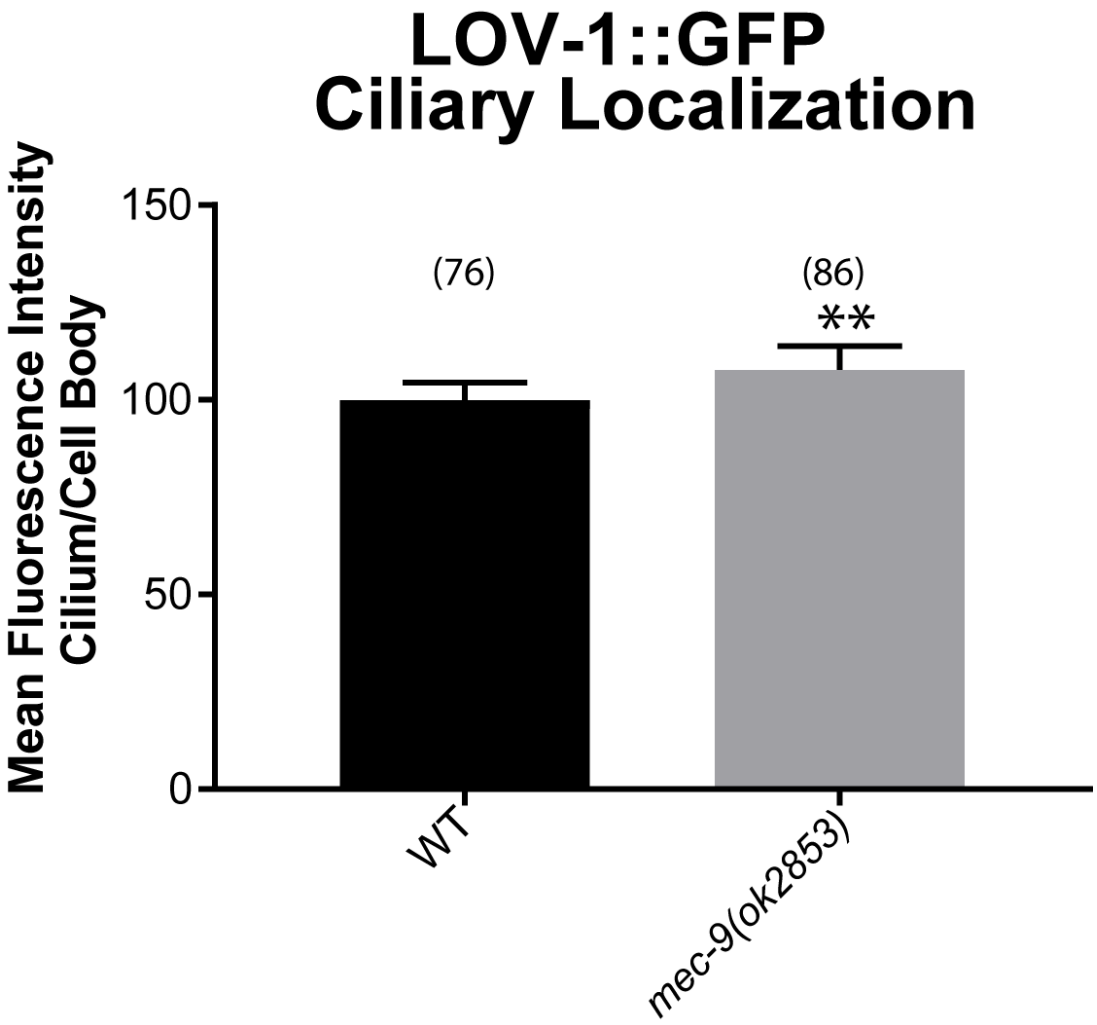


**Figure 3.10 MEC-9 regulates LOV-1::GFP ciliary localization: Fluorescence Intensity quantification** Quantitative measurement of fluorescence intensity in *mec-9* mutants reveal an abundance of LOV-1::GFP at the cilia and cilium proper of male specific CEM neurons when in ratio to CEM cell body. Various measurements were done for maximum and mean fluorescence intensity and for ratio and stand-alone neuronal parts. (Table 3.1) Significance measured by Mann-Whitney test. **p<0.01

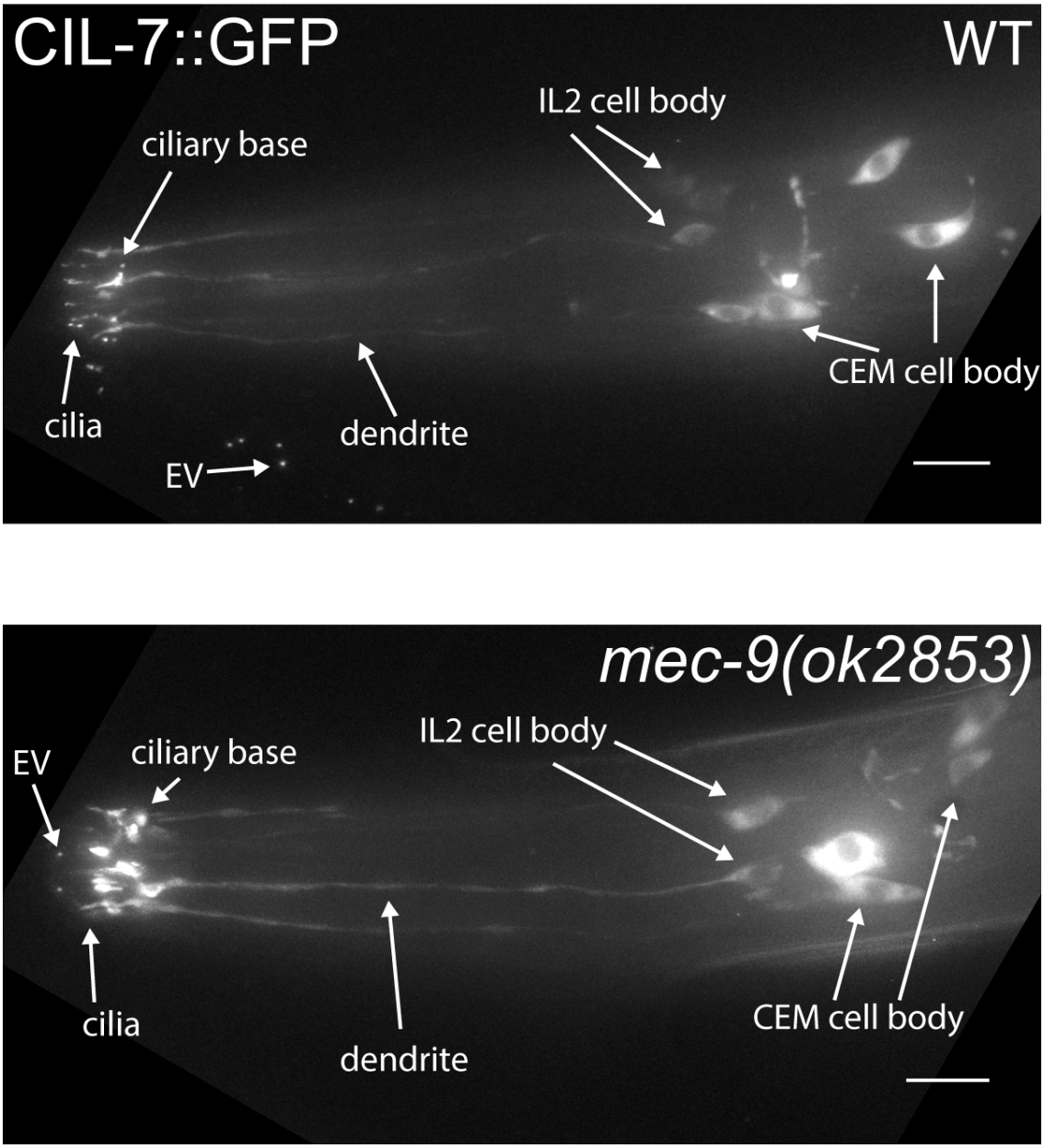


**Figure 3.11 *mec-9* regulates CIL-7::GFP localization** CIL-7::GFP highlights IL2 and CEM neurons in the male head and RnB and HOB tail neurons (not shown). In *mec-9* males, notice the increased accumulation of CIL-7::GFP at ciliary bases of CEM and IL2 neurons, reminiscent of PKD-2::GFP accumulation in the CEM neurons (Figure 2.x). Varicosities are observed in IL2 distal dendrites. Scale bar 10 µm.

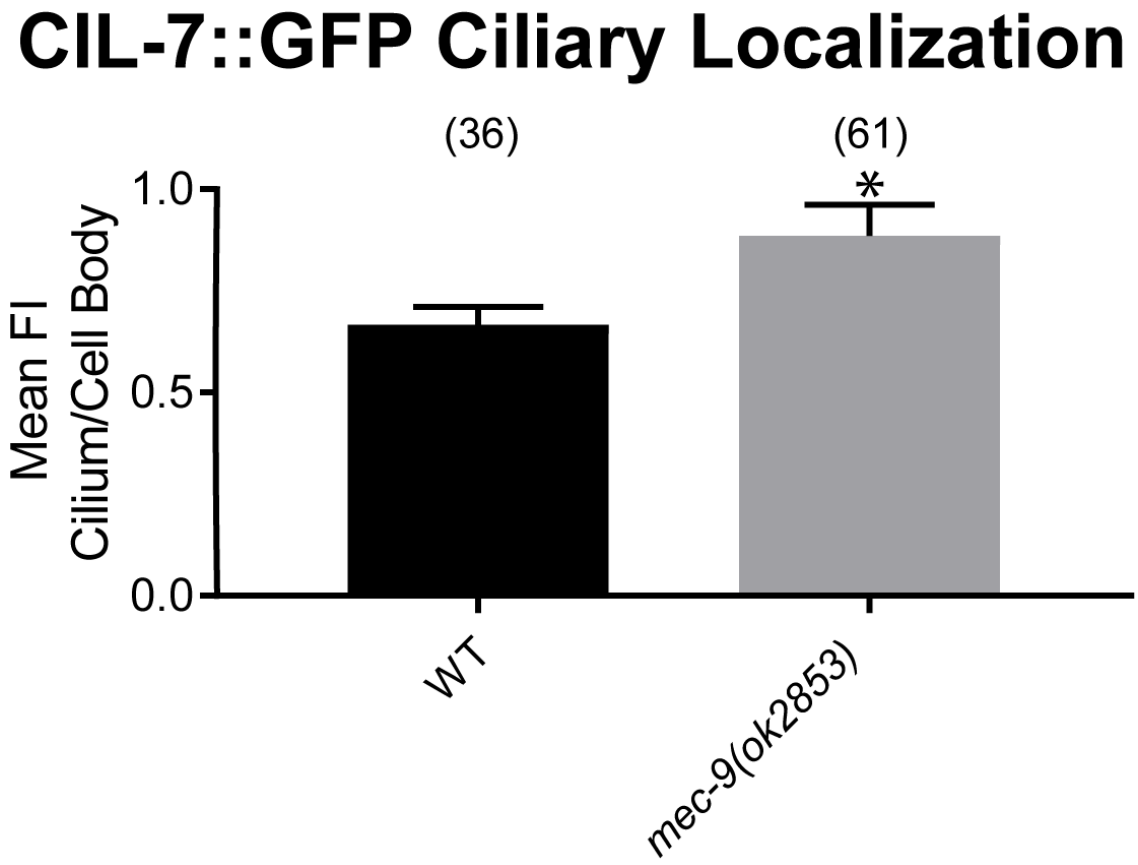


**Figure 3.12 MEC-9 regulates CIL-7::GFP localization.** Quantitative measurement of fluorescence intensity in *mec-9* mutants reveal an abundance of CIL-7::GFP at the cilia and cilium proper of IL2 and male specific CEM neurons when compared in ratio to IL2 and CEM cell bodies. Significance measured by Mann-Whitney test. *$p<0.05$

**Figure 3.13 *mec-9(ok2853)* has no CIL-7::GFP EV release defect** Though *mec-9(ok2853)* animals have a similar ciliary localization defect (Figure 3.11) as that found with PKD-2::GFP (Figure 2.1 H), there is no CIL-7::GFP EV release defect in the male head or tail. Significance measured by Mann-Whitney test. Head p=0.1320, tail p=0.7368.

**Figure 3.13 *mec-9(ok2853)* has no CIL-7::GFP EV release defect**

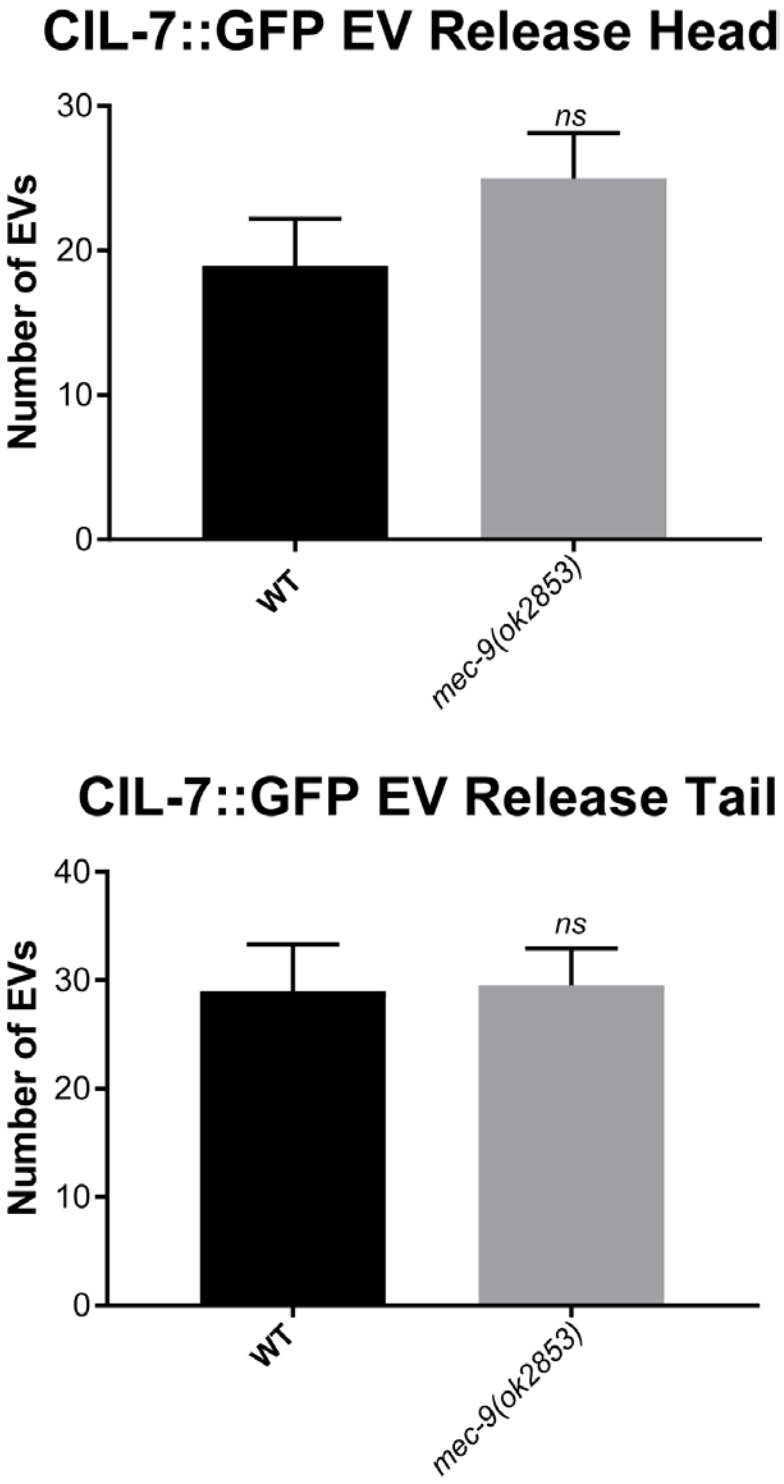

**Figure 3.14 *MEC-9* is not active in IL2 dauer branching.** Top: Oblique transverse schematic of dauer IL2 branching. M, muscle; P, pharynx; H, hypodermis (Schroeder et al., 2013). IL2 cell body is near the pharynx with secondary branching through hypodermis, terminating in perimuscular tertiary and quaternary branching. Bottom: *mec-9* looks like WT. Secondary, tertiary, and quaternary branching are noted. There is no extensive branching in *kpc-1* mutant. There is no obvious dauer branching phenotype during dauer in *mec-9(ok2853)* mutants.

**Figure 3.14 *MEC-9* is not active in IL2 dauer branching.**

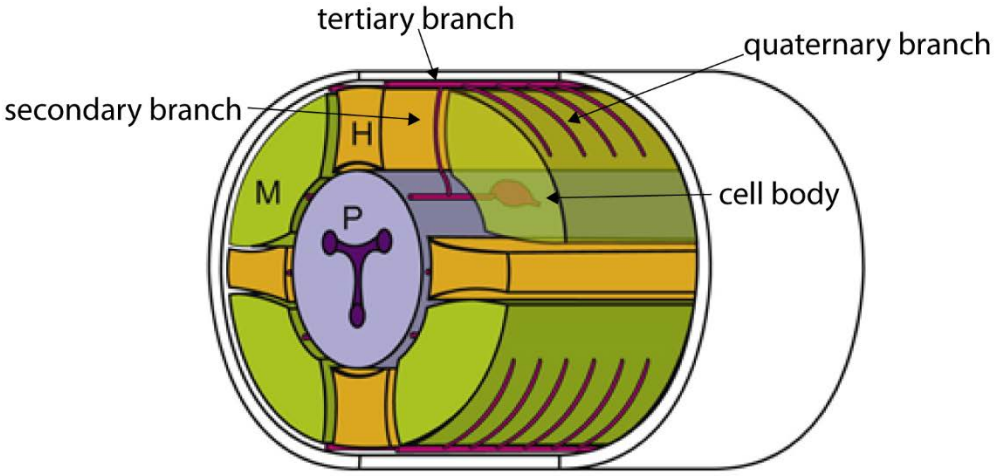


Adapted from Schroeder et. al, *Current Biology* 2013 23, 1527-1535

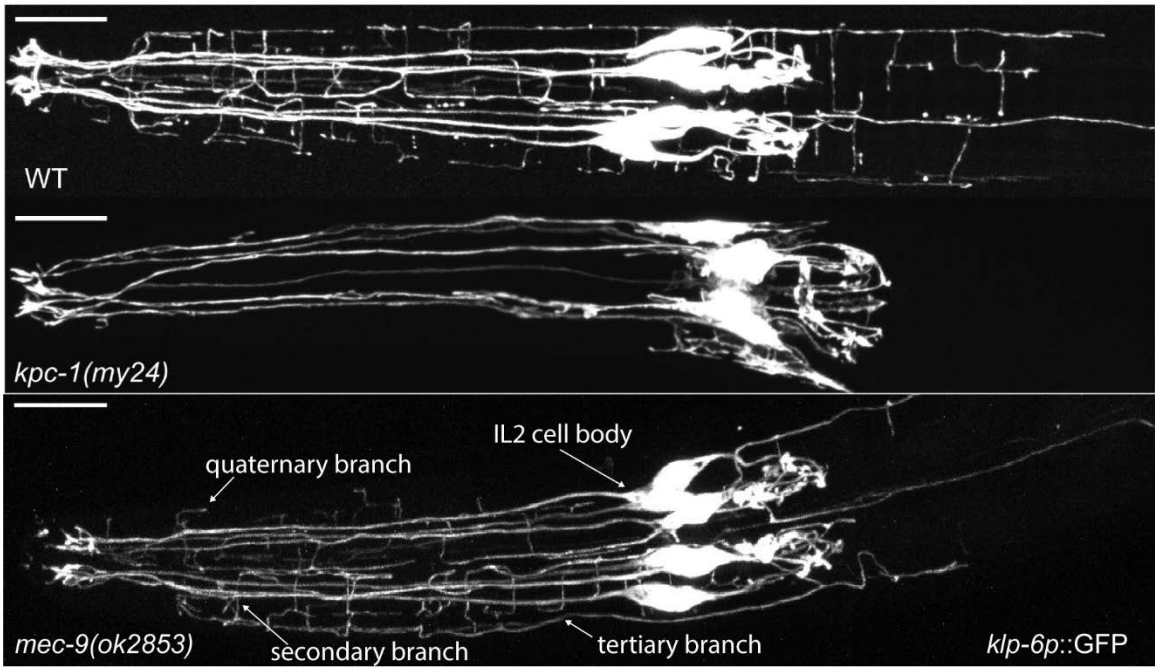

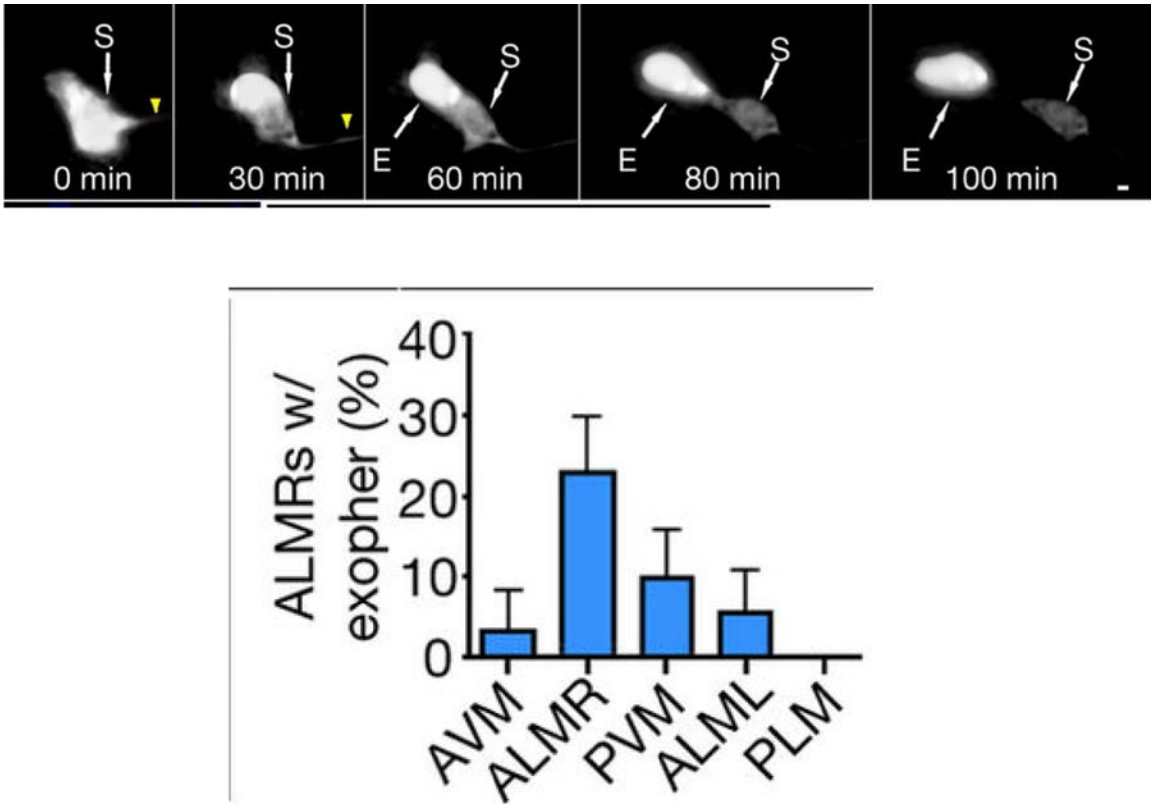


**Figure 3.15 Exophers are released from cell body** Time lapse imaging show exopher budding and release in the soma of the ALM touch neuron. Notice the bright fluorescence then eventual division into a bright exopher and a dim soma (cell body) (Top image; E, exophers; S, soma. Scale bar, 2 μm.) This phenomenon occurs often and in different but not all neurons, as seen in graph of touch neurons. (Bottom) Individual touch neurons differ in their production of detectable exophers. *n* > 500 total for each neuron. Images and data reproduced from Nature 2017 (Ilija Melentijevic et al., 2017)

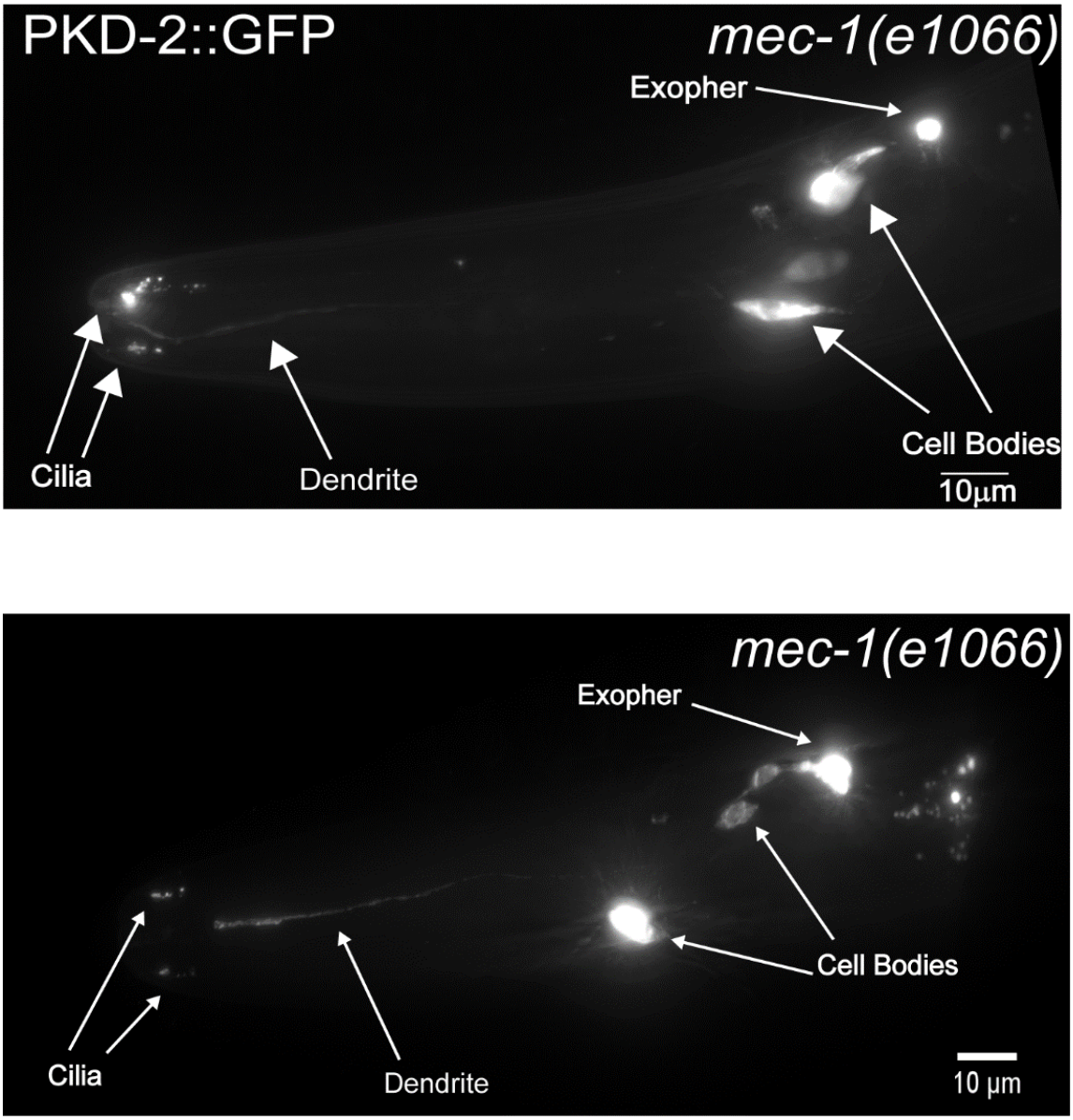


**Figure 3.16 *mec-1(e1066)* exopher release** The top and bottom figure show bright extra-somal bodies posterior to CEM cell bodies. Notice the difference in fluorescence in the exopher and soma in bottom figure. In both these figures, there is also a defect in PKD-2::GFP ciliary localization.

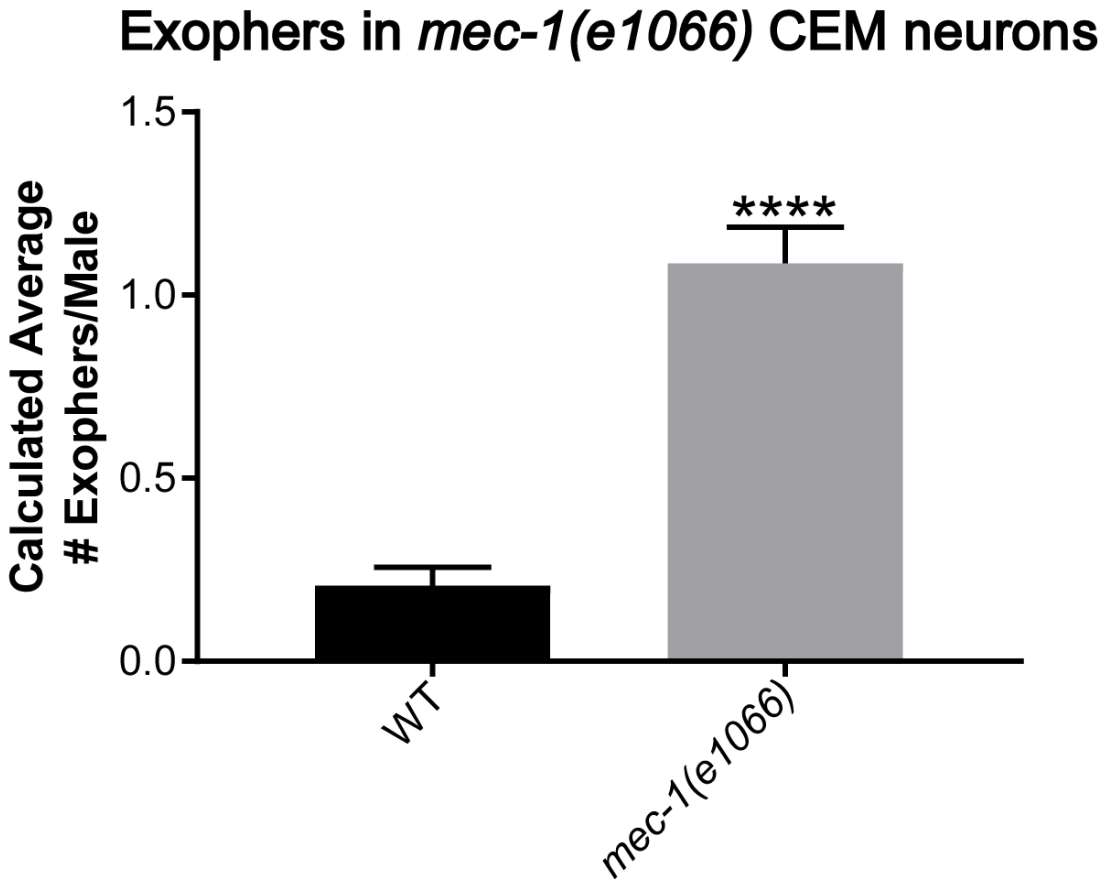


**Figure 3.17 *mec-1(e1066)* release significantly more exophers than WT** Exopher extrusions containing PKD-2::GFP were rarely observed in WT animals. Exophers observed in most *mec-1(e1066)* males. Significance determined by Mann-Whitney test. ****p<0.0001

PROJECT PLAN

**Timeline:**

| | |
|---|---|
| Antigen production and/or quality control | 30 *days* |
| Antibody production | |
| Immunization of four (4) Balb/c mice | *28 days* |
| Fusion, subcloning of 2 – 4 rounds and ELISA screening | 50 *days* |
| Ascites production | 12 *days* |
| Shipping arrangement | 7 *days* |

**Deliverables**

Samples: lyophilized ascites fluid samples of twelve (12) clones, 0.5 ml each

lyopholized decamer peptides of 12 antigens, 0.2 mg each

Data: Titer and epitope information of each clone, determined by ELISA using designed antigens.

**Validation criteria**

Each clone has ELISA titer ≥ 1:100,000 against the designed antigen.

**Figure 3.18 Project plan for anti PKD-2 antibody** timeline, contents, and validation information from direct Abmart correspondence.

**Table 3.2 List of epitopes for antibody production**

| Start | End position | Epitope sequences |
|---|---|---|
| 7 | 18 | DERWANPPQPVA |
| 21 | 32 | EHGPSFDHSMVS |
| 37 | 48 | HDKKKNPAQKEG |
| 57 | 68 | ASGHEKSDGKIK |
| 199 | 210 | EKLEDKTMVGDG |
| 395 | 406 | TNAPFDDVTSSE |
| 556 | 567 | MNKVRGLTKRGK |
| 564 | 575 | KRGKRPDAPGED |
| 603 | 614 | NVTSMTEHVPEK |
| 667 | 678 | TLQTIEKQRVQQ |
| 694 | 705 | QVRNRESAARRP |
| 702 | 713 | ARRPTITSIADK |

**Table 3.2 Two of twelve epitopes worked in *C. elegans* whole mount immunohistochemistry** Twelve epitopes were validated by ELISA at Abmart. I tested all and found two antibodies raised to N terminal and C located epitopes worked in whole-worm immunolocalization experiments (sequences in yellow).

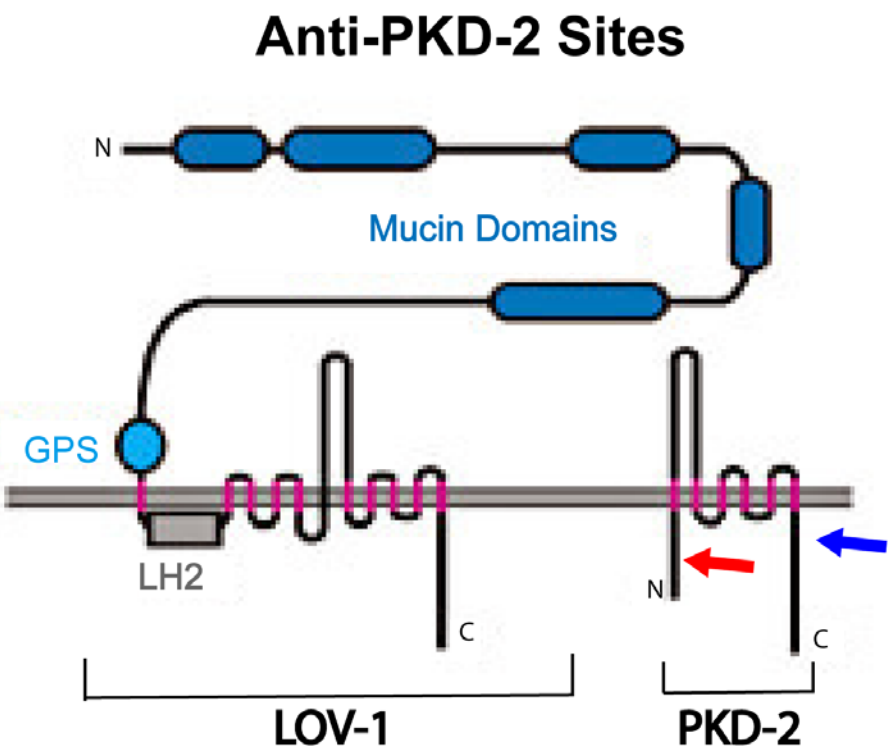


| amino acid start position | amino acid end position | Epitope sequences | Labels |
|---|---|---|---|
| 7 | 18 | DERWANPPQPVA | CEMs/Rays/Sperm |
| 564 | 575 | KRGKRPDAPGED | CEMs/Rays |

**Figure 3.19 N terminal and C terminal ab sites** Top image is a schematic of LOV-1 (left) and PKD-2 (right). Red arrow is the site of the PKD-2 peptide tagged by the N terminal epitope (see information in red in the table). Blue arrow is the site of the PKD-2 peptide tagged by the C terminal epitope (see information in blue in the table). Antibodies raised against the N and C terminal epitopes fluoresce intracellularly. The N terminal antibody may illuminate sperm (Figure 3.24). Both antibodies illuminate endogenous PKD-2 in expected male specific neurons of the head and tail, based on transgenic PKD-2::GFP expression patterns

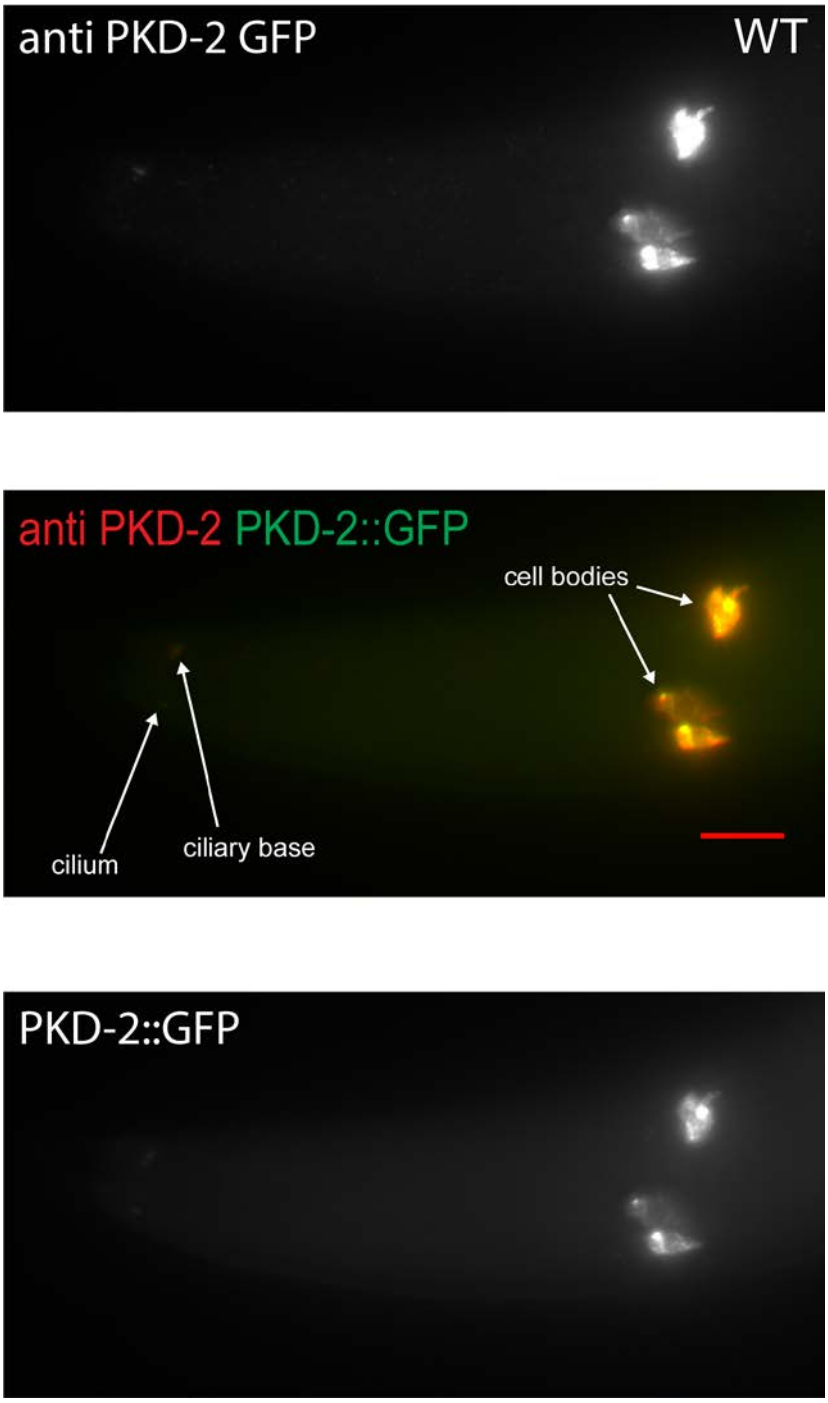


**Figure 3.20 Anti-PKD-2 ab in WT male** Antibody fluoresces in expected parts of CEM neuron. Shown here is the N terminal clone, C111. Notice cell body aggregates.

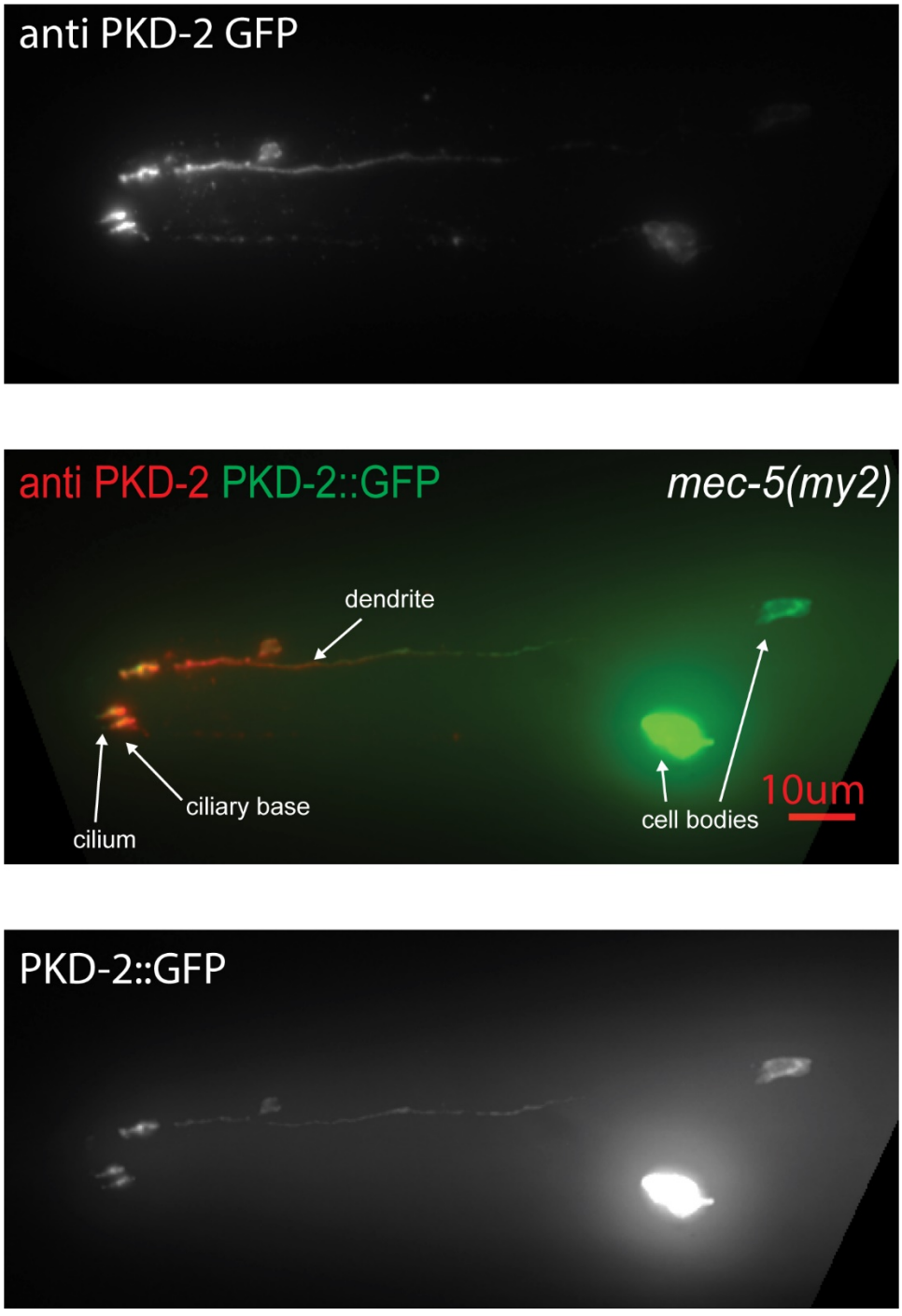


**Figure 3.21 Anti-PKD-2 in *mec-5(my2)* males** Characteristic extradendritic accumulation seen in both antibody and PKD-2::GFP. Shown here is C295, the non-aggregating, N terminus PKD-2 antibody.

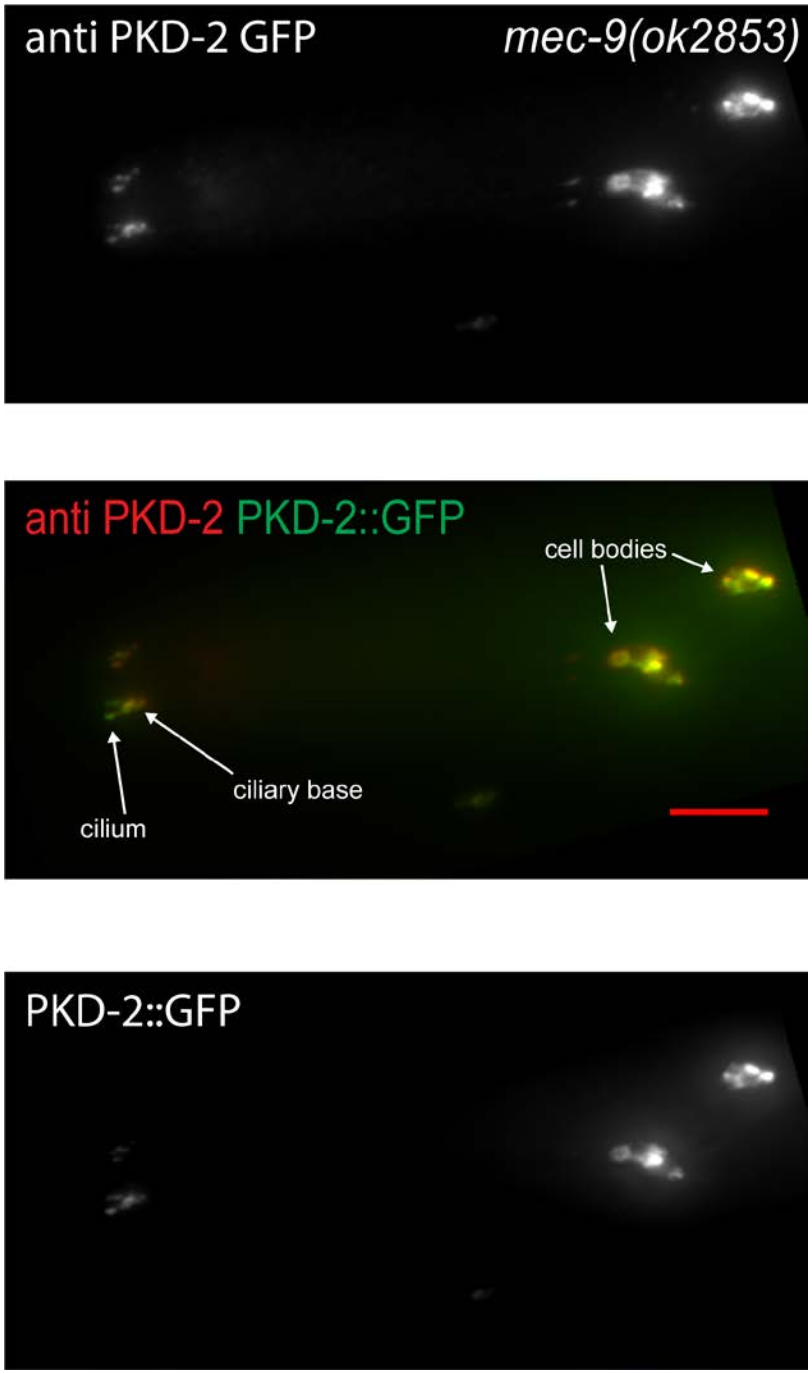


**Figure 3.22 Anti-PKD-2 in *mec-9(ok2853)*** No overt differences in PKD expression or intensity when anti-PKD-2 and PKD-2::GFP are noted. This is C111, an N-terminus PKD-2 antibody. Unlike C295, C111 aggregates in cell body.

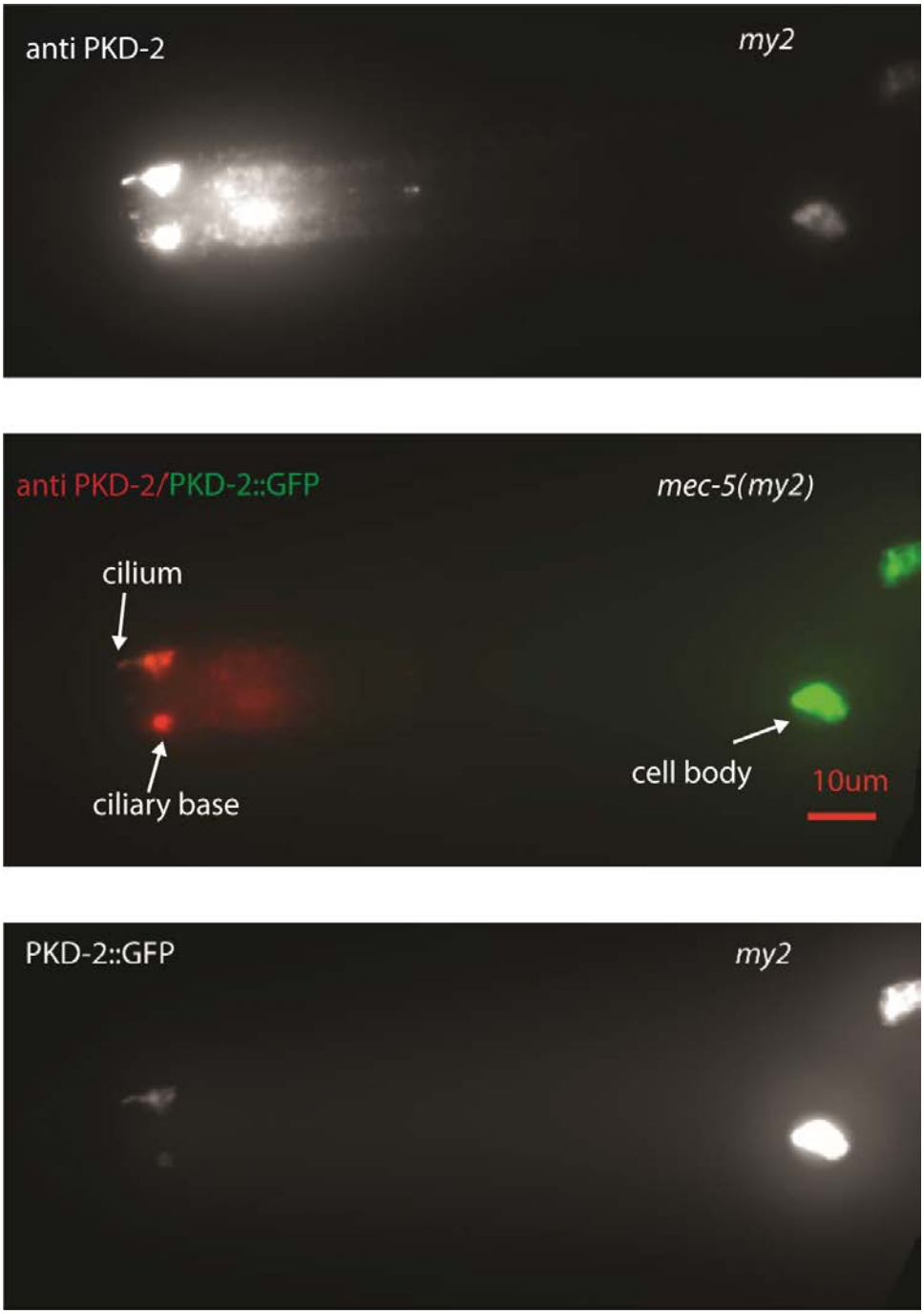


**Figure 3.23 Anti-PKD-2 in *mec-5(my2)*** This is C103, a C-terminus PKD-2 antibody. There is excess fluorescence at the nose of the anti PKD-2 image, possibly due to technician error.

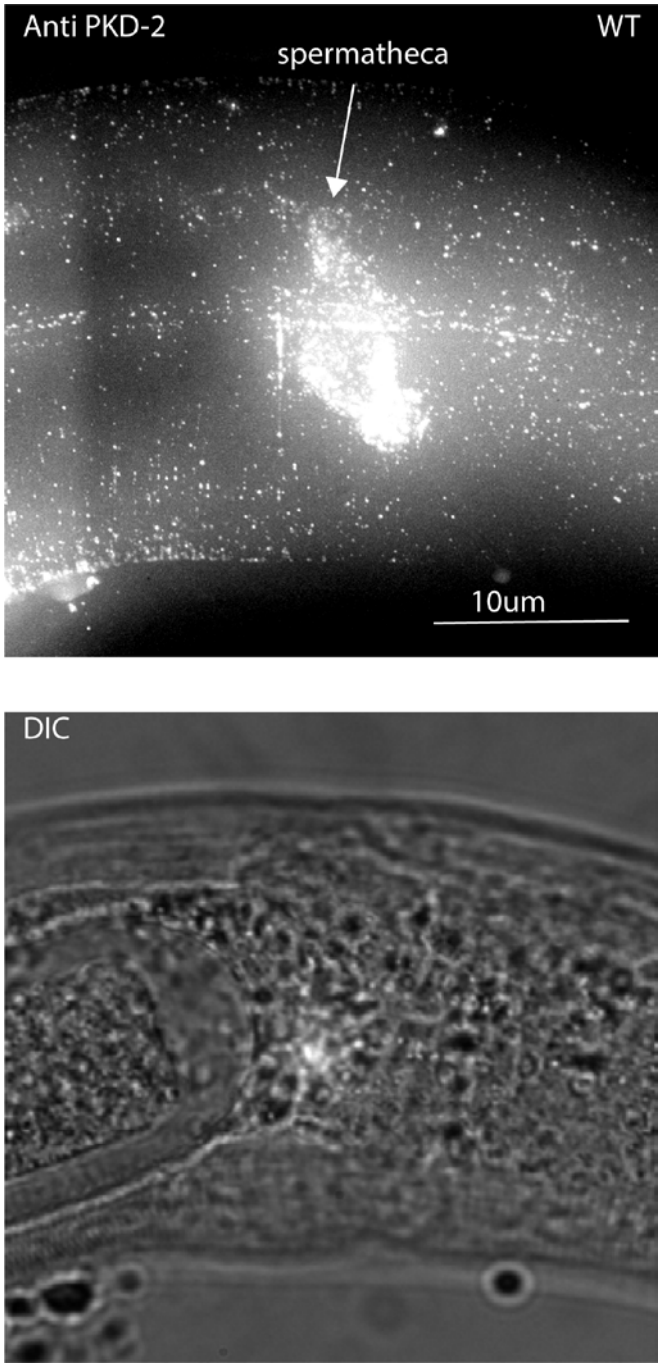


**Figure 3.24 Anti-PKD-2 in WT hermaphrodite spermatheca** This is C103, a C terminus tagging PKD-2 antibody that fluoresces in hermaphrodite spermatheca. 100x magnification. Scale bar 10 µm.

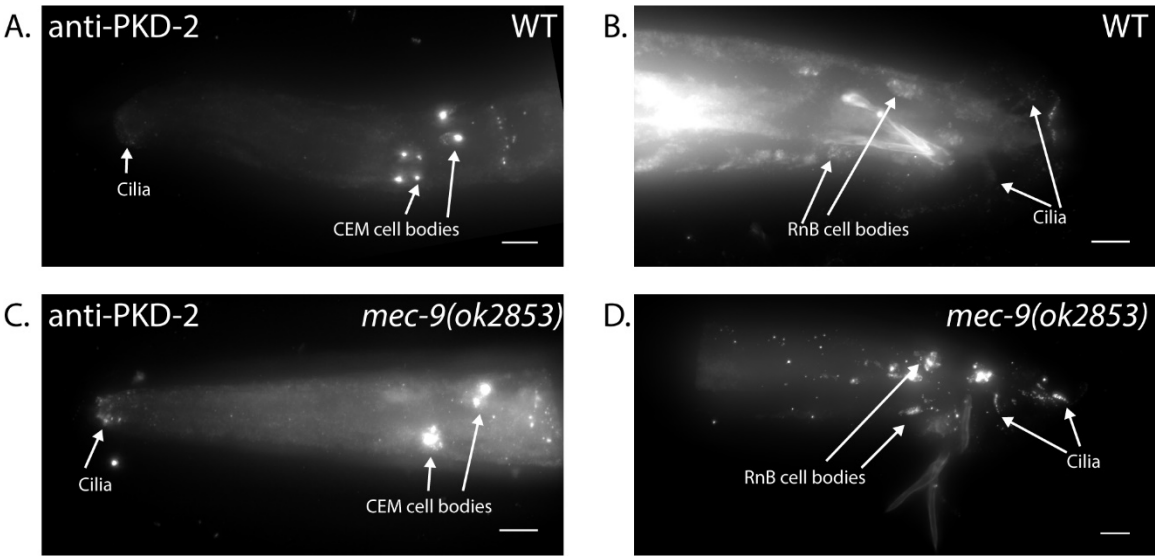


**Figure 3.25 Anti-PKD-2 antibody showed increased, endogenous localization at male specific CEM and RnB cilia.** In WT, endogenous PKD-2 was limited to the cell bodies and cilia of CEM head neurons (Figure 3.23 A) and ray RnB and hook HOB tail neurons (Figure 3.23B). In *mec-9(ok2853)* males, endogenous PKD-2 mislocalized to dendrites and had increased abundance in cilia and cell bodies as shown in FI measurements (Figure 3.23 C and D).

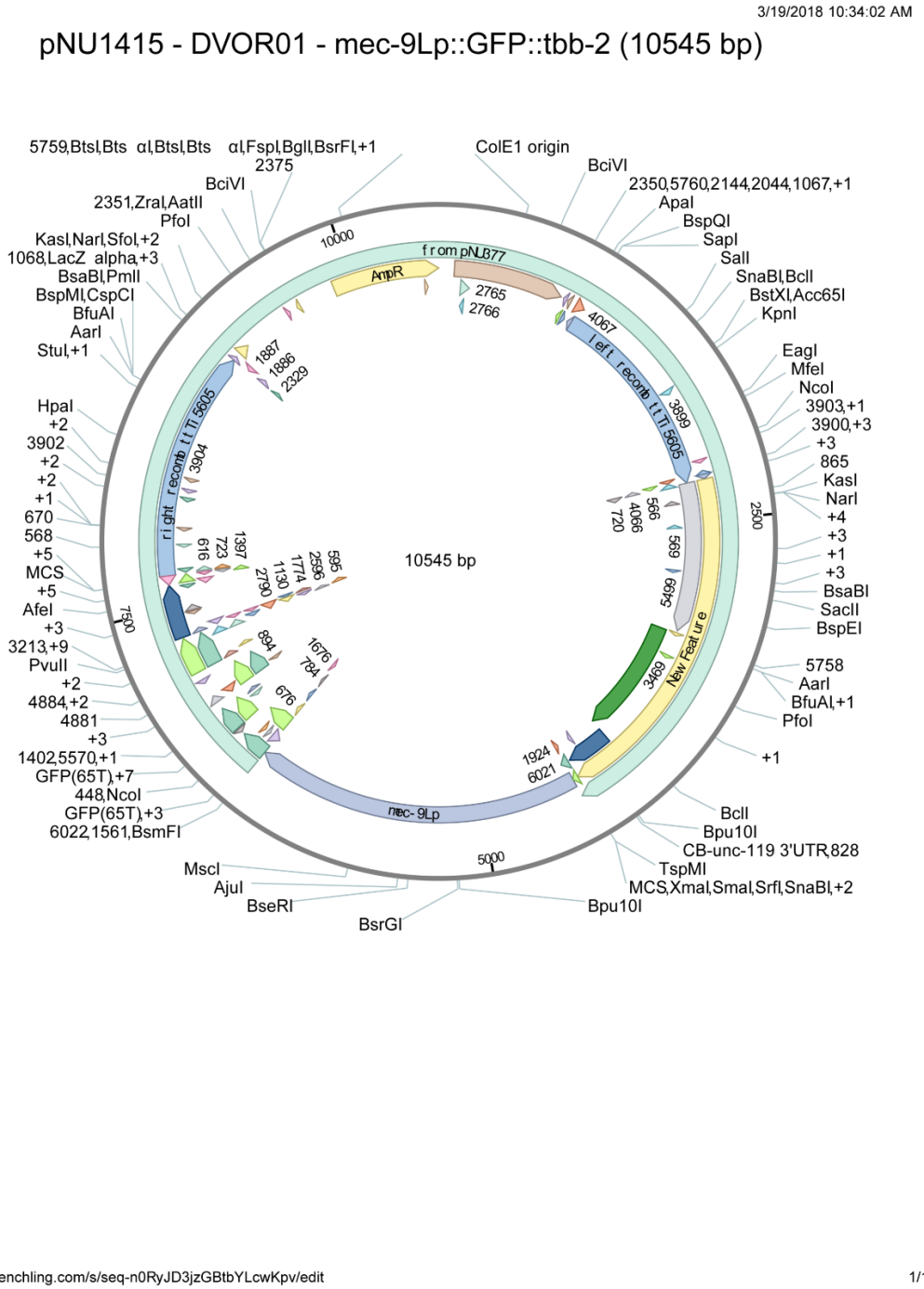




**Figure 3.26 Schematic for *mec-9*L transcriptional reporter** *mec-9*L p (grey at bottom of sphere) denotes the ~2kb upstream sequence. Similar schematic used for construction of *mec-9*S using ~1500 kb of long intron in *mec-9*. Image provided by Knudra through benchling.com.

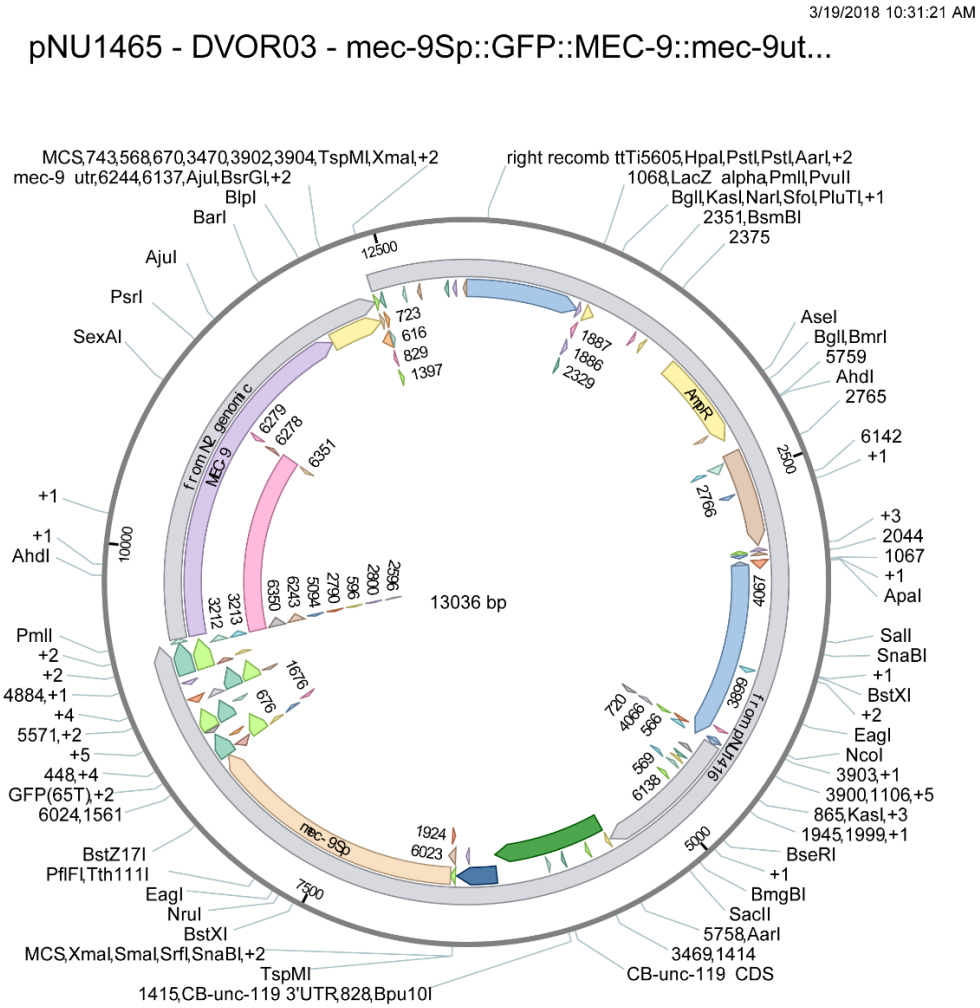


https://benchling.com/s/seq-X0ZHNJ9AgU2G7AejOUZ7/edit 1/1

**Figure 3.27 Schematic for *mec-9S* translational reporter** Reporter included promoter and genomic sequence. Image provided by Knudra through benchling.com.

# CHAPTER 4: CONCLUSIONS AND FUTURE DIRECTIONS

**4.1 Conclusions** Here, I show *mec-1*, *mec-5*, and *mec-9* play multifaceted roles in ciliated sensory organs. ECM components regulate polycystin localization and polycystin-mediated male mating behaviors, control ciliary, dendritic, and glial integrity, and modulate the release of ciliary extracellular vesicles. Intriguingly, *mec-9* has cell-specific functions that are controlled by a short isoform that is differentially expressed in the male and that is not required for touch receptor mechanosensation. Our findings reveal the promiscuity of these ECM components and activity in ciliated and non-ciliated neurons of the worm. While the polycystins have been implicated in sensing and regulating collagen in zebrafish models, roles for ECM proteins in regulating ciliary integrity, ciliary polycystin localization, and ciliary function has not been previously appreciated. This study broadens the scope of activity of the touch receptor extracellular matrix proteins, lends insight on how extracellular matrix proteins contribute to ciliary localization of sensory receptors like PKD-2 and LOV-1, and advance the understanding and expand the options for treatment of ADPKD.

***4.1.1 mec-1*, *mec-5* and *mec-9* have broader roles than previously characterized.** *mec-1*, *mec-5*, and *mec-9* have been previously shown to act in non-ciliated touch receptor neurons and are needed for touch sensitivity (Du et al., 1996). Here I show that these ECM genes act more broadly by revealing that they regulate PKD-2::GFP localization in male specific neurons. PKD-2 localizes to the

cilium of CEM neurons and PKD-2 is necessary for male-specific mating behaviors (Table 2.1, Figures 2.1, and 2.2). We see that alleles of *mec-1, mec-5* and *mec-9* regulate different aspects of male mating behaviors but observed that *mec-9* is necessary for all three of the behaviors tested here, punctuating the specificity and importance of *mec-9* in male-specific neuron and protein activity (Figure 2.2). It would be fascinating to determine if there are other functions for *mec-1*, *mec-5* and *mec-9* in male-specific and other neuron types.

ECM genes regulate activity at male-specific neurons. We wonder if other elements of the well-characterized touch neuron machinery play a role at the male-specific neurons. For example, the paraoxonase POML-1 is homologous to the MEC-6 paraoxonase and is expressed in *C. elegans* neurons that release extracellular vesicles (REF). *mec-6* is also expressed in many neurons, including male-specific ray neurons in the male tail (Chelur et al., 2002). Both POML-1 and MEC-6 are necessary for the functional expression of the DEG/ENaC proteins (Y. Chen et al., 2016) and it is intriguing to speculate that they could perform similarly in polycystin-expressing male-specific neurons.

***4.1.2 mec-9* long and short isoforms have differing expression patterns.** *mec-9* short is expressed in ciliated sensory neurons (Figure 2.3). *mec-9* long isoform is expressed in the six touch receptor neurons (Figure 1.14). It is known that the *mec-9* short isoform, which is the 3' half of the long isoform, is expressed in 25 head and 50 ventral neurons and that this isoform is not necessary for touch

cell activity (Du et al., 1996). Here we show *mec-9* short is expressed in male specific, inner labial, amphid, phasmid, and many other still unidentified neurons (Figure 2.3). Because of this expanded expression pattern, we suspect *mec-9*S is responsible for the phenotypes reported here. We were interested in *mec-9* male-specific expression, but *mec-9* short also is expressed in other non-ciliated, unspecified neurons such as those in the ventral cord. These neurons should also be identified, and their activity elucidated.

*mec-5* also has a broader expression pattern than touch neuron expression: it is expressed in seam cells along the body and other cells in the hermaphrodite head (Du et al., 1996). Further, there are 15 *mec-1* isoforms listed in WormBase and *mec-1* does express in non-touch receptor neurons (Emtage et al., 2004). These expression patterns have only been characterized in hermaphrodites; therefore, male-specific *mec-1* and *mec-5* expression patterns and ultrastructure could be examined.

This *mec-9* male-specific activity is likely directed by a different pathway than that seen in the touch neurons. *mec-3,* is a transcription factor that regulates the levels of *mec-9* long isoform but not that of the short isoform (Du et al., 1996). Also, *mec-3* expression levels can affect dendritic morphology (Albeg et al., 2011). Perhaps another transcription factor regulates *mec-9* short expression. An intriguing candidate would be *daf-19m. daf-19m* is an RFX transcription factor expressed in IL2 and male specific, ciliated neurons and, like *mec-9,* is necessary for male

mating (Wang, Schwartz, & Barr, 2010); it may therefore act upon the *mec-9* short isoform. Further, maybe *mec-3* expression levels are different in males compared to hermaphrodites.

***4.1.3 mec-9* is necessary for EV biogenesis and release.** Extracellular vesicle research is a fledgling field of study and new data is necessary to provide information for cutting edge treatments in drug delivery and disease biomarkers. *C. elegans* is an excellent model for EV research. We previously developed a system to label and visualize EVs in vivo, identified a subset of neurons that release EVs (Wang et al., 2014), and found several genes that affect EV biology (Wang et al., 2015), including the *mec-9* extracellular matrix protein (Figure 2.4). This is valuable information because efforts are being made to classify EVs as a component of the extracellular matrix, as these EVs carry ECM proteins (Rilla & et.al, 2017). Based on my studies, we now know that ECM can regulate EV biogenesis and release in *C. elegans*. We observed increases of EV secretion/storage (Figure 2.4 C) and abnormal dark/light matrix vesicles themselves containing EVs in *mec-9* ECM gene mutants (Figure 2.4 G) suggesting that ECM can negatively regulate EV shedding. We still do not fully understand the mechanism for EV migration through ECM or if and how ECM composition affects EV uptake.

***4.1.4 mec-9* and *pmk-1* act antagonistically in EV biogenesis and release.** *pmk-1* is a kinase that we know is deficient in EV storage at CEM neurons of one

day old males and in EV release from ray neurons in late L4 (Wang et al., 2015) and one day old males. Interestingly, *pmk-1* suppresses the *mec-9* EV hypersecretion phenotype and *mec-9* suppresses *pmk-1* EV hyposecretion (Figure 2.5). This suggests that these genes are antagonistic in EV storage and release. *mec-9* and *pmk-1* also are both defective in PKD-2::GFP ciliary localization (Figure 2.5). These phenotypical similarities, overlapping PKD-2::GFP ciliary localization defects and EV pathway activities, suggest that these genes may interact. This idea that kinases can phosphorylate proteins with EGF domains is not new. CELSR proteins are not ECMs but are transmembranous proteins with long extracellular components. Specifically, CELSR3, a GPCR with similar *mec-9* EGFR domain homology, is necessary for ciliogenesis and dendritic morphology and interacts with a kinase that regulates extension and guidance of sensory neurons in mice (Goffinet & Tissir, 2017)**.**

There are few known ECM kinases and few ECM proteins are known to be extracellularly phosphorylated. Mammalian VLK is a tyrosine kinase that is secreted from platelets and expressed in embryonic stem cells and can phosphorylate various substrates such as matrix metalloproteinases and laminin (Bordoli et al., 2014). FAM20C is another secreted kinase that phosphorylates casein, a secreted milk protein (Tagliabracci, Pinna, & Dixon, 2013). *mec-9* has several predicted phosphorylation sites (data not shown); and maybe the *mec-9;pmk-1* double mutant inhibits PKD-2::GFP localization activity. It would be intriguing to see if *mec-9* is an intracellular or extracellular *pmk-1* substrate or if

there is some reciprocal regulation. This would further expand knowledge of ECM-kinase activity.

***4.1.5 mec-9* regulates neuron anatomy and cilia organization**. It is widely known that ECM is important for neuron anatomy, organization of the brain, and nervous system (Gardiner, 2011). Reelin is necessary for migration of neocortical radial cells in the mammalian brain (Franco et al., 2011). Artichoke regulates morphogenesis of ciliated sensory neurons in *Drosophila* (Marta Andrés et al., 2014a). In *C. elegans*, *dex-1* and *dyf-7* regulate amphid dendrite length which can affect cilia placement (Heiman & Shaham, 2009). *mec-8* and *mec-1* mutants have ciliary fasciculation defects probably caused by interruptions in adhesion proteins (Perkins et al., 1986).

Here we show that CEM, IL2, and amphid neurons in *mec-9* mutant males have abnormal and variable cilia lengths (Figure 2.6 A) and the amphid cilia are disorganized (Figure 2.7). We did not examine *mec-9* hermaphrodite ultrastructure, nor has this been previously reported to our knowledge, though the dye filling defects here were measured in hermaphrodites (Figures 2.7A and 2.11). The abnormal cilia lengths in various neurons is interesting (Figure 2.6 A) because *mec-9* long and short isoform is expressed in non-ciliated touch neurons and *mec-9* long isoform is active at these neurons and now we show that *mec-9* short is also acting in ciliated sensory neurons.

*mec-9* gene mutants have poorly formed or maintained dendrites in the CEM neurons (Figure 2.63), a defect in anterior-posterior positioning of various cilia, and defective amphid cilia organization (Figure 2.7). Again, we do not know how *mec-9* regulates these aspects of neuron anatomy or if this morphology phenotype skews towards males. Electron microscopy can be performed in *mec-9(ok2853)* hermaphrodites to answer this. Further studies are needed to ascertain if MEC-9 protein physically restrains the dendrite or attaches to the ciliary or dendrite membrane to properly position the neuron or if these phenotypes are caused by genetic interactions.

***4.1.6 mec-9* regulates ECM deposition**. Matrix filled vesicles are normally found in the sheath cells surrounding the posterior amphid glia, are vesiculated, and trafficked anteriorly to fuse with the amphid channel enabling matrix to surround cilia (Perkins et al., 1986). *C. elegans* mutants with missing or short amphid cilia (ex- *che-2*, *osm-1*, *daf-6*) tend to accumulate matrix vesicles (Perkins et al., 1986) and we see these vesicles in this *mec-9(ok2853)* mutant. These vesicles can be empty (Figure 2.7 H), filled with smaller vesicles (Figure 2.4 G), or we can find increased ECM surrounding the cilia (Figure 2.7 I). We do not know if *mec-9* regulates the timing or quantity of ECM deposits, specific ECM proteins, or MEC-9 itself (i.e. are these electron dense vesicles excess MEC-9?).

Our findings reveal the promiscuity of ECM components by revealing their activity in ciliated neurons of the worm and broadens the scope of activity of the

extracellular matrix proteins named for the touch receptor neuron activity. We also found ECM proteins contribute to ciliary localization of sensory receptors like PKD-2 which advances the understanding, to consequently expand the options for treatment of ciliopathies like PKD. Here we illustrated that ECM is necessary for the health and well-being of neurons and neural organs. We further propose that ECM regulates aspects of EV biology that builds on the idea that ECM is necessary for extracellular interaction but pushes the envelope enabling us to think of ECM playing a role in extra-organismal communication.

## 4.2 Future directions

**4.2.1 MEC-1 and MEC-5 expression profiles in males** Transcriptional and translational reporters should be examined in males to determine if there is any male specific neuron expression and localization. I began preliminary work using *MEC-5*::YFP, unfortunately this was imaged with a marker for GFP and I was unable to differentiate fluorescence due to close excitation wavelengths. Injecting this construct into animals with a contrasting fluorophore would be beneficial.

**4.2.2 ECM-Polycystin mechanism studies** The connection between ECM and polycystins is still not fully understood. I establish a genetic interaction with the observations presented in this thesis. It would be valuable to test for direct interaction between the two proteins. This might be elucidated by coimmunoprecipitation or attempting to create an anti-*mec-9* antibody (anti-*mec-5* would also be of interest).

**4.2.3 Electron microscopy of other ECM mutants** It would invaluable to view and compare ciliary and dendritic ultrastructure of CEM, IL2, and amphid neurons in *mec-1* and *mec-5* mutants to *mec-9*. I predict that *mec-5(my2)* phenocopies *mec-9(ok2853).* *mec-5(my2)* and *mec-5(e1503)* exhibit the most severe qualitative PKD-2::GFP ciliary localization defective phenotype. I think there would be an increase in extradendritic matrix filled vesicles as seen in the *mec-9(ok2853)* mutant. I would be interested in comparing the structure and substances surrounding the distal dendrites. *mec-1(e1066)* would likely have a less severe CEM phenotype but would provide immeasurable information in male specific neurons as hermaphrodite ultrastructure has been previously remarked upon (Perkins et al., 1986) but other *mec-1* strains listed in (Emtage et al., 2004) were unavailable when requested from Chalfie Lab.

**4.2.4 Electron microscopy of male tail** EM of the WT male tail has been performed (Stephney, 2007) but some details are absent. ECM mutants have a PKD-2::GFP RnB ciliary localization defect (Figure 2.9) and EV release phenotype (Figure 2.4). ECM mutant male tails ultrastructure examination would be beneficial and enable visualization of extracellular vesicles in ray sensilla in wild-type and *mec-9* mutant males and to see if PKD-2::GFP Cil defects correlate to excess EV storage.

**4.2.5 *mec-9* long and short translational localization** I was unable to construct markers, transcriptional or translational for this gene/protein. Knudra had difficulty constructing reporters as well (Chapter 3.7: Project 3-progress notes). The translational construct provided by Knudra does not fluoresce: therefore, we could not discern and provide localization information. Notably, autofluorescence intensity in *MEC-9*sh::GFP is decreased in comparison to WT. There is occasional apolytic (loose cuticle) phenotype that is not exacerbated at 25$^{o}$C: adult worms are mobile but seem to be in mid-molting (data not shown). This differs from WT molting that occurs in larval stage transition during lethargus (Page & Johnstone, 2007). There are no detectable sexually dimorphic localization differences as seen in the transcriptional markers. Therefore, perseverance in seeking a translational marker is necessary to fully appreciate MEC-9 site and mechanism of activity. Alternatively, MEC-9 protein may be produced and secreted at very low levels and therefore undetectable. In support of this possibility, the Chalfie lab has been unable to generate translational reporters for any of the ECM genes.

**4.2.6 Amphid neuron activity assays** *mec-9* mutant ECM may or may not still be able to facilitate transmission of information from the environment to the amphid neurons even though the amphid neurons are decoupled from glia and shorter than WT. Further testing should be done, including assaying the activity of various amphid neurons. We could use osmosensation using glycerol to test ASH activity and thermotaxis using a thermal gradient to test AFD activity. Diacetyl or methyl pyrazine attraction could be used to examine odor sensing AWA activity.

**4.2.7 AWA and AFD ciliary branching.** In *mec-9*, the amphid neurons have a ciliary fasciculation defect (Figure 2.7). *mec-9* amphid neurons may have a ciliary branching defect. The AWA and AFD cilia are extensively branched and testing this would take extensive patience. One could count and measure the many fingers of the AFD; it has been done in WT (Doroquez, Berciu, Anderson, Sengupta, & Nicastro, 2014). This information would be of interest whether or not there is a deficit in the activity of these neurons. If there is a functional phenotype, it could be directly correlated with an increase or decrease in the number of ciliary endings. It would be equally interesting if there is no functional defect even if there is an anatomical or morphological difference.

**4.2.8 Glial cell expression of *mec-9*, *mec-1*, *mec-5.*** It is unclear if *mec-9* short is expressed in glial cells: cephalic or amphid socket and/or sheath. I show via EM that glia are affected in *mec-9* mutants (Figure 2.7). There are occasional images of *mec-9*sP::GFP that show a large punctum where the amphid socket cell soma might be located (data not shown). Further, *mec-9*sP::GFP seems to colocalize with the wide nerve of the amphid, suggesting other structural expression (Figure 2.3 H). Determining coexpression of a glial marker in a contrasting fluorophore with my reporter would address and answer this question.

**4.2.9 Other proteins of interest for PKD-2::GFP ciliary localization** WormBase provides access to Genemania.org which displays gene interaction graphics. In

WormBase, several proteins are predicted to physically or genetically interact with the ECMs discussed in this paper. Further, we have identified an ECM protein that is upregulated in EV neurons via RNA seq.

**4.2.9.1 MTD-1** (**m**ec **t**hree **d**ependent) is a protein with an N terminal extracellular domain and C terminal transmembrane domain. MTD-1 is expressed in touch receptor neurons and enhances the activity of *mec-6* paraoxonase (Zhang & Chalfie, 2002). MTD-1 has a genetic interaction with *mec-5* collagen. It should be characterized to see if there is sexually dimorphic expression and activity.

**4.2.9.2 DEL-1** *del-1* is a Deg/ENaC protein that expresses in ventral cord neurons, like *mec-9* short (Figure 2.3), and is predicted to have mechanosensory activity (Tavernarakis, Shreffler, Wang, & Driscoll, 1997). To my knowledge, there are no recorded phenotypes in the literature, so it would be interesting to see if there are any male specific phenotypes. ASIC-2 is also a DEG/ENaC component, expresses in IL2 neurons, and is shed in EVs (Wang et al 2015). I was unable to construct a stable ASIC-2::GFP line in ECM mutants that expressed this reporter, but ASIC-2 expression and localization could and should be assessed in ECM mutants.

**4.2.9.3 ZK550.3** Our lab identified an unnamed matrix metalloproteinase as a candidate for the PKD gene battery because it contains PKD-motifs. It seems to express in PKD expressing neurons and possibly is an ECM protein. Matrix metalloproteinases purposefully break down matrix proteins (especially collagen)

to facilitate normal body activities such as tissue remodeling and growth and are exploited in disease such as cancer and arthritis (J M Freije et al., 1994; Johansson, Ahonen, & Kähäri, 2000). There could be an interaction with *mec-5* (metalloproteinase using the collagen as a substrate) or with *mec-1* and *mec-9* (conversely, the Kunitz domains negatively regulating the metalloproteinase).

**4.2.10 Motor neuron expression and analysis** *mec-9Sp*::GFP is expressed in the motor neurons in the ventral nerve cord (Figure 2.3). Body bends and muscular activity should be assessed in *mec-9* mutants, and I discussed a possible collaboration with Dr. Gal Haspel at NJIT. My work broadens the expression and activity of these ECMs from non-ciliated touch receptor neurons to include ciliated male specific sensory neurons and motor neurons. Further study in motor neuron activity would further broaden the base of knowledge.

**4.2.11 Exopher analysis** *mec-1(e1066)* mutants exhibit an increased exopher extrusion phenotype (Figure 3.16). The ECM mutants seem to extrude vesicles of many types, but the reasons are not yet known. We could speculate that these mutants are compensating for ineffectual protein clearance, especially since we see an EV biogenesis and storage defect (Figure 2.4). Further inquiry into this phenomenon would expand the breadth of knowledge in this fledgling field of research. To this end, I discussed a possible collaboration with Dr. Monica Driscoll at Rutgers.

# CHAPTER 5: MATERIALS AND METHODS

## 5.1 Culture of *C. elegans* nematodes

Nematodes were maintained using standard conditions(Brenner, 1974). Males and hermaphrodites were isolated at L4 stage ≥24hrs prior to experiments and kept at 20-22$^{o}$C overnight. Because of genetic linkage constraints, mutant alleles such as *mec-9(ok2853)* and *mec-1(e1066)* were outcrossed to *him-8(e1489)*: *him-8* is on chromosome IV and *mec-9* is on chromosome V. In *C. elegans*, the predominant sex is hermaphrodite and males spontaneously arise only rarely (less than 1%).Therefore, in all experiments in which males were tested, we used animals in either the *him-5(e1490)* or *myIs1[pkd-2::GFP] pkd-2(sy606); him-5(e1490)* background to generate a supply of male animals. These backgrounds were considered wild type relative to ECM mutants. Males with the *him-5(e1490)* mutation exhibit normal mating behaviors and are commonly used as wild-type controls for mating assays. WT animals for *mec-1* and *mec-9* animals was *him-8(e1489)* and WT for *mec-5* was *him-5(e1490).* Two plasmids: one containing *mec-5p::MEC-5* and *myo-3p::MEC-5* (gifts from Brian Coblitz-Chalfie Lab) was also used for *my2* rescue.

**5.2 General molecular Biology** PCR amplification PCR amplification was used for genotyping and building transgenic constructs using the following templates: *C. elegans* genomic DNA, cDNA, or prebuilt constructs. High fidelity LA Taq (TaKaRa Bio Inc., Otsu, Shiga, Japan) or Phusion High Fidelity DNA Polymerase (Thermo Fisher Scientific, Vantaa, Finland) were used for amplification of DNA for

constructs. Sequencing reactions were performed on site, and analyzed by IDTDNA Sequencing Facility (Rutgers University, Piscataway, NJ, USA). PCR primer and construct sequences are available upon request.

DNA and protein sequence analysis BLAST (Altschul et al., 1997) was used for identification of gene orthologs in *C. elegans*. Human and nematode protein sequence information was provided by NCBI smartBLAST, and *C. elegans* gene and protein sequence information was also provided by WormBase. Serial Analysis of Gene Expression (SAGE) data provided by WormBase (Release WS221). Structural and domain predictions of gene products are by Exon-Intron Graphic Maker by Nikhil Bhatla (Wormweb.org). Whole genome sequencing was performed and analyzed by Richard Poole using CloudMap.(Gregory Minevich, Danny S Park, Daniel Blankenberg, Richard J Poole, & Oliver Hobert, 2012) ApE 1.17 was used for sequence manipulation.

**5.3 Imaging** Nematodes were anaesthetized with 10 mM levamisole and mounted on agar pads for imaging at room temperature. Epifluorescence images were acquired using a Zeiss Axioplan2 microscope with 10x, 63x (NA 1.4), and 100x (NA 1.4) oil-immersion objectives with a Photometrics Cascade 512B CCD camera using Metamorph software (www.moleculardevices.com) or Zeiss Axio Imager.D1m microscope using a 63x and 100X objective with a Q imaging Regtiga-SRV camera. Optical Z-stack projections were stored as TIFF files and manipulated using ImageJ and Adobe Illustrator. Scale bars are 10 microns for head and tail images. EM scale bars are 200 nm unless otherwise stated.

**5.4 Transmission Electron Microscopy** *mec-9* and wild-type young adult animals were fixed using high-pressure freeze fixation and freeze substitution in 2% OsO4 + 2% water in acetone as the primary fixative (Weimer 2006). Samples were slowly freeze substituted in an RMC freeze substitution device, before infiltration with Embed-812 plastic resin. For TEM, serial sections (`70-75 nm thickness) of fixed animals were collected on copper slot grids coated with formvar and evaporated carbon and stained with 4% uranyl acetate in 70% methanol, followed by washing and incubating with aqueous lead citrate. Images were captured on a Philips CM10 transmission electron microscope at 80kV with a Morada 11-megapixel TEM CCD camera driven by iTEM software (Olympus Soft Imaging Solutions). Images were analyzed using ImageJ (FIJI) and manipulated with Adobe Illustrator.

**5.5 Extracellular vesicle release**

As done in Silva 2017- EV release performed by counting all EVs from one-day old young adult males. Individual animals are mounted on agar into four quadrants of agar slide. Free and newly released EVs that float to the cover slip are counted. One high powered field of the head and one of the tail are counted and reported as “number of EVs released.”

**5.6 EV biogenesis**-Using ImageJ (FIJI) software, WT and mutant electron micrograms are compared at and around the CEM TZ. Qualitative and quantitative

examination is reported. EV diameter measurements performed using by drawing a line across the widest diameter of an EV and taking a measurement via FIJI measurement tool reporting diameter in nm.

**5.7 Cilia length measurements** Electron micrograms are used and stacked using the TRAKEM component of ImageJ(FIJI) software. TZ zone is identified and used as the bottom measurement. Cilium tip is identified and used as the top measure. The Z stack position is multiplied by the thickness of the cut (~70-75 nm as specified by Ken Ngyuen) and length is reported in nm.

**5.8 Antibody staining** Animals were staged young adults and washed off plates with M9. Antibodies were prepared using Abmart protocols and staining against PKD-2 was prepared and performed using a Finney Ruvkun protocol [(Bettinger, Lee et al. 1996); Wormatlas.org]. The monoclonal PKD-2 primary antibody was created by Abmart. It was created against the intracellular N-terminal domain and an intracellular C-terminal domain. The secondary antibody used was α mouse Alexa Fluor ® 568 donkey anti-mouse IgG (H + L) (2 mg/ml) by Invitrogen TM. Concentrations and incubation times used: primary antibodies 1:200 overnight (18-24 hours); secondary antibody 1:1000 for two hours.

**5.9 Response behavior assay** Control Strains used: CB1490, CB1489, PT9, and CB169. L4 larval males were moved to a fresh plate approximately 24 hours before mating. Males used were either from the strains listed above or were males

resulting from crossing CB1490 (in *mec-5* studies) or CB1489 (in *mec-1* and *mec-9* studies) with ECM mutant hermaphrodites. *unc-31* mutant hermaphrodites were also picked as L4 larvae ~24 hours before experiments. Male mating assays were conducted on a fresh NGM agar plate with a small lawn of *E. coli* (OP50) containing 25 young-adult *unc-31* hermaphrodites. One, two, or three males were placed in the center of the lawn and observed for four minutes. A response was scored as positive when a male began scanning a hermaphrodite and the tail maintained contact with a mate for at least ten seconds.

**5.10 Location of vulva assay** Performed as described. (Barr & Sternberg, 1999) Location of vulva efficiency is calculated by successful vulva location divided by the total number of vulva encounters for each male. Total time measured was four minutes.

**5.11 Male leaving assay** Performed according to Barrios 2008.(Barrios et al., 2008) L4 males were picked and isolated from hermaphrodites on plates, then assayed 24 hours later in 20 µl food on a 9 cm diameter plate. Animals are positive for leaving when males exhibit tracks that approach within 1 cm of the edge of the plate. Time points scored were 2, 5, 8, and 24 hours after the males were placed on the spot of food. A minimum of 20 animals per strain and three replicates were scored for each genotype assayed. Statistical significance determined by R software.

**5.12 Dye filling assays** Standard dye-filling assays were performed using DiI (Invitrogen) (Perkins et al., 1986; Warburton-Pitt, 2015). The number of amphid and phasmid cell bodies were counted, and the results reported as number of neurons out of 12 (amphid) or 4 (phasmid) that fill with DiI.

**5.13 Gentle touch assay** Performed as previously described (Chalfie & Sulston, 1981). Touch neuron activity was measured by lightly touching animals alternatively and repeatedly near the head and near the tail and reporting the number of times out of ten animal retracted in opposite direction. Numerical data reported as number of responses out of ten.

**5.14 Cloning and rescue** Performed using normal standards. (*WormBook*2005) *MEC-5* constructs were gifted from Chalfie Lab and injected at 20 ng/ul for rescue unless otherwise stated.

**5.15 Temperature sterility** Isolated L4 hermaphrodites were plated and placed in 25°C to and examined for presence of offspring. Number of plates with eggs and larva counted and reported as percentage of animals that "complemented" the *my2* temperature sensitive sterility phenotype.

**5.16 Velocity measurements** To directly measure in vivo velocity of PKD-2::GFP in CEM dendrites, I acquired time lapse image stacks, which were later converted to kymographs using the KymographClear V2.0 plugin in FIJI. Motile particles were

automatically and indiscriminately detected and traced, and velocities analyzed with KymographDirect as described (Mangeol, Prevo, & Peterman, 2016). We observed a reduction of overall observed velocities as compared to Morsci 2012 (Morsci, 2012). This reduction does not affect our analysis or overall conclusions, as our model is not based on absolute velocities of individual IFT components but rather on their relative changes.

**5.19 Ciliary localization and fluorescence intensity** Ciliary localization was performed by blind assay of a stack of images collected into a maximum intensity image using the “Z project” function in ImageJ software. Animals were scored as defective if excess or misplaced protein tagged fluorescence protein detected (ex-excess in cilium, ciliary base, or dendrite). Fluorescence intensity was measured using ImageJ by drawing a range of interest and using measurement tool. All measurements have background subtracted to create final value.

**5.20 Strains used**

| | |
|---|---|
| CB1066 | *mec-1(e1066)V* |
| CB1292 | *mec-1(e1292)V* |
| CB1494 | *mec-9(e1494)V* |
| CB1503 | *mec-5(e1503)X* |
| CB169 | *unc-31(e169)IV* |
| COP1472 | *knuEx206[pNU1416-mec-9Sp::GFP::tbb-2utr,unc-119(+)];unc-119(ed3)III* |
| COP1473 | *knuEx207[pNU1415-mec-9Lp::GFP::tbb-2utr,unc-119(+)];unc-119(ed3)III* |
| COP1597 | *knuEx218 [pNU1465 - mec-9sp::GFP::MEC-9::mec-9utr unc-119(+)] ; unc-119 (ed3) III* |

| | |
|---|---|
| COP1621 | *knuEx219 [(pNU1465 - mec-9sp::GFP::MEC-9::mec-9utr unc-119(+)]; unc-119 (ed3) III* |
| KU25 | *pmk-1(km25)IV* |
| PT3296 | *mec-9(ok2853),pmk-1(km25)IV;myIs4 him-5(e1490) V* |
| PT3168 | *him-8(e1489) myIs1[PKD-2::GFP + cc::GFP] IV;* |
| PT277 | *unc-119(ed3)III; him-5(e1490) V* |
| PT1213 | *myIs4 him-5(e1490) V; my2 X* |
| PT1852 | *pha-1(e2123) III; him-5(e1490) V; Ex [LOV-1::GFP1]* |
| PT2434 | *dyf-1(m335); myIs1; him-5* |
| PT2679 | *him-5(e1490)V;myIs23[Pcil-7::gCIL-7::GFP_3'UTR+ccRFP]* |
| PT2962 | *him-8(e1489) myIs1[PKD-2::GFP + cc::GFP] IV; mec-1(e1066) V* |
| PT2963 | *him-8(e1489) myIs1[PKD-2::GFP + cc::GFP] IV; mec-1(e1336) V* |
| PT2964 | *him-8(e1489) myIs1[PKD-2::GFP + cc::GFP] IV; mec-1(e1292) V* |
| PT2965 | *him-8(e1489) myIs1[PKD-2::GFP + cc::GFP] IV; mec-9(e1494) V* |
| PT2966 | *him-8(e1489) myIs1[PKD-2::GFP + cc::GFP] IV; mec-9(ok2853) V* |
| PT2967 | *him-5(e1490) myIs4[PKD-2::GFP + cc::GFP] V; mec-5(e1790) X* |
| PT2968 | *him-5(e1490) myIs4[PKD-2::GFP + cc::GFP] V; mec-5(e1503) X* |
| PT2969 | *uIs31[MEC-17::GFP] III; him-5(e1490) myIs4[PKD-2::GFP + cc::GFP] V; mec-5(u444) X* |
| PT3038 | *unc-31(e169)IV; him-5(e1490), myIs4 V* |
| PT3203 | *mec-9(ok2853); pha-1; him-5(e1490); syEx301[pBx+LOV-1::GFP1]* |
| PT3213 | *mec-9(ok2853)V,him-5(e1490)V;myIs23[pcil-7::gCIL-7::GFP::3'UTR+ccRFP]* |
| PT443 | *myIs1 pkd-2(sy606) IV; him-5(e1490) V* |
| PT621 | *myIs4 him-5(e1490) V* |
| RB2140 | *mec-9(ok2853) V* |
| SP261 | *mnDp1(X;V)/+ V; mnDf2 X* |
| SP265 | *mnDp1(X;V)/+ V; mnDf4 X* |
| SP272 | *mnDp1(X;V)/+ V; mnDf11 X* |

| | |
|---|---|
| SP273 | *mnDp1(X;V)/+ V; mnDf13 X* |
| SP275 | *mnDp1(X;V)/+ V; mnDf17 X* |
| SP395 | *mnDp1(X;V)/+ V; mnDf42 X* |

# References

Albeg, A., Smith, C. J., Chatzigeorgiou, M., Feitelson, D. G., Hall, D. H., Schafer, W. R., . . . Treinin, M. (2011). C. elegans multi-dendritic sensory neurons: Morphology and function. *Molecular and Cellular Neuroscience, 46*(1), 308-317. 10.1016/j.mcn.2010.10.001 Retrieved from https://www.sciencedirect.com/science/article/pii/S1044743110002460

API histology. Retrieved from https://legacy.owensboro.kctcs.edu/gcaplan/anat/Notes/API%20Notes%20F%20Connective%20Tissues.htm

Armato, U., Chakravarthy, B., Pacchiana, R., & Whitfield, J. F. (2012). Alzheimer's disease: An update of the roles of receptors, astrocytes and primary cilia (review). *International Journal of Molecular Medicine,* 10.3892/ijmm.2012.1162; 10.3892/ijmm.2012.1162

B.E. Vogel, & E.M. Hedgecock. (2001). Hemicentin, a conserved extracellular member of the immunoglobulin superfamily, organizes epithelial and other cell attachments into oriented line-shaped junctions. *Development, 128*(6), 883. Retrieved from http://dev.biologists.org/content/128/6/883.abstract

Bae, Y. K., Lyman-Gingerich, J., Barr, M. M., & Knobel, K. M. (2008). Identification of genes involved in the ciliary trafficking of C. elegans PKD-2.

*Developmental Dynamics : An Official Publication of the American Association of Anatomists, 237*(8), 2021-2029. 10.1002/dvdy.21531

Bae, Y. K., Qin, H., Knobel, K. M., Hu, J., Rosenbaum, J. L., & Barr, M. M. (2006). General and cell-type specific mechanisms target TRPP2/PKD-2 to cilia. *Development (Cambridge, England), 133*(19), 3859-3870. 10.1242/dev.02555

Barr, M. M., DeModena, J., Braun, D., Nguyen, C. Q., Hall, D. H., & Sternberg, P. W. (2001). The caenorhabditis elegans autosomal dominant polycystic kidney disease gene homologs lov-1 and pkd-2 act in the same pathway. *Current Biology : CB, 11*(17), 1341-1346.

Barr, M. M., & Garcia, L. R. (2006). Male mating behavior. *WormBook : The Online Review of C.Elegans Biology,* , 1-11. 10.1895/wormbook.1.78.1

Barr, M. M., & Sternberg, P. W. (1999). A polycystic kidney-disease gene homologue required for male mating behaviour in C. elegans. *Nature, 401*(6751), 386-389. 10.1038/43913

Barragan, I., Shah, A., Mena, M., Abd El-Aziz, M. M., El-Ashry, M. F., Cheetham, M. E., . . . Bhattacharya, S. S. (2008). EYS , encoding an ortholog of drosophila spacemaker, is mutated in autosomal recessive retinitis pigmentosa. *Nature Genetics, 40*(11), 1285-1287. 10.1038/ng.241 Retrieved from http://dx.doi.org/10.1038/ng.241

Barrios, A., Nurrish, S., & Emmons, S. W. (2008). Sensory regulation of C. elegans male mate-searching behavior. *Current Biology, 18*(23), 1865-1871. 10.1016/j.cub.2008.10.050 Retrieved from http://www.sciencedirect.com/science/article/pii/S096098220801419X

Barstead R, Moulder G, Cobb B, Frazee S, Henthorn D, Holmes J, Jerebie D, Landsdale M, Osborn J, Pritchett C, Robertson J, Rummage J, Stokes E, Vishwanathan M, Mitani S, Gengyo-Ando K, Funatsu O, Hori S, Imae R, Kage-Nakadai E, Kobuna H, Machiyama E, Motohashi T, Otori M, Suehiro Y, Yoshina S, Smith M, Moerman D, Edgley M, Adair R, Allan BJ, Au V, Chaudhry I, Cheung R, Dadivas O, Eng S, Fernando L, Fisher A, Flibotte S, Gilchrist E, Hay A, Huang P, Worsley Hunt R, Kwitkowski C, Lau J, Lee N, Liu L, Lorch A, Luck C, Maydan J, McKay S, Miller A, Mullen G, Navaroli C, Neil S, Hunt-Newbury R, Partridge M, Perkins J, Rankin A, Raymant G, Rezania N, Rogula A, Shen B, Stegeman G, Tardif A, Taylor J, Veiga M, Wang T, Zapf R. (2012). Large-scale screening for targeted knockouts in the caenorhabditis elegans genome. *G3 (Bethesda, Md.), 2*(11), 1415-1425. 10.1534/g3.112.003830 Retrieved from http://www.ncbi.nlm.nih.gov/pubmed/23173093

Benjamin D. Williams, & Robert H. Waterston. (1994). Genes critical for muscle development and function in caenorhabditis elegans identified through lethal mutations. *The Journal of Cell Biology, 124*(4), 475-490. 10.1083/jcb.124.4.475 Retrieved from http://www.jstor.org/stable/1616191

Bhatta, N.Exon-intron graphic maker.

Bordoli, M. R., Yum, J., Breitkopf, S. B., Thon, J. N., Italiano, J., Joseph E, Xiao, J., . . . Whitman, M. (2014). A secreted tyrosine kinase acts in the extracellular environment. *Cell, 158*(5), 1033-1044. 10.1016/j.cell.2014.06.048 Retrieved from http://www.ncbi.nlm.nih.gov/pubmed/25171405

Brenner, S. (1974). The genetics of caenorhabditis elegans. *Genetics, 77*, 71-94.

Bruckner-Tuderman, L., & Bruckner, P. (1998). Genetic diseases of the extracellular matrix: More than just connective tissue disorders. *Journal of Molecular Medicine, 76*(3-4), 226-37.

Calvet, J. P. (1993). Polycystic kidney disease: Primary extracellular matrix abnormality or defective cellular differentiation? *Kidney International, 43*(1), 101-108. 10.1038/ki.1993.17 Retrieved from https://www.sciencedirect.com/science/article/pii/S0085253815578897

Chalfie, M. (2009). Neurosensory mechanotransduction. *Nature Reviews.Molecular Cell Biology, 10*(1), 44-52. 10.1038/nrm2595

Chalfie, M., & Sulston, J. (1981). Developmental genetics of the mechanosensory neurons of caenorhabditis elegans. *Developmental Biology, 82*(2), 358-370.

Chelur, D. S., Ernstrom, G. G., Goodman, M. B., Yao, C. A., Chen, L., O'Hagan, R., & Chalfie, M. (2002). The mechanosensory protein MEC-6 is a subunit of the C. elegans touch-cell degenerin channel. *Nature, 420*(6916), 669-673. 10.1038/nature01205

Chen, C., Chen, Y., Jiang, H., Chen, C., & Pan, C. (2013). Neuronal aging: Learning from C. elegans. *Journal of Molecular Signaling, 8*(1), 14. 10.1186/1750-2187-8-14 Retrieved from http://www.ncbi.nlm.nih.gov/pubmed/24325838

Chen, Y., Bharill, S., Altun, Z., O'Hagan, R., Coblitz, B., Isacoff, E. Y., & Chalfie, M. (2016). Caenorhabditis elegans paraoxonase-like proteins control the functional expression of DEG/ENaC mechanosensory proteins. *Molecular Biology of the Cell, 27*(8), 1272. Retrieved from http://www.ncbi.nlm.nih.gov/pubmed/26941331

Chorev, M., & Carmel, L. (2012). The function of introns. *Frontiers in Genetics, 3*, 55. 10.3389/fgene.2012.00055 Retrieved from http://www.ncbi.nlm.nih.gov/pubmed/22518112

Chun-Liang Pan, Chiu-Ying Peng, Chun-Hao Chen, & Steven McIntire. (2011). Genetic analysis of age-dependent defects of the caenorhabditis elegans touch receptor neurons. *Proceedings of the National Academy of Sciences of the United States of America, 108*(22), 9274-9279.

10.1073/pnas.1011711108 Retrieved from https://www.jstor.org/stable/25831123

The collagen molecule. Retrieved from https://www.proto-col.com/blog/2014/07/30/collagen/

Colognato, H., & Yurchenco, P. D. (2000). Form and function: The laminin family of heterotrimers. *Developmental Dynamics : An Official Publication of the American Association of Anatomists, 218*(2), 213-234. AID-DVDY1>3.0.CO;2-R Retrieved from http://www.ncbi.nlm.nih.gov/pubmed/10842354

Common diabetes drug may halt growth of cysts in polycystic kidney disease. (2010, Nov 14,). *Web News Wire*

Compagnon, J., Barone, V., Rajshekar, S., Kottmeier, R., Pranjic-Ferscha, K., Behrndt, M., & Heisenberg, C. (2014). The notochord breaks bilateral symmetry by controlling cell shapes in the zebrafish laterality organ. *Developmental Cell, 31*(6), 774-783. 10.1016/j.devcel.2014.11.003 Retrieved from http://www.ncbi.nlm.nih.gov/pubmed/25535919

Corcoran, C., Rani, S., & O'Driscoll, L. (2014). miR-34a is an intracellular and exosomal predictive biomarker for response to docetaxel with clinical relevance to prostate cancer progression. *The Prostate, 74*(13), 1320-1334. 10.1002/pros.22848

Cox, G. N., Kramer, J. M., & Hirsh, D. (1984). Number and organization of collagen genes in caenorhabditis elegans. *Molecular and Cellular Biology, 4*(11), 2389-2395.

Daniel R. Zerbino, et al. (2018). *Ensembl: Tps-1 caenorhabditis elegans*.10.1093/nar/gkx1098 Retrieved from http://useast.ensembl.org/Caenorhabditis_elegans/Transcript/Domains?db=core;g=WBGene00006602;r=X:17467137-17473698;t=ZK54.2b.1

Davis, E. E., Zhang, Q., Liu, Q., Diplas, B. H., Davey, L. M., Hartley, J., . . . Katsanis, N. (2011). TTC21B contributes both causal and modifying alleles across the ciliopathy spectrum. *Nature Genetics, 43*(3), 189-196. 10.1038/ng.756

Depuydt, G., Shanmugam, N., Rasulova, M., Dhondt, I., & Braeckman, B. P. (2016). Increased protein stability and decreased protein turnover in the caenorhabditis elegans ins/IGF-1 daf-2 mutant. *The Journals of Gerontology, Series A, 71*(12), 1553-1559. 10.1093/gerona/glv221 Retrieved from https://search.proquest.com/docview/1842820133

Doitsidou, M., Poole, R. J., Sarin, S., Bigelow, H., & Hobert, O. (2010). C. elegans mutant identification with a one-step whole-genome-sequencing and SNP mapping strategy. *PloS One, 5*(11), e15435. 10.1371/journal.pone.0015435

Donnelly, E., Ascenzi, M., & Farnum, C. (2010). Primary cilia are highly oriented with respect to collagen direction and long axis of extensor tendon. *Journal of Orthopaedic Research : Official Publication of the Orthopaedic Research Society, 28*(1), n/a. 10.1002/jor.20946 Retrieved from http://www.ncbi.nlm.nih.gov/pubmed/19603516

Doroquez, D. B., Berciu, C., Anderson, J. R., Sengupta, P., & Nicastro, D. (2014). A high-resolution morphological and ultrastructural map of anterior sensory cilia and glia in caenorhabditis elegans. *eLife, 3*, e01948. 10.7554/eLife.01948 Retrieved from http://www.ncbi.nlm.nih.gov/pubmed/24668170

Drummond, I. A. (2011). Polycystins, focal adhesions and extracellular matrix interactions. *BBA - Molecular Basis of Disease, 1812*(10), 1322-1326. 10.1016/j.bbadis.2011.03.003 Retrieved from https://www.sciencedirect.com/science/article/pii/S0925443911000524

D'Souza, S. E., Ginsberg, M. H., & Plow, E. F. (1991). Arginyl-glycyl-aspartic acid (RGD): A cell adhesion motif. *Trends in Biochemical Sciences, 16*(7), 246-250. 10.1016/0968-0004(91)90096-E Retrieved from http://www.sciencedirect.com/science/article/pii/096800049190096E

Du, H., Gu, G., William, C. M., & Chalfie, M. (1996). Extracellular proteins needed for C. elegans mechanosensation. *Neuron, 16*(1), 183-194.

Emmons, S. W. (2005). Male development. *WormBook : The Online Review of C. Elegans Biology,* , 1. 10.1895/wormbook.1.33.1 Retrieved from http://www.ncbi.nlm.nih.gov/pubmed/18050419

Emtage, L., Gu, G., Hartwieg, E., & Chalfie, M. (2004). Extracellular proteins organize the mechanosensory channel complex in C. elegans touch receptor neurons. *Neuron, 44*(5), 795-807. 10.1016/j.neuron.2004.11.010

Engel, F. B., & Cazorla-Vazquez, S. (2018). Adhesion GPCRs in kidney development and disease. *Frontiers in Cell and Developmental Biology, 6*10.3389/fcell.2018.00009 Retrieved from https://doaj.org/article/e66f40ee7418420999f4ef4b52a81f78

Engel, J. (1989). *EGF-like domains in extracellular matrix proteins: Localized signals for growth and differentiation?*. NETHERLANDS: Elsevier B.V.10.1016/0014-5793(89)81417-6 Retrieved from http://www.sciencedirect.com.proxy.libraries.rutgers.edu/science/article/pii/0014579389814176

Fais, S., O'Driscoll, L., Borras, F. E., Buzas, E., Camussi, G., Cappello, F., . . . Giebel, B. (2016). Evidence-based clinical use of nanoscale extracellular vesicles in nanomedicine. *ACS Nano, 10*(4), 3886. Retrieved from http://www.ncbi.nlm.nih.gov/pubmed/26978483

Fay, D. (2006a). Genetic mapping and manipulation: Chapter 2--two-point mapping with genetic markers. *WormBook : The Online Review of C. Elegans Biology,* , 1. 10.1895/wormbook.1.91.1 Retrieved from http://www.ncbi.nlm.nih.gov/pubmed/18050462

Fay, D. (2006b). Genetic mapping and manipulation: Chapter 3--three-point mapping with genetic markers. *WormBook : The Online Review of C. Elegans Biology,* , 1. 10.1895/wormbook.1.92.1 Retrieved from http://www.ncbi.nlm.nih.gov/pubmed/18050461

Fay, D., & Bender, A. (2008). SNPs: Introduction and two-point mapping. *WormBook : The Online Review of C. Elegans Biology,* , 1. Retrieved from http://www.ncbi.nlm.nih.gov/pubmed/18819170

Franco, S. J., Martinez-Garay, I., Gil-Sanz, C., Harkins-Perry, S. R., & Müller, U. (2011). Reelin regulates cadherin function via Dab1/Rap1 to control neuronal migration and lamination in the neocortex. *Neuron, 69*(3), 482-497. 10.1016/j.neuron.2011.01.003 Retrieved from https://www.sciencedirect.com/science/article/pii/S0896627311000286

Gao, J., DeRouen, M. C., Chen, C., Nguyen, M., Nguyen, N. T., Ido, H., . . . Marinkovich, M. P. (2008). Laminin-511 is an epithelial message promoting dermal papilla development and function during early hair morphogenesis. *Genes & Development, 22*(15), 2111-2124. 10.1101/gad.1689908 Retrieved from http://www.ncbi.nlm.nih.gov/pubmed/18676816

Garcia-Gonzalo, F. R., & Reiter, J. F. (2012). Scoring a backstage pass: Mechanisms of ciliogenesis and ciliary access. *The Journal of Cell Biology, 197*(6), 697-709. 10.1083/jcb.201111146

Gardiner, N. J. (2011). Integrins and the extracellular matrix: Key mediators of development and regeneration of the sensory nervous system. *Developmental Neurobiology, 71*(11), 1054-1072. 10.1002/dneu.20950 Retrieved from http://www.ncbi.nlm.nih.gov/pubmed/21761574

Goffinet, A., & Tissir, F. (2017). Seven pass cadherins CELSR1-3. *Seminars in Cell and Developmental Biology,* 10.1016/j.semcdb.2017.07.014 Retrieved from http://hdl.handle.net/2078.1/191623

Goodman, M. (2006). Mechanosensation. Retrieved from http://www.wormbook.org

Goodman, M. B., Ernstrom, G. G., Chelur, D. S., O'Hagan, R., Yao, C. A., & Chalfie, M. (2002). MEC-2 regulates C. elegans DEG/ENaC channels needed for mechanosensation. *Nature, 415*(6875), 1039-1042. 10.1038/4151039a

Gordon, M., & Hahn, R. (2009). Collagens. *Cell Tissue Res, 339*, 247-257.

Gregory Minevich, Danny S Park, Daniel Blankenberg, Richard J Poole, & Oliver Hobert. (2012). CloudMap: A cloud-based pipeline for analysis of mutant genome sequences. *Genetics, 192*(4), 1249-1269.

10.1534/genetics.112.144204 Retrieved from http://www.ncbi.nlm.nih.gov/pubmed/23051646

Gu, G., Caldwell, G. A., & Chalfie, M. (1996). Genetic interactions affecting touch sensitivity in caenorhabditis elegans. *Proceedings of the National Academy of Sciences of the United States of America, 93*(13), 6577-6582.

Gupta, M. C., Graham, P. L., & Kramer, J. M. (1997). Characterization of alpha1(IV) collagen mutations in caenorhabditis elegans and the effects of alpha1 and alpha2(IV) mutations on type IV collagen distribution. *The Journal of Cell Biology, 137*(5), 1185-1196. Retrieved from http://www.ncbi.nlm.nih.gov/pubmed/9166417

Hanaoka, K., Qian, F., Boletta, A., Bhunia, A. K., Piontek, K., Tsiokas, L., . . . Germino, G. G. (2000). Co-assembly of polycystin-1 and -2 produces unique cation-permeable currents. *Nature, 408*(6815), 990-994. 10.1038/35050128

Heiman, M. G., & Shaham, S. (2009). DEX-1 and DYF-7 establish sensory dendrite length by anchoring dendritic tips during cell migration. *Cell, 137*(2), 344-355. 10.1016/j.cell.2009.01.057 Retrieved from https://www.sciencedirect.com/science/article/pii/S0092867409001597

The histology Guide=Connective tissue. Retrieved from http://histology.leeds.ac.uk/tissue_types/connective/connective_fibres.php

Hochgreb-Hägele, T., Yin, C., Koo, D. E. S., Bronner, M. E., & Stainier, D. Y. R. (2013). Laminin β1a controls distinct steps during the establishment of digestive organ laterality. *Development (Cambridge, England), 140*(13), 2734-2745. 10.1242/dev.097618 Retrieved from http://www.ncbi.nlm.nih.gov/pubmed/23757411

Hodgkin, J., Horvitz, H. R., & Brenner, S. (1979). Nondisjunction mutants of the nematode caenorhabditis elegans. *Genetics, 91*(1), 67-94. Retrieved from http://www.genetics.org/cgi/content/abstract/91/1/67

Hofherr, A., & Kottgen, M. (2011). TRPP channels and polycystins. *Advances in Experimental Medicine and Biology, 704*, 287-313. 10.1007/978-94-007-0265-3_16

Honda, Y., Tanaka, M., & Honda, S. (2010). Trehalose extends longevity in the nematode caenorhabditis elegans. *Aging Cell, 9*(4), 558-569. 10.1111/j.1474-9726.2010.00582.x Retrieved from http://www.ingentaconnect.com/content/bsc/ace/2010/00000009/00000004/art00011

Igarashi, P., & Somlo, S. (2002). Genetics and pathogenesis of polycystic kidney disease. *Journal of the American Society of Nephrology : JASN, 13*(9), 2384-2398. 10.1097/01.ASN.0000028643.17901.42 Retrieved from http://www.ncbi.nlm.nih.gov/pubmed/12191984

Ilija Melentijevic, Marton L Toth, Meghan L Arnold, Ryan J Guasp, Girish Harinath, Ken C Nguyen, . . . Monica Driscoll. (2017). C. elegans neurons jettison protein aggregates and mitochondria under neurotoxic stress. *Nature, 542*(7641), 367-371. 10.1038/nature21362 Retrieved from https://search.proquest.com/docview/1869485786

Iraci, N., Leonardi, T., Gessler, F., Vega, B., & Pluchino, S. (2016). Focus on extracellular vesicles: Physiological role and signalling properties of extracellular membrane vesicles. *International Journal of Molecular Sciences, 17*(2), 171. 10.3390/ijms17020171 Retrieved from http://www.ncbi.nlm.nih.gov/pubmed/26861302

J M Freije, I DÃez-Itza, M BalbÃn, L M SÃ¡nchez, R Blasco, J Tolivia, & C LÃ³pez-OtÃn. (1994). Molecular cloning and expression of collagenase-3, a novel human matrix metalloproteinase produced by breast carcinomas. *Journal of Biological Chemistry, 269*(24), 16766. Retrieved from http://www.jbc.org/content/269/24/16766.abstract

Jennifer F Barger, Mohammad A Rahman, Devine Jackson, Mario Acunzo, & S Patrick Nana-Sinkam. (2016). *Extracellular miRNAs as biomarkers in cancer*10.1016/j.fct.2016.06.010

Jingdong Liu, Bertold Schrank, & Robert H. Waterston. (1996). Interaction between a putative mechanosensory membrane channel and a collagen.

*Science, 273*(5273), 361-364. 10.1126/science.273.5273.361 Retrieved from http://www.sciencemag.org/content/273/5273/361.abstract

Johansson, N., Ahonen, M., & Kähäri, V. -. (2000). Matrix metalloproteinases in tumor invasion. *Cellular and Molecular Life Sciences, 57*(1), 5-15. 10.1007/s000180050495 Retrieved from http://www.ncbi.nlm.nih.gov/pubmed/10949577

Joseph P. Ardizzi, & Henry F. Epstein. (1987). Immunochemical localization of myosin heavy chain isoforms and paramyosin in developmentally and structurally diverse muscle cell types of the nematode caenorhabditis elegans. *The Journal of Cell Biology, 105*(6), 2763-2770. 10.1083/jcb.105.6.2763 Retrieved from https://www.jstor.org/stable/1612705

Kain, K. H. (2010). The extracellular matrix and disease: An interview with zena werb. *Disease Models & Mechanisms, 3*(9-10), 513-516. 10.1242/dmm.006338

Kalra, H., Drummen, G. P. C., & Mathivanan, S. (2016). Focus on extracellular vesicles: Introducing the next small big thing. *International Journal of Molecular Sciences, 17*(2), 170. 10.3390/ijms17020170 Retrieved from http://www.ncbi.nlm.nih.gov/pubmed/26861301

Keryer, G., Pineda, J. R., Liot, G., Kim, J., Dietrich, P., Benstaali, C., . . . Saudou, F. (2011). Ciliogenesis is regulated by a huntingtin-HAP1-PCM1 pathway

and is altered in huntington disease. *The Journal of Clinical Investigation, 121*(11), 4372-4382. 10.1172/JCI57552; 10.1172/JCI57552

Kim, N., Dempsey, C. M., Kuan, C. J., Zoval, J. V., O'Rourke, E., Ruvkun, G., . . . Sze, J. Y. (2007). Gravity force transduced by the MEC-4/MEC-10 DEG/ENaC channel modulates DAF-16/FoxO activity in caenorhabditis elegans. *Genetics, 177*(2), 835-845. genetics.107.076901 [pii]

Kobe, B., & Kajava, A. V. (2001). The leucine-rich repeat as a protein recognition motif. *Current Opinion in Structural Biology, 11*(6), 725-732.

Le Corre, S., Eyre, D., & Drummond, I. A. (2014). Modulation of the secretory pathway rescues zebrafish polycystic kidney disease pathology. *Journal of the American Society of Nephrology : JASN, 25*(8), 1749-1759. 10.1681/ASN.2013101060 Retrieved from http://www.ncbi.nlm.nih.gov/pubmed/24627348

Lee, K., Boctor, S., Barisoni, L. M. C., & Gusella, G. L. (2015). Inactivation of integrin-β1 prevents the development of polycystic kidney disease after the loss of polycystin-1. *Journal of the American Society of Nephrology : JASN, 26*(4), 888. Retrieved from http://www.ncbi.nlm.nih.gov/pubmed/25145933

Liebscher I, S. T. (2016). Tethered agonism: A common activation mechanism of adhesion GPCRs. *Handb Exp Pharmacol, 234*, 111-125.

Liebscher, I., Monk, K. R., & Schöneberg, T. (2015). How to wake a giant. *Oncotarget, 6*(27), 23038. Retrieved from http://www.ncbi.nlm.nih.gov/pubmed/26405160

Liebscher, I., Schön, J., Petersen, S., Fischer, L., Auerbach, N., Demberg, L., . . . Schöneberg, T. (2014). A tethered agonist within the ectodomain activates the adhesion G protein-coupled receptors GPR126 and GPR133. *Cell Reports, 9*(6), 2018-2026. 10.1016/j.celrep.2014.11.036 Retrieved from https://www.sciencedirect.com/science/article/pii/S221112471401002X

Liu Xiaowen, Vien Thuy, Duan Jingjing, Sheu Shu-Hsien, DeCaen Paul, G., & Clapham David, E. (2018). Polycystin-2 is an essential ion channel subunit in the primary cilium of the renal collecting duct epithelium. *eLife, 7*10.7554/eLife.33183 Retrieved from https://search.proquest.com/docview/2009161162

Liu, B., Li, C., Liu, Z., Dai, Z., & Tao, Y. (2012). Increasing extracellular matrix collagen level and MMP activity induces cyst development in polycystic kidney disease. *BMC Nephrology, 13*(1), 109. 10.1186/1471-2369-13-109 Retrieved from http://www.ncbi.nlm.nih.gov/pubmed/22963260

Liu, K. S., & Sternberg, P. W. (1995). Sensory regulation of male mating behavior in caenorhabditis elegans. *Neuron, 14*(1), 79-89. 10.1016/0896-6273(95)90242-2 Retrieved from https://www.sciencedirect.com/science/article/pii/0896627395902422

Lockwood, C. A., Lynch, A. M., & Hardin, J. (2008). Dynamic analysis identifies novel roles for DLG-1 subdomains in AJM-1 recruitment and LET-413-dependent apical focusing. *Journal of Cell Science, 121*(9), 1477-1487. 10.1242/jcs.017137 Retrieved from http://jcs.biologists.org/cgi/content/abstract/121/9/1477

Lodish, H. F. (2000). *Molecular cell biology* (4. ed., 1. print. ed.). New York, NY: Freeman. Retrieved from http://www.ncbi.nlm.nih.gov/books/NBK21475/

Ma M, Gallagher AR, Somlo S. (2017). Ciliary mechanisms of cyst formation in polycystic kidney disease. *Cold Spring Harb Perspect Biol, 9*, 11.

Maguire, J. E., Silva, M., Nguyen, K. C. Q., Hellen, E., Kern, A. D., Hall, D. H., & Barr, M. M. (2015). Myristoylated CIL-7 regulates ciliary extracellular vesicle biogenesis. *Molecular Biology of the Cell, 26*(15), 2823-2832. 10.1091/mbc.E15-01-0009 Retrieved from http://www.ncbi.nlm.nih.gov/pubmed/26041936

Maguire, J. E. (2015). *Myristoylated CIL-7 is required for polycystin associated behaviors and extracellular vesicle biogenesis in C. elegans* Available from Dissertations & Theses Europe Full Text: Science & Technology. Retrieved from https://search.proquest.com/docview/1749024119

Mangeol, P. J. J., Prevo, B., & Peterman, E. J. G. (2016). KymographClear and KymographDirect: Two tools for the automated quantitative analysis of

molecular and cellular dynamics using kymographs. *Molecular Biology of the Cell, 27*(12), 1948-1957. 10.1091/mbc.E15-06-0404 Retrieved from http://www.narcis.nl/publication/RecordID/oai:research.vu.nl:publications%2F136d4326-a912-4f73-a6ba-c250cafdcb5c

Mangos, S., Lam, P. Y., Zhao, A., Liu, Y., Mudumana, S., Vasilyev, A., . . . Drummond, I. A. (2010). The ADPKD genes pkd1a/b and pkd2 regulate extracellular matrix formation. *Disease Models & Mechanisms, 3*(5-6), 354-365. 10.1242/dmm.003194

Markus Delling, Paul G DeCaen, Julia F Doerner, Sebastien Febvay, & David E Clapham. (2013). Primary cilia are specialized calcium signalling organelles. *Nature, 504*(7479), 311. Retrieved from http://www.ncbi.nlm.nih.gov/pubmed/24336288

Marta Andrés, Enrique Turiégano, Martin C Göpfert, Inmaculada Canal, & Laura Torroja. (2014a). The extracellular matrix protein artichoke is required for integrity of ciliated mechanosensory and chemosensory organs in drosophila embryos. *Genetics, 196*(4), 1091-1102. 10.1534/genetics.113.156323 Retrieved from http://www.ncbi.nlm.nih.gov/pubmed/24496014

Marta Andrés, Enrique Turiégano, Martin C Göpfert, Inmaculada Canal, & Laura Torroja. (2014b). The extracellular matrix protein artichoke is required for integrity of ciliated mechanosensory and chemosensory organs in drosophila

embryos. *Genetics, 196*(4), 1091-1102. 10.1534/genetics.113.156323 Retrieved from http://www.ncbi.nlm.nih.gov/pubmed/24496014

Merritt, C., Rasoloson, D., Ko, D., & Seydoux, G. (2008). 3′ UTRs are the primary regulators of gene expression in the C. elegans germline. *Current Biology, 18*(19), 1476-1482. 10.1016/j.cub.2008.08.013 Retrieved from https://www.sciencedirect.com/science/article/pii/S0960982208010531

Ming Ma, Xin Tian, Peter Igarashi, Gregory J Pazour, & Stefan Somlo. (2013). Loss of cilia suppresses cyst growth in genetic models of autosomal dominant polycystic kidney disease. *Nature Genetics, 45*(9), 1004. 10.1038/ng.2715 Retrieved from http://www.ncbi.nlm.nih.gov/pubmed/23892607

Morsci, N. S. (2012). *The role of kinesin-like protein 6 in structure and function of ciliated sensory neurons* Available from Dissertations & Theses Europe Full Text: Science & Technology. Retrieved from http://www.riss.kr/pdu/ddodLink.do?id=T13063669

Nandadasa, S., Nelson, C., & Apte, S. (2015). ADAMTS9-mediated extracellular matrix dynamics regulates umbilical cord vascular smooth muscle differentiation and rotation. *Cell Reports, 11*(10), 1519-1528. 10.1016/j.celrep.2015.05.005 Retrieved from https://www.sciencedirect.com/science/article/pii/S2211124715005033

Nauli, S. M., Alenghat, F. J., Luo, Y., Williams, E., Vassilev, P., Li, X., . . . Zhou, J. (2003). Polycystins 1 and 2 mediate mechanosensation in the primary cilium of kidney cells. *Nature Genetics, 33*(2), 129-137. 10.1038/ng1076

Nucleic acids research. (2018). *Nucleic Acids Research, 45*(5), 2699.

O'Hagan, R. e. a. (2017). Glutamylation regulates transport, specializes function, and sculpts the structure of cilia. *Current Biology, 27*(22), 3430-3441.

O'Hagan, R., Chalfie, M., & Goodman, M. B. (2005). The MEC-4 DEG/ENaC channel of caenorhabditis elegans touch receptor neurons transduces mechanical signals. *Nature Neuroscience, 8*(1), 43-50. 10.1038/nn1362

O'Hagan, R., Wang, J., & Barr, M. M. (2014). Mating behavior, male sensory cilia, and polycystins in caenorhabditis elegans. *Seminars in Cell & Developmental Biology, 33*, 25. 10.1016/j.semcdb.2014.06.001 Retrieved from http://www.ncbi.nlm.nih.gov/pubmed/24977333

Page, A. P., & Johnstone, I. L. (2007). The cuticle. *The Wormbook,* Retrieved from http://www.wormbook.org

Paul G DeCaen, Markus Delling, Thuy N Vien, & David E Clapham. (2013). Direct recording and molecular identification of the calcium channel of primary cilia. *Nature, 504*(7479), 315. Retrieved from http://www.ncbi.nlm.nih.gov/pubmed/24336289

Perkins, L. A., Hedgecock, E. M., Thomson, J. N., & Culotti, J. G. (1986). Mutant sensory cilia in the nematode caenorhabditis elegans. *Developmental Biology, 117*(2), 456-487.

Rachel Jones. (2010). Day and night: Circadian rhythms in worms. *PLoS Biology, 8*(10)10.1371/journal.pbio.1000511 Retrieved from https://search.proquest.com/docview/1292285058

Raman A, Reif GA, Dai Y, Khanna A, Li X, Astleford L, Parnell SC, Calvet JP, Wallace DP. (2017). Integrin-linked kinase signaling promotes cyst growth and fibrosis in polycystic kidney disease. *J Am Soc Nephrol, 9*, 2708-2719.

Reichardt, L. F., & Prokop, A. (2011). Introduction: The role of extracellular matrix in nervous system development and maintenance. *Developmental Neurobiology, 71*(11), 883-888. 10.1002/dneu.20975; 10.1002/dneu.20975

Renu Batra-Safferling, Karin Abarca-Heidemann, Heinz Gerd KÃ¶rschen, Christos Tziatzios, Matthias Stoldt, Ivan Budyak, . . . U. Benjamin Kaupp. (2006). Glutamic acid-rich proteins of rod photoreceptors are natively unfolded. *Journal of Biological Chemistry, 281*(3), 1449-1460. 10.1074/jbc.M505012200 Retrieved from http://www.jbc.org/content/281/3/1449.abstract

Ricard-Blum, S. (2011). The collagen family. *Cold Spring Harbor Perspectives in Biology, 3*(1), a004978. 10.1101/cshperspect.a004978; 10.1101/cshperspect.a004978

Riddle, D. L. (1997). *C. elegans II*. New York: Cold Spring Harbor Laboratory Press.

Rilla, K., & et.al. (2017). Extracellular vesicles are integral and functional components of the extracellular matrix. *Matrix Biology,*

Rondanino, C., Poland, P. A., Kinlough, C. L., Li, H., Rbaibi, Y., Myerburg, M. M., . . . Hughey, R. P. (2011). Galectin-7 modulates the length of the primary cilia and wound repair in polarized kidney epithelial cells. *American Journal of Physiology.Renal Physiology, 301*(3), 622. 10.1152/ajprenal.00134.2011

Rong Luo, Sung-Jin Jeong, Annie Yang, Miaoyun Wen, David E Saslowsky, Wayne I Lencer, . . . Xianhua Piao. (2014). Mechanism for adhesion G protein-coupled receptor GPR56-mediated RhoA activation induced by collagen III stimulation. *PLoS One, 9*(6), e100043. 10.1371/journal.pone.0100043 Retrieved from http://www.ncbi.nlm.nih.gov/pubmed/24949629

Ruhlen, R. |., K. (2014). The chondrocyte primary cilium. *Osteoarthritis and Cartilage, 22*(8), 1071-1076. 10.1016/j.joca.2014.05.011 Retrieved from https://www.clinicalkey.es/playcontent/1-s2.0-S1063458414010905

Satir, P., Pedersen, L. B., & Christensen, S. T. (2010). The primary cilium at a glance. *Journal of Cell Science, 123*(Pt 4), 499-503. 10.1242/jcs.050377

Scholz N, Monk KR, Kittel RJ, Langenhan T. (2016). Adhesion GPCRs as a putative class of metabotropic mechanosensors. *Handb Exp Pharmacol, 234*, 221-247.

Schroeder, N. E., Androwski, R. J., Rashid, A., Lee, H., Lee, J., & Barr, M. M. (2013). Dauer-specific dendrite arborization in C. elegans is regulated by KPC-1/furin. *Current Biology : CB, 23*(16), 1527-1535. 10.1016/j.cub.2013.06.058 Retrieved from http://www.ncbi.nlm.nih.gov/pubmed/23932402

Seeger-Nukpezah, T., & Golemis, E. A. (2012). The extracellular matrix and ciliary signaling. *Current Opinion in Cell Biology, 24*(5), 652-661. 10.1016/j.ceb.2012.06.002; 10.1016/j.ceb.2012.06.002

Selander-SunnerhagenSQ, M. e. a. (1992). How an epidermal growth factor (EGF)-like domain binds calcium. *Journal of Biological Chemistry, 267*, 19642-19649.

Shen, P. S., Yang, X., DeCaen, P. G., Liu, X., Bulkley, D., Clapham, D. E., & Cao, E. (2016). The structure of the polycystic kidney disease channel PKD2 in lipid nanodiscs. *Cell, 167*(3), 773.e11. 10.1016/j.cell.2016.09.048

Shigetomi, H., Onogi, A., Kajiwara, H., Yoshida, S., Furukawa, N., Haruta, S., . . . Kobayashi, H. (2010). Anti-inflammatory actions of serine protease inhibitors containing the kunitz domain. *Inflammation Research, 59*(9), 679-687. 10.1007/s00011-010-0205-5 Retrieved from http://www.ncbi.nlm.nih.gov.proxy.libraries.rutgers.edu/pubmed/20454830

Sigurdson, D. C., Spanier, G. J., & Herman, R. K. (1984). Caenorhabditis elegans deficiency mapping. *Genetics, 108*(2), 331-345.

Silva, M. S. (2017). *Ultrastructure of cephalic male cilia of caenorhabditis elegans: Development and specialization* Retrieved from https://search.proquest.com/docview/2002539882

Silva, M., Morsci, Natalia, Nguyen, Ken, Rizvi, A., Rongo, C., Hall, D., & Barr, M. (2017). Cell-specific alpha-tubulin isotype regulates ciliary microtubule ultrastructure, intraflagellar transport and extracellular vesicle biology. *Current Biology, 27*, 968-980.

Song CJ, Zimmerman KA, Henke SJ, Yoder BK. (2017). Inflammation and fibrosis in polycystic kidney disease. *Results Probl Cell Differ, 60*, 323-344.

Stephney, G. (2007). The teachable worm: C. elegans, worm atlas, worm image and the slidable worm: From the webpage to the classroom. *Microscopy and Microanalysis, 13*(S02), 208-209. 10.1017/S1431927607073916 Retrieved from http://journals.cambridge.org/abstract_S1431927607073916

Sulston, J. E., Albertson, D. G., & Thomson, J. N. (1980). The caenorhabditis elegans male: Postembryonic development of nongonadal structures. *Developmental Biology, 78*(2), 542-576.

Sutters, M., & Germino, G. G. (2003). Autosomal dominant polycystic kidney disease: Molecular genetics and pathophysiology. *The Journal of Laboratory and Clinical Medicine, 141*(2), 91-101. 10.1067/mlc.2003.13

Tagliabracci, V. S., Pinna, L. A., & Dixon, J. E. (2013). Secreted protein kinases. *Trends in Biochemical Sciences, 38*(3), 121-130. 10.1016/j.tibs.2012.11.008 Retrieved from http://www.ncbi.nlm.nih.gov/pubmed/23276407

Takiar, V., & Caplan, M. J. (2011). Polycystic kidney disease: Pathogenesis and potential therapies. *BBA - Molecular Basis of Disease, 1812*(10), 1337-1343. 10.1016/j.bbadis.2010.11.014 Retrieved from https://www.sciencedirect.com/science/article/pii/S0925443910002693

Tavernarakis, N., & Driscoll, M. (1997). Molecular modeling of mechanotransduction in the nematode caenorhabditis elegans. *Annual Review of Physiology, 59*(1), 659-689. 10.1146/annurev.physiol.59.1.659 Retrieved from http://www.ncbi.nlm.nih.gov/pubmed/9074782

Tavernarakis, N., Shreffler, W., Wang, S., & Driscoll, M. (1997). Unc-8, a DEG/ENaC family member, encodes a subunit of a candidate mechanically gated channel that ModulatesC. elegansLocomotion. *Neuron, 18*(1), 107-

119. 10.1016/S0896-6273(01)80050-7 Retrieved from https://www.sciencedirect.com/science/article/pii/S0896627301800507

Thein, M. C., Winter, A. D., Stepek, G., McCormack, G., Stapleton, G., Johnstone, I. L., & Page, A. P. (2009). Combined extracellular matrix cross-linking activity of the peroxidase MLT-7 and the dual oxidase BLI-3 is critical for post-embryonic viability in caenorhabditis elegans. *The Journal of Biological Chemistry, 284*(26), 17549-17563. 10.1074/jbc.M900831200

Toomer, K. A., Fulmer, D., Guo, L., Drohan, A., Peterson, N., Swanson, P., . . . Norris, R. A. (2017). A role for primary cilia in aortic valve development and disease. *Developmental Dynamics, 246*(8), 625-634. 10.1002/dvdy.24524 Retrieved from https://onlinelibrary.wiley.com/doi/abs/10.1002/dvdy.24524

Waaijers, S., De Amil Da Costa Jacob Ramalho, Joao, Koorman, T., Kruse, E., & Boxem, M. (2015). The C. elegans crumbs family contains a CRB3 homolog and is not essential for viability. *Biology Open, 4*(3), 276. Retrieved from http://www.narcis.nl/publication/RecordID/oai:dspace.library.uu.nl:1874%2F320999

Wade, R. J., & Burdick, J. A. (2012). Engineering ECM signals into biomaterials. *Materials Today, 15*(10), 454-459. 10.1016/S1369-7021(12)70197-9

Wang, J., Schwartz, H. T., & Barr, M. M. (2010). Functional specialization of sensory cilia by an RFX transcription factor isoform. *Genetics, 186*(4), 1295-1307. 10.1534/genetics.110.122879

Wang, J., Kaletsky, R., Silva, M., Williams, A., Haas, L. A., Androwski, R. J., . . . Barr, M. M. (2015). Cell-specific transcriptional profiling of ciliated sensory neurons reveals regulators of behavior and extracellular vesicle biogenesis. *Current Biology : CB, 25*(24), 3232-3238. 10.1016/j.cub.2015.10.057 Retrieved from http://www.ncbi.nlm.nih.gov/pubmed/26687621

Wang, J., Silva, M., Haas, L. A., Morsci, N. S., Nguyen, K. C. Q., Hall, D. H., & Barr, M. M. (2014). C. elegans ciliated sensory neurons release extracellular vesicles that function in animal communication. *Current Biology : CB, 24*(5), 519-525. 10.1016/j.cub.2014.01.002 Retrieved from http://www.ncbi.nlm.nih.gov/pubmed/24530063

Warburton-Pitt, S. R. F. (2015). *The ciliopathy gene nphp-2 functions in multiple gene networks and regulates ciliogenesis in C. elegans* Available from Dissertations & Theses Europe Full Text: Science & Technology. Retrieved from https://search.proquest.com/docview/1704864810

Ward, S., Thomson, N., White, J. G., & Brenner, S. (1975). Electron microscopical reconstruction of the anterior sensory anatomy of the nematode caenorhabditis elegans.?2UU. *The Journal of Comparative*

*Neurology, 160*(3), 313. Retrieved from http://www.ncbi.nlm.nih.gov/pubmed/1112927

Ware, R., Clark, D., Crossland, K., & Russell, R. (1975). The nerve ring of the nematode caenorhabditis elegans: Sensory input and motor output. *Journal of Computational Neurobiology, 162*, 71-110.

WormBase. Retrieved from http://www.wormbase.org/species/c_elegans/gene/WBGene00003165#0-9g84f6-10

*WormBook* (2005). Retrieved from http://data.theeuropeanlibrary.org/BibliographicResource/3000080810773

Xie, P., Kondeti, V. K., Lin, S., Haruna, Y., Raparia, K., & Kanwar, Y. S. (2011). Role of extracellular matrix renal tubulo-interstitial nephritis antigen (TINag) in cell survival utilizing integrin (alpha)vbeta3/focal adhesion kinase (FAK)/phosphatidylinositol 3-kinase (PI3K)/protein kinase B-serine/threonine kinase (AKT) signaling pathway. *The Journal of Biological Chemistry, 286*(39), 34131. Retrieved from http://www.ncbi.nlm.nih.gov/pubmed/21795690

Xu Q, Liu X, Liu W, Hayashi T, Yamato M, Fujisaki H, Hattori S, Tashiro SI, Onodera S, Ikejima T. (2018). Type I collagen-induced YAP nuclear

expression promotes primary cilia growth and contributes to cell migration in confluent mouse embryo fibroblast 3T3-L1 cells. *Mol Cell Biochem,*

Yook, Y. J., Woo, Y. M., Yang, M. H., Ko, J. Y., Kim, B. H., Lee, E. J., . . . Park, J. H. (2012). Differential expression of PKD2-associated genes in autosomal dominant polycystic kidney disease. *Genomics & Informatics, 10*(1), 16-22. 10.5808/GI.2012.10.1.16; 10.5808/GI.2012.10.1.16

Yu, M., Liu, Y., Li, J., Natale, B. N., Cao, S., Wang, D., . . . Hu, H. (2016). Eyes shut homolog is required for maintaining the ciliary pocket and survival of photoreceptors in zebrafish. *Biology Open, 5*(11), 1662-1673. 10.1242/bio.021584 Retrieved from https://doaj.org/article/7d185410e32e4043ada5890bf3acc609

Zhang, Y., & Shen, H. (2016). (2016). Improve signal peptide prediction by using functional domain information. Paper presented at the 1814-1819. 10.1109/CISP-BMEI.2016.7853012 Retrieved from http://ieeexplore.ieee.org/document/7853012

Zhang, Y., & Chalfie, M. (2002). MTD-1, a touch-cell-specific membrane protein with a subtle effect on touch sensitivity. *Mechanisms of Development, 119*(1), 3-7. 10.1016/S0925-4773(02)00293-9 Retrieved from https://www.sciencedirect.com/science/article/pii/S0925477302002939